6-13-2011 12:00 AM

Supercritical Water Gasification of Biomass & Biomass Model Compounds

Emhemmed A.E.A Youssef, *The University of Western Ontario*

Supervisor: George Nakhla, *The University of Western Ontario*
Joint Supervisor: Paul Charpentier, *The University of Western Ontario*
A thesis submitted in partial fulfillment of the requirements for the Doctor of Philosophy degree in Chemical and Biochemical Engineering

SUPERCRITICAL WATER GASIFICATION OF BIOMASS & BIOMASS MODEL COMPOUNDS

(Thesis format: Integrated-Article)

The thesis by

Emhemmed A. Youssef

Graduate Program in Engineering Science
Department of Chemical and Biochemical Engineering

A thesis submitted in partial fulfillment
of the requirements for the degree of
Doctor of Philosophy

School of Graduate and Postdoctoral Studies
The University of Western Ontario
London, Ontario, Canada

Certificate of Examination

Supervisor

_____
Dr. George Nakhla

Co-supervisor

_____
Dr. Paul Charpentier

Examiners

_____
Dr. Prabir Basu

_____
Dr. Clare Robinson

_____
Dr. Lars Rehmann

_____
Dr. Chunbao Xu

The thesis by

Emhemmed A Youssef

entitled:

SUPERCRITICAL WATER GASIFICATION OF BIOMASS & BIOMASS MODEL COMPOUNDS

is accepted in partial fulfilment of the requirements for the degree of

DOCTOR OF PHILOSOPHY

Date_____

_____
Chair of the Thesis Examination Board

Abstract and Keywords

Supercritical water gasification (SCWG) is an innovative, modern, and effective destruction process for the treatment of organic compounds. Hydrogen production using SCWG of biomass or waste feedstocks is a promising approach towards cleaner fuel production while simultaneously providing novel solution for hard-to-treat organic wastes. The main premise of this work was to experimentally examine real waste biomass sources i.e. hog manure and waste biomass model compounds using gasification in SCW while examining various commercial catalysts. The improvement of the SCWG process requires a understanding of the waste/biomass reaction chemistry, and thus a knowledge of the reaction mechanisms is critically important for proper catalyst selection and design. The main possible reactions that occurred through the formation and disappearance of intermediate compounds as well as the final gaseous and liquid final products are reported.

In this work, gasification and partial oxidation of glucose 0.25 Molarity (M) was conducted using different metallic Ni loadings (7.5, 11, and 18 wt %) on different catalyst supports (θ-Al_2O_3 and γ-Al_2O_3) in supercritical water at 400-500°C, and compared with a commercial catalyst (65 wt % Ni on Silica-Alumina). Results showed that the presence of metallic Nickel increases the yield of gases and the total gas yield increased with increasing nickel in the 7.5-18 wt % Ni/Al_2O_3 catalyst. This study showed that the same hydrogen yield can be obtained from the synthesized low nickel alumina loading (18 wt %) catalyst as the high (65 wt %) nickel on silica-alumina commercial catalyst.

In this work, oleic acid was examined as a model compound for lipids. Results showed that an increase of temperature coupled with the use of catalyst enhanced the gas

yield dramatically. The H_2 yield was 15 mol/ mol oleic acid converted using both the pelletilized Ru/Al_2O_3 and powder Ni/Silica-alumina catalysts which yielded 4 times higher than the calculated equilibrium yield of 3.5 mol/mol oleic acid fed. The composition of residual liquid products was studied and a generalized reaction pathway of oleic acid decomposition in SCW reported.

Cysteine gasification in supercritical water in the presence of Ru/Al_2O_3, Ru/AC and activated carbon (AC) catalysts was also investigated. The main sulfur-containing compound in the gaseous effluents in all experiments was H_2S. It was found that the formation of H_2S was neither dependent on temperature nor on the catalyst. The composition of residual liquid products revealed the presence of residual organic sulfur components that include diethyl sulfide, diethyl tri sulfide, and ethanone. A generalized reaction pathway for organo-sulfur compounds was reported.

The catalytic co-gasification of starch and catechol as models of carbohydrates and phenol compounds was investigated. Employing TiO_2 as a catalyst alone had no significant effect on the H_2 yield but when combined with CaO increased the hydrogen yield by 35%, while promoting higher total carbon (TOC) reduction efficiencies. The process liquid effluent characterization showed that the major non-polar components were phenol, substituted phenols, and cresols. An overall reaction scheme was provided.

Catalytic hydrogen production with various catalysts from hog manure using supercritical water partial oxidation was investigated. The order of H_2 production was the following: $Pd/AC > Ru/Al_2O_3 > Ru/AC > AC > NaOH$. A 35% reduction in the H_2 and CH_4 yields was observed in the sequential gasification partial oxidation (oxidant at an 80% of theoretical requirement) experiments compared to the gasification experiments

(catalyst only). Moreover, this reduction in gas yields coincided with a 45% reduction in the liquid effluent chemical oxygen demand (COD), 60% reduction of the ammonia concentration in the liquid effluent, and 20% reduction in the H_2S concentration in the effluent gas.

The scientific contribution of this study culminated in the development of a qualitative mechanistic understanding of the reaction chemistry of organic matters presented in waste streams such as waste biomass, sewage sludge, and hog manure. This understanding of the SCW reaction chemistry is required for the potential applications of SCW for energy recovery from waste streams through hydrogen production.

Keywords: Catalysis, Hydrogen production, Gasification, TOC destruction, Supercritical water, Hog manure, Sewage sludge, Biomass, Oleic acid, Cysteine, Starch, Catechol.

Co-Authorship

Chapter 2: Supercritical Water Gasification for Hydrogen Production

Youssef E, Nakhla G, Charpentier P.

A Book chapter in: Handbook of Hydrogen Energy. 1st edition, Edited by: S.A.Sherif. CRC/Taylor and Francis. 2010. in press

Chapter 4: Effect of Nickel Loading on Hydrogen Production and Chemical Oxygen Demand (COD) Destruction from Glucose Oxidation and Gasification in Supercritical Water

Youssef E, Chowdhury M, Nakhla G, Charpentier P.

Published in the *Int J Hydrogen Energy*. 2010; 35: 5034-5042.

Chapter 5: Oleic Acid Gasification over Supported Metal Catalysts in Supercritical Water: Hydrogen Production and Product Distribution.

Youssef E, Nakhla G, Charpentier P.

Published in the *Int. J. Hydrogen Energy*. 2011; 36: 4830-4842.

Chapter 6: Fate of Sulfur during Catalytic and Non-catalytic Cysteine Gasification in Supercritical Water for Hydrogen Production

Youssef E, Nakhla G, Charpentier P.

Submitted to *Int. J. Hydrogen Energy*.

Chapter 7: Co-gasification of catechol and starch in supercritical water for hydrogen production

Youssef E, Nakhla G, Charpentier P.

Submitted to Bioresource Tech.

Chapter 8: Sequential Supercritical Water Gasification and Partial Oxidation of Hog Manure for Hydrogen Production

Youssef E, Elbeshbishy E, Hafez H, Nakhla G, Charpentier P.

Published in the *Int. J. Hydrogen Energy*. 2010; 35: 11756-11767.

Dedication

To my beloved wife, Naziha, for her love and patience, thanks for waiting.

To my daughters, Danah and Ala, you filled my life

To my parents and siblings for their continuous support

And

Last but not the least, to all brave Libyan men, women, and children who wrote the history with their blood

Acknowledgements

Praise be to Allah, the most gracious and the most merciful, who gave me the health and ability to start and end this study.

My deep appreciation and thanks to my supervisors Dr. George Nakhla and Dr. Paul Charpentier for their guidance, and support.

I also would like to thank the Libyan Secretariat of High Education for help and financial support throughout this study.

I would like to convey my appreciation to my family members for their support; May Allah bless them

I would like to thank my colleagues at the Chemical and Biochemical Engineering Department at the University of Western Ontario for the friendly environment and help.

Last but not the least, I would like particularly to extend and express my deepest and sincere gratitude to my beloved wife, Naziha, and my daughters Danah and Ala for their continuous support and encouragement.

Table of Contents

List of Tables

List of Figures

CHAPTER 1

General Introduction

1.1 Background

Conversion of biomass and waste biomass into fuels has attracted significant recent attention [1-3]. Dwindling reserves of fossil fuels and their negative environmental impacts has shifted the focus towards the development of alternative energy sources [4]. Hydrogen (H_2) is a promising alternative clean energy source. Hydrogen's viability as a clean fuel is greatly enhanced if it is produced from renewable sources such as sewage sludge, manure, or other waste biomass types. Waste biomass contains up to 80-85% water and 15-20% dry solids [5], 75% of which is organic. Conversion of such waste streams to valuable fuels such as hydrogen and chemicals using conventional techniques such as pyrolysis or catalytic gasification is energy intensive due to the high energy input required for drying.

Hydrogen's role in today's economy is essential since it is used in many applications. It is also a valuable component of the current petroleum industries because it is employed to upgrade petroleum products such as naphtha reforming, ammonia, and methanol production [5-7]. More recently, there has been growing interest in developing new technologies for hydrogen production from renewable sources [8]. The rapid increase in energy demand, the depletion of fossil resources such as petroleum as well as the necessity to protect the environment have contributed to the current active search for renewable and environmentally friendly energy sources. Considerable research efforts have been made to introduce hydrogen as an alternative energy source especially in the transportation sector where fuel cells are emerging as a viable long term clean solution [6-8]. Hydrogen contains no carbon that harms the environment through the formation of green house gases. Hydrogen is the lightest element, has a high energy yield of

122 MJ/kg, which is 2.8 times greater than an average hydrocarbon fuel. Hydrogen is the cleanest fuel since its combustion produces only water [10].

Hydrogen is produced primarily from two sources: non-renewable which mainly uses fossil fuels and renewable resources such as biomass and waste biomass.

- Non-renewable hydrogen production technologies such as SMR (steam reforming of methane) represented by the reforming of hydrocarbon-steam mixture into H_2 and CO_2.
- Renewable hydrogen production technologies through gasification of renewable feedstocks such as biomass using either steam reforming or supercritical water gasification (SCWG) techniques.

Supercritical water gasification (SCWG) provides a powerful means to transform toxic organic materials into simple inert oxides [9-10]. Over the past two decades, the basic understanding of the fundamental chemistry of the process has increased markedly, due to the rising research interest in this area. Water above its critical state i.e. critical pressure and critical temperature exhibits unique change in its properties. At the supercritical conditions (373°C, 221 atm) water becomes supercritical (SCW), a non-polar fluid that has a gas-like and liquid –like properties [1-5, 8-12]. The dielectric constant drops sharply and the hydrogen bonding becomes very weak which allows for fast and effective C-C bond cession. It also allows for fast reaction kinetics as the mass transfer resistance becomes insignificant as a result of the high solubility and diffusivity [1&2]. For most organic compounds, these conditions are sufficient to achieve more than 99.99% destruction and removal efficiencies in only 30-60 seconds. The properties of water change drastically in the critical region as they behave as a non-polar solvent, and the inorganic salts become insoluble and precipitate. The high pressure of the SCW increases the mixture

density which in combination with solubility of the organic combustion gases and fast reaction kinetics allows complete oxidation in a relatively short reaction time frame [3].

The improvement of SCWG process depends on better understanding of the waste/biomass reaction chemistry. However, gasification of real biomass is difficult due to its complex chemical structure. Waste biomass is defined as consisting of all plant and plant-derived materials including livestock manures and sludges. Lignocellulosic waste biomass is composed primarily of carbohydrate polymers (cellulose and hemi-cellulose) and phenolic polymers (lignin). Lower concentrations of various other compounds, such as proteins, acids, salts, and minerals, are also present. The structural and chemical composition of lignocellulosic waste biomass is highly variable because of genetic and environmental influences and their interactions [10-12]. For example, quantitative and qualitative composition of sewage sludge is very complicated. It is rich in organic matter, nitrogen, phosphorus, calcium, magnesium, and sulphur. However, sewage sludge mainly consisted of lipids (about 10%), proteins (about 40%), carbohydrates, lignin (about 17%), and ash [13]. To gain an understanding of the reaction chemistry of waste biomass gasification, studying compounds that model real biomass components is an invaluable to gain insight into the complex structure of waste biomass.

1.2 Selection of the model compounds

There are limited studies reported in the literature on hydrogen production from sewage sludges using supercritical water. This motivated this thesis to break down the proposed investigation into two categories by which the behavior of sewage sludges in supercritical water can be examined. The first category is to investigate sewage sludges (SS) model compounds at the SCW conditions whereas the second category deals with real waste stream such as hog manure. The model compounds were selected based on the fact that sewage sludge (SS) typically

consists of 41% protein, 25% lipid, 14% carbohydrate [13]. Therefore, the following five model compounds were selected:

- Polysaccharides:

  Glucose ($C_6H_{12}O_6$): serves as a simple model compound for SCW because it mimics the chemical structure for cellulosic wastes and sludges. Glucose was primarily used for testing and catalyst development in the constructed SCW batch unit.

- Lipids:

  Oleic acid ($C_{18}H_{34}O_2$): a long chain fatty acid can serve as a model compound for lipids, it has the formula. The saturated form of this acid is stearic acid and it is a waxy solid.

Oleic acid

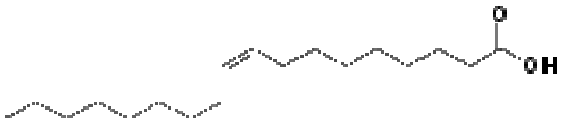

- Proteins:

  Cysteine; is an α-amino acid with the chemical formula $HO_2CCH(NH_2)CH_2SH$. Cysteine is classified as a hydrophobic amino acid. Because of the high reactivity of this thiol, cysteine is also an important structural and functional component of many proteins. Also, since cysteine contains the sulfide group in its structural formula, it is well suitable to represent sulfur containing sewage sludge proteins. Another reason for selecting cysteine is that in the literature, there has not been any investigations of the behavior of sulfur compounds present in sewage sludge (SS).Therefore, investigating cysteine would give an invaluable addition to the understanding of the behavior of sulfur compounds present in sewage sludges. To the best of the author's knowledge, neither oleic acid nor cysteine has been investigated previously.

Cysteine

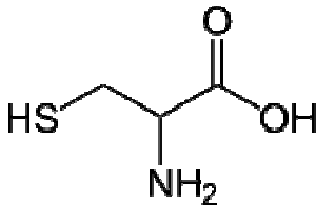

- Carbohydrate:

  Starch with a chemical formula $(C_6H_{10}O_5)_n$ is a polysaccharide carbohydrate consisting of a large number of glucose units joined together by glycosidic bonds, and thus starch serves as carbohydrate model compound.

Starch

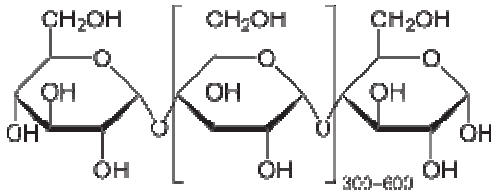

- Lignin:

  Catechol or Pyrocatechol is used as a model compound for lignin thermal degradation intermediates and for aromatic compounds in wastewater. Catechol, formerly known as pyrocatechol, is a 1,2-dihydroxybenzene, an organic compound with the formula $C_6H_4(OH)_2$.

Catechol

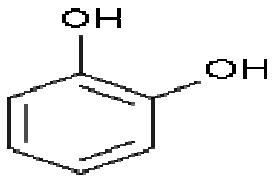

1.3 Catalysts selection & screening

Homogeneous and heterogeneous catalysis in SCW has been systematically examined for few years. It is clear that catalysts enhance the efficacy of SCW (i.e., substantially higher conversions and higher selectivities to H_2, CH_4 lower reaction temperatures, and selectivity toward CO) and numerous types of catalysts have been investigated. In supercritical water, the catalyst selection is extremely important. The need to produce a tar-free product gas from the gasification of biomass, the removal of tars, and the reduction of the methane has been the main focus of several literature studies. Several catalysts have been identified for complete oxidation in supercritical water. These include hetero-polyacids, alkali carbonates, and carbons. However, the criteria for the catalyst are fundamentally the same and may be summarized as follows:

- The catalysts must be effective in the removal of tars.
- The catalysts should be resistant to deactivation as a result of carbon fouling and sintering.
- The catalysts should be easily regenerated, strong, and inexpensive.

Adding to the above criteria in the case of hydrogen production using supercritical water, the catalyst should give reasonable hydrogen yield. In other words, the SCW catalytic process is an optimized combination of catalyst (components, manufacturing process, and morphology), reactants, reaction environment, process parameters such as temperature, pressure, and residence time, and reactor configuration.

The effect of catalysts on the production of hydrogen gas results point to the importance of identifying effective catalysts for the production of a hydrogen rich synthesis gas from waste biomass. From the tabulated literature review in chapter 2 section 6, precious metals, activated carbon, and metal oxide catalysts appear to have a strong influence on the hydrogen production

yield and showed higher H_2 and CO selectivity during the gasification of lignin and woody biomass as other compounds that model biomass and waste biomass. Thus, the catalyst selection procedure during this study was based on the aforementioned catalyst along with careful consideration and regular follow-up of literature.

Activated carbon has been shown to be effective for the decomposition of sewage sludge and other biomass feed-stocks along with noble metals, metallic nickel, and titanium dioxide giving the ability to increase hydrogen yield from the model compounds and hog manure. Therefore, several commercial catalysts have been selected for testing in this study. Besides nickel and titanium dioxide based catalysts, the selected catalysts were mainly activated carbon based with traces of different noble metals (about 0.5-5 % wt). Activated carbon was selected as the base line for catalyst comparison. Additionally, different catalyst supports such as alumina and silica alumina with the same percentage of noble metals were also compared with the selected catalysts.

1.4 Objectives

The main purpose of this research is to provide a qualitative mechanistic understanding of the reaction chemistry of organic matters present in waste streams including waste biomass, sewage sludge, and hog manure in supercritical water gasification. The effects of different commercial catalysts, reaction temperature, reaction time and oxidant stoichiometric ratio on the gaseous product distributions of sewage sludges model compounds, and hog manure as a selected agricultural waste stream, using SCW gasification and partial oxidation were evaluated in an attempt to maximize the hydrogen yield concomitantly with the chemical oxygen demand

(COD) and total organic carbon (TOC) destruction. The following specific objectives can be formulated in order to meet the main objectives of this work:

- Design, construct and operate a batch supercritical water oxidation unit able to work at temperature of 500°C and pressure of 28 MPa.
- Experimental assessment of the selected pollutant model contaminants for hydrogen production in batch SCW gasification over activated carbon, carbon doped with noble metals, and metallic commercial catalysts.
- Study and investigate the behavior and yield of the sulfur compounds that are the main sources of odor in sludges in the SCW process.
- Investigate and postulate the reaction schemes for the decomposition of model compounds in SCW based on the main products observed in both the gas and liquid phases. The main possible reactions contributing to the formation and disappearance of some intermediate compounds as well as the final gaseous and liquid products are postulated.
- Investigating the synergistic/inhibitory effects of co-gasification in the presence of CaO solely as well as combination of CaO and TiO_2 catalyst on the product gas composition.
- Investigation of treatment of real wastes.i.e. hog manure by applying the gasification and partial oxidation techniques studied for the model contaminants.

1.5 Thesis Organization

This thesis encompasses nine chapters and conforms to the “integrated-article” format as outlined in the Thesis Regulation Guide by the School of Graduate and Postdoctoral Studies

(SGPS) of the University of Western Ontario. The aforementioned chapters are organized as follows:

- Chapter 1 provides a general introduction that includes the background information pertaining to this work.
- Chapter 2 introduces a thorough review of the pertinent literature including background and a thorough assessment of information on the supercritical water (SCW) process from all aspects including design considerations, hydrogen production, and catalytic SCW gasification.
- Chapter 3 provides details of the batch SCW process unit as well as the related information pertaining to materials and analysis methods employed.
- Chapter 4 introduces the sequential partial oxidation of glucose in SCW with and without catalysts at various temperatures.
- Chapter 5 provides the detailed experimental results of oleic acid gasification in SCW in the presence of ruthenium on activated carbon catalysts.
- Chapter 6 introduces the experimental results of cysteine gasification in SCW and discuses the fate of sulfur during this work.
- Chapter 7 provides the experimental investigation of catalytic co-gasification of starch and catechol as models of carbohydrates and phenol compounds in the presence of TiO_2 and CaO catalysts.
- Chapter 8 discusses the effect of different commercial catalysts on hydrogen production from hog manure in SCW.
- Chapter 9 summarizes the major conclusions of this research and provides recommendations for future research directions based on the findings of this study.

1.6 Thesis contribution and significance

In addition to the valuable contribution of designing, installing, and operating the supercritical water gasification unit, this thesis represent an invaluable addition to the efforts for better understanding of the SCWG reaction chemistry and eventually improving the SCWG process. Other valuable scientific contributions to the recently extensive research being conducted in the literature are summarized in the following points:

- The aim of the work presented is filling several gaps found in the literature. Studying the products of the model compounds gasification in supercritical water was expanded with the identification of the persistent intermediates in the liquid effluent stream. Both gaseous and liquid products of the tested model contaminants were analyzed. The analysis techniques used for gas and liquid products allows for the derivation of the generalized reaction pathways for each model compound tested.
- Two new model untested compounds have been examined in this study i.e. oleic acid and cysteine and their impact on both gas and liquid products from the process has been evaluated.
- This study will also help identify any synergistic and/or inhibitory impacts on both gas and liquid product distribution using an employed co-gasification.
- Investigation of particular waste stream i.e. hog manure containing nitrogen, sulfur, and phosphorus, and chlorides still represents an important class of wastes that have not been studied in the literature.
- Testing the effect of different commercial catalysts on the gas and liquid products from SCW. As it has been shown that carbonaceous catalysts have a catalytic effect on

supercritical water gasification of organic compounds, carbonaceous materials might also effectively catalyze supercritical water gasification.

- However, precious metals and metal oxides doped on carbonaceous supports have been investigated as possible candidate catalysts for use in supercritical water oxidation.

1.7 References

[1] Savage PE. Organic Chemical Reactions in Supercritical Water. Chem. Rev 1999; 99: 603–621.

[2] Antal M J, Schulman S D, Xu X. Biomass Gasification in Supercritical Water. Ind. Eng. Chem. Res.2000; 39: 4040-4053.

[3] Kruse A. Supercritical water gasification. Biofuels, Bioprod. Bioref. 2008; 2: 415–437.

[4] Marquevich M, Coll R, Montane D. Steam Reforming of Sunflower Oil for Hydrogen Production. Ind. Eng. Chem. Res. 2000; 39: 2140-2147.

[5] Savage P E. A perspective on catalysis in sub- and supercritical water. The Journal of Supercritical Fluids. 2009; 47: 407-414.

[6] Elliott D, Todd R, Gary G. Chemical Processing in High-Pressure Aqueous Environments; Improved Catalysts for Hydrothermal Gasification. Ind. Eng. Chem. Res. 1993; 32: 1542-1548.

[7] Demirbas A. Hydrogen-rich gas from fruit shells via supercritical water extraction. Int. J. Hydrogen Energy. 2004; 29: 1237-1243.

[8] David S, Brian K., Julian R. Review of literature on catalysts for biomass gasification. Fuel Processing Technology. 2001; 73: 155–173

[9] Yu D, Aihara M, Antal M J. Hydrogen Production by Steam Reforming Glucose in Supercritical Water. Energy & Fuels. 1993; 7: 574.

[10] Guo L, Lu Y, Zhang X, Guan Y, Pei A. Hydrogen production by biomass gasification in supercritical water: A systematic experimental and analytical study. Catal. Today. 2007; 129: 275-286.

[11] Kritzer P, Dinjus E. An assessment of supercritical water oxidation (SCWO) Existing problems, possible solutions and new reactor concepts**.** Chemical Engineering Journal. 2001; 83:207–214.

[12] Furness D, Hoggett L, Judd S. Thermochemical treatment of sewage sludge. Water Environ. J. 2000; 14: 57-65.

[13] Goto M, Nada M, Kodama T, Hirose A. Kinetic Analysis for Destruction of Municipal Sewage Sludge and Alcohol Distillery Wastewater by Supercritical Water Oxidation. Ind. Eng. Chem. Res. 1999; 38*: 1863–1865*

CHAPTER 2

Literature Review

2.1Supercritical Fluids:

2.1.1 *Fundamentals of supercritical fluids*

A fluid heated to above the critical temperature and compressed to above the critical pressure is known as a supercritical fluid. The phenomena and behavior of supercritical fluids has been the subject of research since the 1800's [1]. Two supercritical fluids are of particular interest, carbon dioxide and water. Carbon dioxide has a low critical temperature of 31 □C and a moderate critical pressure of 7.3 MPa. It is non-flammable, non-toxic and environmentally friendly. It is often used to replace toxic freons and certain organic solvents. Furthermore, it is miscible with a variety of organic solvents and is readily recovered after processing.

2.1.2 *Supercritical water and pressurized hot water*

Any fluid is defined as a supercritical fluid when its temperature and pressure are above its critical conditions i.e. 374°C, 22 MPa for water. In Figure 2.1, the upper right quadrant portrays the phase in which water is in its supercritical state. It can be noted that at the critical point there is no distinction between the vapor and liquid phases in the P-T phase diagram. Therefore, if the liquid is heated at constant pressure until its temperature exceeds its critical temperature, it expands and becomes a state that is like vapor but with no phase transition.

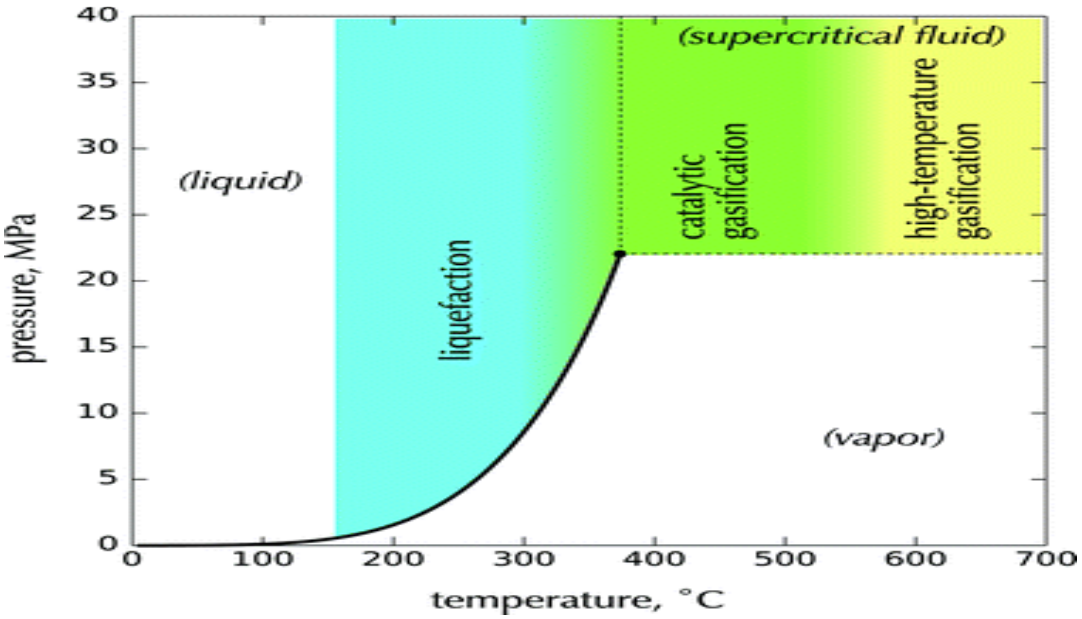

Fig 2.1 Water pressure and temperature diagram [2, 3].

2.1.3 *Properties of Supercritical Water*

Under normal conditions, water has three states; ice, steam, and liquid. When water is heated and compressed to a high temperature and pressure, above 374°C and 22 MPa, the water enters its supercritical state. Water above its critical point has unique gas-like and liquid-like properties, which are conducive to destruction of organic compounds. The solvation properties of water at 30 MPa as a function of temperature are portrayed in Figure 2.2. The viscosity and diffusivity are more gas-like whereas the density is comparable with liquid water. The mass transfer resistance in SCW becomes insignificant because of the high solubility and diffusivity of gases and organic material. Under supercritical conditions, the dielectric constant of water and hydrogen bonding drops sharply, thus providing high solvating power for organic compounds. This results in supercritical water acting as a single phase, non-polar, dense gas that has solvation properties similar to low polarity organics [1-4].

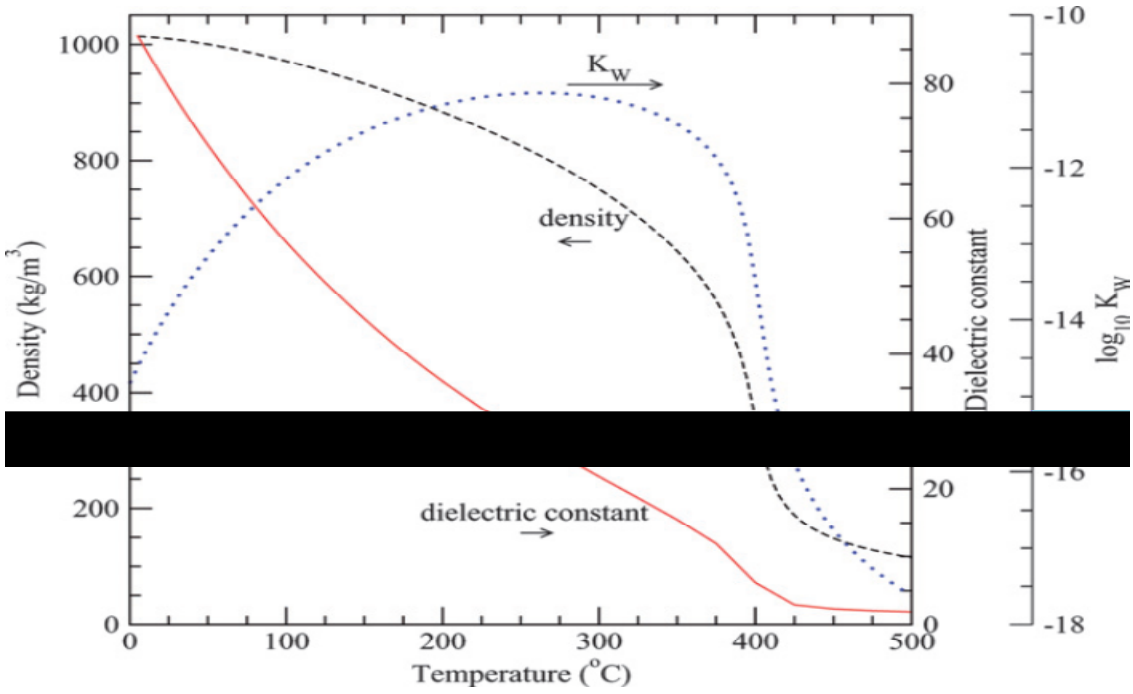

Fig 2.2: Density, static dielectric constant and ion dissociation constant (Kw) of water at 30 MPa as a function of temperature [2-3].

Moreover, increasing the value of the ionic product increases the concentration of both hydrogen and OH ions, which leads to a significant increase in the power of the hydrolysis reaction. Hence, hydrocarbons and gases such as CO_2, N_2, and O_2 are highly soluble while ionic species, namely inorganic salts, are practically insoluble in supercritical water. This enhances the oxidation kinetics of organic species, especially because of the absence of mass transfer limitations. Therefore, although SCW is applicable to a wide range of feed mixtures and is not limited to aqueous organics , organic wastes containing carbon, hydrogen, oxygen and nitrogen atoms are of particular interest and oxidized to primarily carbon dioxide, water, molecular nitrogen and other small molecules.

2.2 Development of SCW process.

2.2.1 *Current status of the SCW process*

The supercritical water (SCW) process was first known in the late 1970s, thanks to the pioneering work of Modell and co-workers [4] at the Massachusetts Institute of Technology (MIT); SCW was first developed for the treatment of hazardous wastes and materials such as warfare agents. However, SCW has emerged rapidly in the last two decades mainly because of the need to develop an alternative and environmentally friendly fuel source. This attraction was driven by the fact that SCW produces considerable amounts of gaseous fuels such as hydrogen and methane. Although it is still in the developmental stage, Yoshida [5] reported that, from an energy point of view, biomass gasification using SCW is technically feasible compared to other existing technologies such as anaerobic digestion or incineration. This is driven by the fact that SCW converts the feedstock organic contents fully leaving no residue which simultaneously achieves the ultimate goal of energy production as well as water treatment.

Several laboratory studies have focused on improving the understanding of the SCW process, in order to overcome its commercialization challenges. Preeminent research groups in SCW include Tester and coworkers at the MIT, Savage and coworkers at the University of Michigan, the Advanced Institute of Science and Technology in Korea, the Japanese National Institute for Resources and Environment, the Forschungszentrum Karlsruhe in Germany, University of Twente in the Netherlands, and the State Key Laboratory of Multiphase Flow in Power Engineering in China. Pilot scale plant operations using SCW are countable and are being conducted either by agencies such as General Atomics of USA, Chematur of UK, Mitsubishi Heavy Industries of Japan or institutions such as the High Pressure Process Group, Department

of Chemical Engineering and Environmental Technology, University of Valladolid (Spain) or private companies.

2.2.2 *Modeling and Thermo-physical properties of SCW*.

Modeling of the SCW process has gained more attention recently facilitated by the growth of experimental results. Properties of SCW significantly differ from those at the ambient conditions, as the increase of temperature increases the tendency for ion pairing which increases the salts concentration in the mixture. Thus, using numerical techniques for the calculation of the SCW properties is of utmost importance since these properties are usually unknown and difficult to experimentally estimate. The aim of this important step is the scaling up of the SCW process for commercial applications. Therefore, required knowledge of SCW thermo-physical properties such as densities, enthalpies, and heat capacities has motivated several researchers to investigate and overcome the poor prediction capabilities of the conventional cubic Equations of States (EoS) [6]. However, the Peng-Robinson EoS with volume translation correlation as reported by Bermejo et al. [6] and Li et al [7] showed a rather accurate reproducibility of both the water-air system behavior when analyzing SCWO reactors. In their comprehensive review of high-temperature electrolyte solutions, Anderko and co-workers [8] reported that the development and integration of a universal model using the combined high temperature ion-pair-based model with low-and-moderate temperature approach would be invaluable. Such a model; if computationally sufficient, could cover the wide range of temperatures required for practical applications, and thus circumvent the impractical thermodynamic properties prediction resulting from the current EoS.

2.2.3 *Reactions in SCW.*

The fundamental understanding of reactions in supercritical water (SCW) has increased remarkably in the last two decades. According to Savage et al. [9], the unique physical and transport properties of SCW are intermediate between those of a liquid and a gas. This makes SCW an attractive media for chemical reactions. The aforementioned authors pointed out that among ambient reactions in SCW are homogeneous and heterogeneous catalysis, waste oxidation, and green fuels production such as hydrogen.

Before proceeding into detailed reactions in SCW, and from an organizational point of view, SCW research activities fall into four main categories i.e. pyrolysis, total oxidation, gasification, and partial oxidation in SCW. An attempt to classify the cases in which SCW is used to gasify different compounds is presented below:

1. **Pyrolysis in SCW** which stands for the hydrolysis of the organic compounds at SCW conditions in the absence of both catalyst and oxidant.
2. **Total oxidation in SCW** which stands for gasifying the organic compounds in the absence of catalyst and the presence of excess oxidant at oxygen to carbon molar ratios (MR) of 1.0 or higher (the stoichiometric requirement i.e. M.R $\geq$ 1.0).
3. **Gasification in SCW (SCWG)** which stands for gasifying the organic compounds in the absence of oxidant while using a catalyst, which is also known as low temperature gasification.
4. **Partial oxidation in SCW (SCWPO)** which stands for oxidizing the organic compounds in the presence of oxidant at oxygen to carbon molar ratio of lower 1.0 (M.R < 1.0) and with an absence of catalyst.

5. **Sequential gasification partial oxidation** which stands for gasifying the organic compounds in the presence of active catalyst (heterogeneous or homogenous) followed by further gasifying the organic compounds in the presence of oxidant at oxygen to carbon ratios below the theoretical requirements i.e. an approach using a combination of step 3 followed by step 4.

Sequential gasification partial oxidation was studied in detail for glucose as a waste biomass model compound and hog manure by Youssef et al. [10] respectively to determine the product distribution in both the gas and liquid phases. Product distribution is important as it facilitates detailed analysis of the reactions and transformation paths that take place in SCW as well as providing insight into the process design and operating conditions i.e. temperature, pressure, oxidant stoichiometric ratios as well as the selection of the catalyst.

The chemistry of total oxidation in SCW has undoubtedly received the most attention to date. In this process, organic compounds are converted to carbon dioxide and water at typical operating conditions of about 25 MPa and 400-800°C, and in the presence of excess oxidant (O_2). The general reaction equation is given by:

$$Cx\ Hy + (x + y/4)\ O_2 \rightarrow x\ CO_2 + (y/2)\ H_2O \quad (1)$$

As a waste destruction process, supercritical water oxidation (SCWO) has several advantages over conventional processes and even some of the relatively modern processes such as wet-air oxidation and incineration. As a medium for chemical reactions, depending on its density, SCW's low dielectric constant promotes dissolution of non-polar organic compounds whereas gas-like low viscosity promotes mass transfer and the solvation is enhanced by the liquid-like density. The pioneering work of Thomason and Modell 1978 [4] was the first to apply SCWO as a powerful technology for the transformation of hazardous and toxic organic wastes,

and reported destruction efficiencies of 99.99% of organic compounds, including polychlorinated biphenyls. Bermejo et al. [6] reported the use of the SCWO technique for the treatment of municipal sewage sludge and paper mill waste as sewage sludge was converted to clear water and gases. Goto et al. [11] reported a study on the destruction of municipal sludge and alcohol distillery wastewater. The aforementioned authors reported that the composition of the molasses-rich wastewater mainly consisted of saccharide, carbohydrate, and ash (mainly KCl) whereas the sewage sludge composition consisted of lipid (about 10%), protein (about 40%), carbohydrate, lignin (about 17%), and ash. The experiments were conducted at three different temperatures of 400, 450, and 500°C with hydrogen peroxide as oxidant at 300% of the stoichiometric demand. The aforementioned authors characterized the liquid effluent by means of total organic carbon (TOC) and used it as a tool for developing a global rate model to express reduction of components by SCWO of the used wastes since the development of more rigorous kinetic models was more intricate given the complexity of the feed and the intermediates originating from the reactions involved in SCWO.

For partial oxidation in SCW, and in order to generate effectively H_2 from cellulose or glucose as biomass model compounds, water is used as a suitable solvent and reactant in accordance with equations 2 and 3:

$$C_6H_{10}O_5 + 7H_2O \rightarrow 12H_2 + 6CO_2 \quad (2)$$

$$C_6H_{12}O_6 + 6H_2O \rightarrow 12H_2 + 6CO_2 \quad (3)$$

According to Cortright et al. [12], the H_2 selectivity is evaluated to know how many hydrogen atoms in an organic compound can be taken out as H_2 by the following (Equation 4):

H_2 selectivity, mol % =

$$\{(H_2 \text{ produced, mol})/(\text{C atom in the gas phase})\} \text{ X } \{1/2\} \text{ X } 100 \quad (4)$$

The aforementioned authors considered H_2/CO_2 reforming ratio as ½. For glucose which is represented as $C_6H_{12}O_6$, the maximum hydrogen is 12 moles of H_2 with 6 moles of CO_2.In other words, 6 moles of H_2 produced from glucose reforming and the 6 moles of CO produced from glucose reacts with moles of H_2O to produce another 6 moles of H_2 through the water-gas shift reaction. The above equations suggest that by employing partial oxidation followed by the water-gas shift reaction could enhance the H_2 production rate. The general equation of this theme could be approximated by the following general reactions:

Gasification:

$$C_mH_{n\ \{Catalyst\}} \rightarrow CO_2 + H_2 + CH_4 + \text{Intermediate products} \quad (5)$$

Partial oxidation:

$$[C_mH_n]_{\{\ \%O2<1\}} + \text{Intermediate products} \rightarrow CO + H_2 + \text{other components} \quad (6)$$

Water-gas shift reaction:

$$CO + H_2O \rightarrow \text{active hydrogenating species} \rightarrow CO_2 + H_2 \quad (7)$$

The water-gas shift reaction represented by equation (7) is of the utmost importance for hydrogen production from waste biomass. However, Watanabe et al.[13] reported that at pressure below 30 MPa, the pressure-dependence of kinetics is insignificant. Thus, the acceleration of the water-gas shift reaction by increasing the temperature or employing the appropriate catalyst is possible. Rice et al. [14] who evaluated the water-gas shift reaction in SCW in the absence of a catalyst, reported that the increase in the reaction temperature coupled with an increase in pressure up to 60 MPa resulted in a significant acceleration of the conversion rates, although the observed water-gas shift reaction conversion rates in SCW were much lower than those of catalytic industrial processes.

2.2.4. *SCW product distribution*

Identifying the SCW intermediate products could help understand the reaction mechanisms and eventually foster the development of kinetic models that are required for reactor design. Thus, several studies regarding the analysis of intermediate products from the SCW process have been reported in the literature [10, 15-20]. However, most of these studies have focused on the identification of the intermediate products from model compounds such as glucose, cellulose, and starch with fewer data reported for real waste biomass feed stocks such as municipal wastewater sludge and hog manure.

Pyrolysis products

Tester's group at MIT reported the SCW liquid effluent characteristics above the water critical temperature from glucose hydrolysis (pyrolysis) and oxidation in a continuous flow reactor at a pressure of 246 bar and temperature range of 425 to 600°C [19]. Since the identification and analysis of all liquid-phase products was challenging, the aforementioned authors employed literature results for glucose hydrolysis below and near critical water to obtain a list of 40 suspected products [21-24]. In order to clearly identify each peak from HPLC analysis, two different wavelengths of 210 and 290 nm were used to discrimination between functional groups, and allowed identification of additional species that were not detectable using a single wavelength. The authors reported that the number of products in the oxidation experiments were substantially reduced compared to the hydrolysis experiments products, although many peaks formed during glucose hydrolysis were unidentified. This conclusion was supported by a good carbon balance closure obtained for the oxidation experiments of glucose.

Sasaki et al. [16] studied cellulose hydrolysis in sub and supercritical water in a continuous flow reactor at a temperature range of 290 to 400 °C and pressure of 25 MPa. The aforementioned

authors employed a H-NMR and FAB-MS for the liquid-phase product analysis identification and HPLC for the quantitative analysis of the identified compounds. At temperatures of 320°, 350°, and 400°C, the main components at 100% conversion of cellulose liquid-phase were erythrose, dihydroxyacetone, fructose, glucose, glyceraldehydes, pyruvaldehyde, and oligomers such as cellobiose, cellotriose, cellotetraose, cellopentaose, and cellohexaose. Comparing the results obtained in this study with previous ones for glucose decomposition in sub and supercritical water Sasaki et al. [25], pointed out that glucose had a faster conversion rate than cellulose even with the formed glucose as a hydrolysis product from cellulose. Furthermore, the authors reported that around and above the water critical point, the hydrolysis products yield was higher than those of sub-critical water. Figure 2.3 portrays the suggested reaction pathways of cellulose decomposition in SCW.

Oxidation products

Onwudili and Williams [18] investigated the decomposition of cellulose, starch, and glucose as a biomass model compounds, and real biomass in the form of Cassava waste in subcritical and supercritical water. The experiments were conducted in a batch reactor at a temperature range from 330 to 380°C, a pressure of 25MPa and using hydrogen peroxide (H_2O_2) as a source of oxygen. The liquid-phase products for each model compound were divided into three main areas i.e. water soluble products (WSP), char, and oil. The product oil was analyzed using Fourier transform infrared spectrometry (FT-IR) with the mass of the WSP determined as total dissolved solids (TDS), and the char removed by filtration. For the oil analysis, the authors reported that using the functional group assignment could help identify the various peaks of the spectrogram. Thus, the presence of carboxyl acids was confirmed by the presence of C=O between the wavelengths of 1650 and 1850 cm^{-1} together with the -OH functional groups.

Similarly, the authors confirmed the presence of other functional groups such as ketones and aldehydes, primary, secondary, and tertiary alcohols, alkane and alkene groups. Wahyudiono et al. [26] reported on an experimental study for the behavior of catechol as a model compound representing lignin. Experiments were conducted in a batch reactor at temperatures of 370 to 420°C and pressures of 25 to 40 MPa.

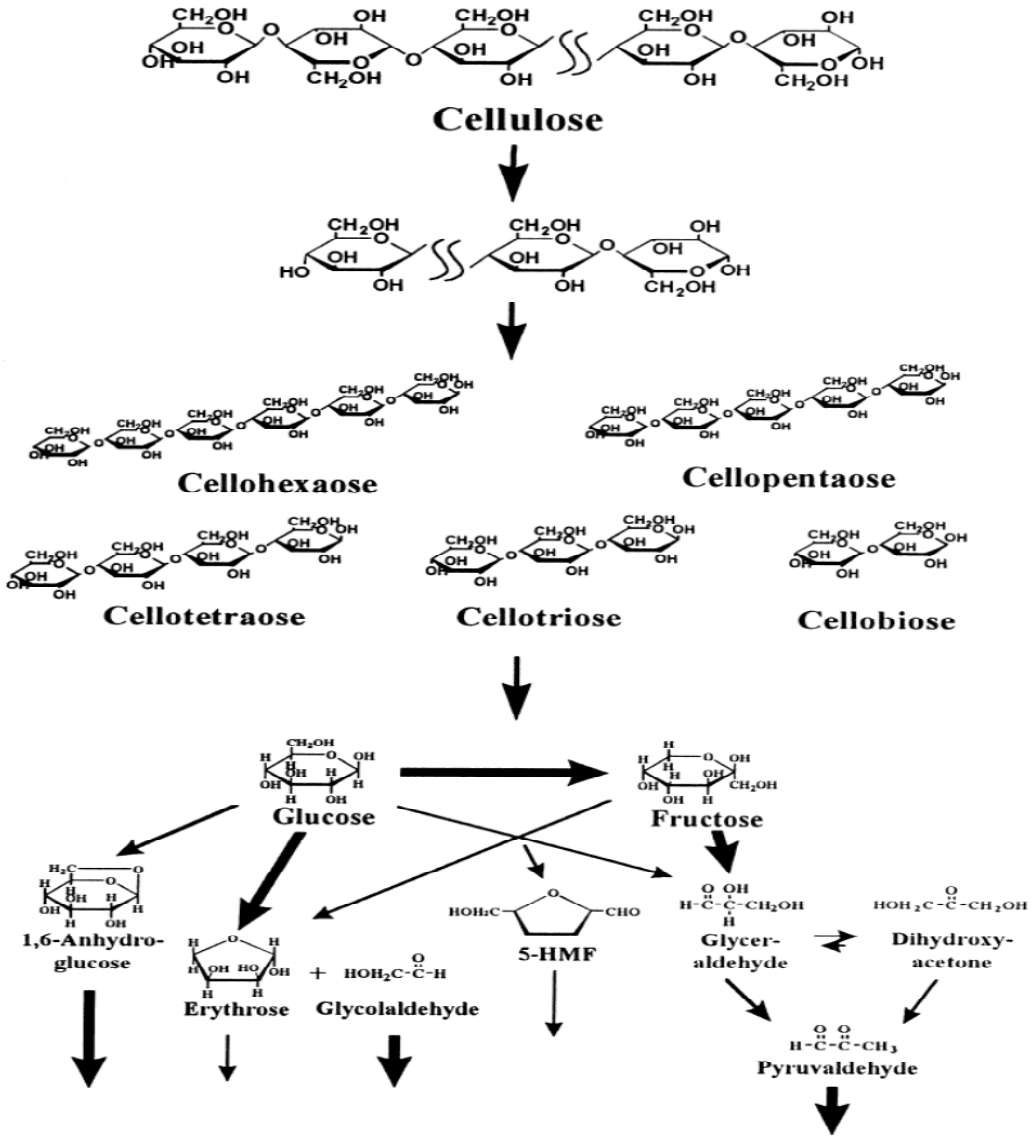

Fig. 2.3 The main reaction pathways of cellulose hydrolysis in SCW [25].

The aforementioned authors reported that the variation of temperature resulted in a variation of higher and lower molecular weight products as identified by GC-MS. Phenol was the major component identified with several other components presented in small amounts as summarized in Table 2.1. The presence of phenol as a major intermediate compound was attributed to the fact that higher temperatures hydrolyzed the dissolved compounds with ether linkages to single ring phenolic compounds as reported by [13, 27].

Gasification products

Onwudili and Williams [28] reported the product distribution and characterization of crude glycerol gasification as a model of waste biomass derived from a bio-diesel production plant. The experiments were conducted in a batch reactor at a temperature range of 300°C to 450°C and pressures between 8.5 MPa and 31 MPa. The liquid-phase analysis was performed by first transferring the entire contents of the reactor to a separating funnel in which the organic fraction was partitioned using a liquid-liquid extraction technique. The extracted oil was then analyzed using GC-FID and GC-MS for qualitative and quantitative analysis. The extracted water soluble products (WSP) were analyzed by evaporating the water content, drying and weighing each sample to determine the mass of the WSP. The distribution of oil products present in the liquid phase was examined by varying the reaction temperature and reaction time. Table 2.1 reports some of the results obtained in this study with methyl oleate, methyl stearate, methyl palmitate, palmitic acid and mleic acid as the major compounds in the liquid phase that exhibit significant resistance to a temperature increase. The degree of decomposition of fatty acids was influenced by the temperature increase with the major products formed at lower temperatures being a waxy material containing glycerol, fatty acids and methyl esters.

Table 2.1 Main intermediate compounds produced during SCW of different model and real waste compounds.

Name of the Feed Compound	Process Description	Main Intermediate Compounds		References
Glucose	Plug flow reactor made of Inconel 625 tubing having 6.36 mm O.D and 1.7 mm I.D with an internal volume of 10.7cm^3.	Acetic acid, Propenoic acid		[19]
		5-Hydroxymethylfurfural		
		Acetaldehyde, Acetonylacetone		
		Formic acid, Lactic acid		
Cellulose, coconut oil solutions, brewery and dairy effluents	A batch reactor made of stainless steel 316 coiled tubing having length of 76.2 cm, O.D of 1.27cm, and 0.21 cm wall thickness. A continuous flow reactor made of stainless steel 316 tubing length of 400 cm, O.D of 0.318cm,and ID of 0.14 cm.	Acetic acid	Major component	[15]
		Formic acid	Major component	
		Lactic acid	Minor component	
		Glycolic	Minor component	
crude glycerol	Hastelloy-C batch reactor having 75ml capacity , design pressure of 40MPa, and temperature of 600°C	Compound	Concentration (μg/goil)	[28]
		Methyl oleate	108,000	
		Methyl stearate	32,800	
		Oleic acid	68,300	
		Palmitic acid	67,500	
		Methyl palmitate	63,700	
		Dimethyl phenol	26,400	
		1-Nonene	39,600	
		Xylene	44,600	
		1-Octene	46,900	
Glucose	subcritical experiments (stainless steel (SUS 316) reactor with ID of 0.118 cm); supercritical experiments (stainless steel (SUS 316) reactor with ID of 0.077 cm)	saccharinic acids		[17]
		fructose		
		glyceraldehyde		
		erythrose, pyruvaldehyde		
		1,6-anhydroglucose		
		dihydroxyacetone 12.6		

Table 2.1 Cont'd

Name of the Feed Compound	Process Description	Main Intermediate Compounds	References
Catechol	A hastelloy C-276 tube reactor having internal volume of 5 cm^3	Phenol	[11]
		cyclopentanone	
		2-cyclopentenone	
		1,2-benzenedicarboxylic acid	
		nonylphenol	
		1,4-dipropylbenzene	
		acetophenone	
		2,6-di-tert-butylnaphthalene	
		4-butoxyphenol	
		o-ethoxyphenol	
		2-methylterephthalaldehyde	
		p-diethoxybenzene	
		5-methoxy-2,3,4-trimethylphenol	
Cellulose	An Inconel 600 tube reactor having a length of 35.56 cm, OD of 0.635 cm, ID of 0.279 cm, and a volume of 2.18 mL	Cellobiose	[59]

2.3 SCW Process Design Considerations

2.3.1 *SCW reactors (concepts and facts)*

The discovery of the advantages of the SCWO process generated widespread optimism in anticipation of a large number of possible applications. The underestimation of the main SCW problems including reaction hot spots and corrosion hindered the process from realizing widespread industrial application. To date, a considerable number of SCWO reactor concepts and process designs have been described in the literature. These reactors are either for laboratory use i.e. small scale applications or pilot-scale applications [29]. The types of these reactors can be classified into five main categories as follows:

- Batch reactors
- Tubular reactors
- Transpiring wall reactors
- Flame reactors
- Other types such as quartz reactors.

For the batch reactors, they vary considerably in size from small bomb reactors of volume 2 to 9 cm^3 to as large as 1000 cm^3. The advantage of the batch reactor system is that the structure is simple, no high-pressure pump transport system is necessary, and they can be used for almost all biomass and waste biomass feedstock gasification [29]. However, there is a finite time required for heat-up and cool-down of the reactor system including the feedstock and reaction products. For biomass gasification in supercritical water, there are a significant amount of reactions occurring during the heat-up stages of the experiments in the batch reactor. Feedstock transformation appears to become significant before reaching 250°C although little gas formation occurs at these lower temperatures.

For the case of tubular reactors [1, 6, 29] primarily simple tubular reactors consisting of preheat, reaction, and cool-down sections are employed. Although these reactors are prone to corrosion and plugging problems, they are easily accessible, cheap and practical for lab scale taking into account the tremendous cost of other types of reactors because of the special requirements for the demanding SCW process i.e. high pressure and temperature. Because of the nature of the SCW environment, not only high pressures (mechanical load) and high temperatures (thermal load) are observed, but also the very corrosive aqueous environment of the input reactor materials must be considered. In addition to reactor plugging, the corrosion of the SCW reactor and related components is the other main technical problem pertaining to SCW systems [30, 31]. As previously mentioned, heteroatoms are converted to the corresponding acids and the reactive ions lead to corrosion. It must be stressed that chloride is the most important corrosive species in SCWO processes. Furthermore, the pH of the solutions is frequently very low after oxidation. Therefore, the reactor design also needs to account for material fatigue resulting from temperature cycles, loads exerted by thermal shock, and the weakening of material through corrosion.

2.3.2 *Corrosion in SCW*

The supercritical water process operates at a high temperature of 400 to 800°C and high pressure of 24 to 40 MPa. Thus, the SCW process must be able to sustain the resulting mechanical and thermal load, and high corrosion environment. Several studies pertaining to corrosion in SCW have been reported in the literature. Kritzer et al. [2, 32] investigated the corrosion behavior of several Ni based alloys and stainless steels in oxygen and chloride containing aqueous solutions. All materials exhibited a similar corrosion pattern of slight intergranular corrosion below approximately 150°C; pitting between approximately 150 and

300°C; shallow pitting and penetration of the whole surface at near critical temperatures. The aforementioned authors classified the types of corrosion that occur in the SCW into four types as follows:

- Pitting corrosion

Pitting corrosion is defined as a localized form of corrosion that occurs in the passive state of the metal. This type of corrosion is caused mainly by penetration and local destruction of some aggressive anions to the previously formed metal oxide film as a result of initial oxidation. The pits started small and increase as the oxidation and dissolution of metal components and their following reaction with water proceeds. This eventually leads to a strong acidification environment inside the pit [3]. Thus, the corrosion becomes more aggressive especially after the oxide film weakens as the temperature increases.

- General corrosion

Taking advantage of the weakness of the metal oxide film, general corrosion attacks the entire surface although its morphology is typically shallow, typical in high temperature oxidation environments. General corrosion usually occurs when the alloy is unable to form a protective layer. Bogaerts and Bettendor [33] reported that some forms of pitting corrosion transformed to general corrosion at temperatures of around 250°C, and this usually occurs with stainless steel alloys.

- Stress corrosion cracking

The stochastic occurrence behavior of stress corrosion cracking makes it the most dangerous form of corrosion as the alloy failure is also stochastic and not predictable. It usually occurs either in the transition ranges between the active compounds such as hydrogen and the passive ones such as oxygen, or the passive and the transpassive potential, respectively. Careful

and professional design of the SCW process is a must because even at low values of stress corrosion cracking can lead to the failure or leakage of the SCW reactor. This can cause fires or even explosions from the presence of hydrogen and high temperatures.

2.3.3 *Materials of construction*

In light of the high corrosion potential from SCW, it is obvious that the materials of construction of the SCW process must be carefully selected. This selection is based on the ability of the alloy to resist corrosion as well as withstanding the mechanical and thermal loads of the process. As reported by Kritzer [2], the corrosion of alkaline solutions is improved by nickel whereas chromium improves the resistance against acidic and oxidizing media and reduces pitting corrosion. Moreover, molybdenum causes the lowest passivating effect compared to other elements leading to high corrosion rates as the conventional high chromium, nickel and iron-based alloys tend to lose their protective layers in highly oxidizing, acidic solutions at moderate to high temperatures [2, 29]. Thus, an alloy that forms a protective layer or oxide film that covers the entire alloy is preferable to other types of alloys. Some elements such as zirconium, titanium, and yttrium form stable oxides in high temperature oxidizing environments. As suggested by Kritzer [2], this could be a potential for future research on some alloys based on the previously mentioned elements.

Mitton et al. [34] investigated the behavior of different alloys by exposing these alloys to a highly chlorinated oxygenated organic feed stream at temperature of 600°C for different times to a maximum of 65 hours. The aforementioned authors reported that the G-30 alloy exhibited the best corrosion resistance whereas the Ni-based alloys C-22, C-276, 625 showed comparable corrosion rates, with 316-L stainless steel corroding rate of 10 times faster than G-30. In

conclusion, although there is still no optimum alloy for use in the SCW process, inconel 625 and Hastelloy C-276 have been recommended in the literature as the most corrosion resistant alloys available so far [1].

2.4 Applications of SCW for Hydrogen Production

Considerable attention has been focused on the development of alternative energy sources since the energy crisis in the 1970's, and the realization that the world's energy demand is increasing exponentially [35]. Also, the reserve of fossil fuels has been dwindling, not to mention the negative effects of the fossil fuels on the environment because of the carbon dioxide (CO_2) emission. Hydrogen (H_2) has been gaining more attention as a promising alternative energy form. It is considered as an alternative fuel and its use is gaining more acceptance as the environmental impacts of hydrocarbon fuels become more evident [36]. Hydrogen is the lightest element, and it is the most abundant element in the universe although it is found in the free state in only trace amounts. Hydrogen has a high energy yield of 122 MJ/kg, which is 2.75 times greater than an average hydrocarbon fuel. Hydrogen is the cleanest fuel since its combustion produces only water. Nevertheless, hydrogen's viability as a clean fuel is greatly enhanced if it is produced from renewable sources. On the other hand, and in the past two decades, wastewater treatment has gained significant interest due to water shortages [37]. As a result of expanded wastewater treatment, the amount of sewage sludge has also increased in accordance with this development. Compost produced from sewage sludge is a small percent of the total amount produced. Consequently, the valuable energy contained in organic sludge is lost without utilization in the energy cycle since the main use of the obtained product of composting is agricultural use - fertilization of soils, planting of trees and shrubs [38]. Sewage sludge has a

potential to produce hydrogen-rich gaseous fuel. Thus, hydrogen production from sewage sludge may be a solution for cleaner fuel as well as sewage sludge disposal problems.

Sewage sludge typically consists of 41% protein by weight, 25% lipid, 14% carbohydrate, and the rest is ash and biodegradable and recalcitrant organic compounds, as well as pathogens and heavy metals [11]. It is considered as a waste biomass that has a chemical energy content of 9-29 MJ per kg of total suspended solids that can be potentially recovered by various biological or thermochemical processes [39]. Sludge has a very high water content of greater than 90% on a wet mass basis, which makes it more suitable for a supercritical water oxidation process than other conventional thermochemical treatment processes. The latter requires high energy input for drying the sludge to make them suitable for processes such as combustion and pyrolysis [35]. Therefore, supercritical water gasification (SCWG), which primarily involves catalytic conversion in water without oxidation, eliminates the need for drying processes since water participates in the steam reforming and water-gas shift reactions during the SCWG process. In addition, the organic compounds in sewage sludge are mainly soluble in the SCW which makes it easier to gasify them into useful gases such as hydrogen and methane [29, 40-42]. Due to the complexity of SCW, previous research activities have focused primarily on compounds that model sewage sludge. Employing SCW to produce green energy from waste streams such as sewage sludge has many advantages. Indeed, using SCW as a reaction medium avoids the expensive step of drying. In fact, estimated feedstocks of 30% or higher moisture content are preferable and more economical in SCW [43]. Antal et al. [44-46] research group at the University of Hawaii was the first to publish an extensive work on catalyzed hydrogen production from biomass and sewage sludge. The aforementioned authors realized and pointed out the advantages of SCW compared to conventional methods such as pyrolysis. This is due to

SCW supporting ionic chemistry, which could be much more selective and more controllable than the free-radical chemistry that occurs in pyrolysis.

2.5 Catalytic SCW gasification

The high temperatures required for some particularly recalcitrant compounds, such as ammonia beside the formation of undesired products in the un-catalyzed SCWO free-radical reactions, has increased the interest in employing catalysts in order to increase the selectivity to complete oxidation products as well as to decrease the temperature required [43, 47]. Homogeneous and heterogeneous catalysts have been systematically examined in SCW for several years. Table 2.2 reports a brief review of the investigated catalysts reported in the literature.

It is clear that catalysts enhance the efficiency of SCW i.e. provide substantially higher conversions and higher selectivities to H_2, CH_4 and lower reaction temperatures, and selectivity toward CO [44-46]. Catalysts also increase the economic viability of the biomass gasification process [43]. For supercritical water, the catalyst selection is extremely important. The need to produce a tar-free product gas from the gasification of biomass, the removal of tars, and the reduction of methane has been the main focus of several literature studies. Dunn et al. [48] examined the effects of reaction time, water density, and the concentrations of catalyst, p-xylene, and oxidant on terephthalic acid synthesis in SCW at 380°C using simple tubing-bomb mini batch reactors. Several catalysts were identified for complete oxidation in supercritical water. These include heteropolyacids, alkali carbonates, and carbons.

Table 2.2 SCW literature reported catalysts.

Compound	Catalysts	Main product gas	Refernces
Ammonia	MnO_2	N/A	[74, 81]
Benzene	V_2O_5, Cr_2O_3, MnO_2	N/A	[47]
MEK	Pt/TiO_2	N/A	[50]
Acetic Acid	CuO/ZnO, TiO_2, MnO_2	N/A	[50]
Alcohols	CuO/ZnO	N/A	[52]
Pyridine	Pt/TiO_2	N/A	[50]
Quinoline	$ZnCl_2$	N/A	[83]
Glucose	Ni/AC	Hydrogen	[77]
Glucose & Glycerol	Ru/TiO_2	Hydrogen & Methane	[64]
Glucose	ZrO_2	Methane	[41]
Glucose	KOH and Na_2CO_3	Hydrogen & Methane	[29]
Glucose & Glycerol	Ru/Al_2O_3	Hydrogen	[59, 69]
Catechol & Vanillin	KOH & K_2CO_3	Hydrogen	[60]
Catechol	KOH	Hydrogen	[63]
Cellulose, Xylan, and Lignin mixture	Engelhard 5132P nickel catalyst	Hydrogen & Methane	[5]
Lignin	NaOH and ZrO_2	Hydrogen	[13]
Cellulose	K_2CO_3 and $Ca(OH)_2$	Hydrogen & Methane	[67]

Table 2.2 Cont'd

Cellulose	Ru/C, Pd/C, CeO_2 particles, nano-CeO_2 and nano-(CeZr)*x* O_2	Hydrogen	[68]
Phenol and glycerol	Nickel wire	Hydrogen	[61]
Phenol	Activated carbon (AC)	N/A	[62]
Cellulose	Reduced nickel (Ni)	Hydrogen	[65]
Glucose	Ni, K_2CO_3	Hydrogen	[89]
Cellulose, softwood, and grass lignin	Ni	Hydrogen	[17]
Organic wastewater	Ni/carbon	Hydrogen & Methane	[41]
Glycerol, glucose, celloboise, bagasse, and sewage sludge	Charcoal activated carbon	Hydrogen	[45]
Organosolv-lignin	ZrO_2	Hydrogen	[41]
Vanilin, glycine, straw, sewage, sludge, lignin, pyrocatechol	K_2CO_3 & KOH	Hydrogen	[42]
glycine and glycerol	Na_2CO_3	Hydrogen & Methane	[33]
Pyridine	Pt/*ç*-Al_2O_3, MnO_2/*γ*-Al_2O_3, and MnO_2/CeO_2	N/A	[74]
N/A	Cr_2O_3	N/A	[73]

However, the criteria for the catalyst are fundamentally the same and may be summarized as follows:

- The catalysts must be effective in the removal of tars.
- The catalysts should be resistant to deactivation as a result of carbon fouling and sintering.
- The catalysts should be easily regenerated, strong, and inexpensive.
- Higher hydrogen yield is a highly desirable criterion in the case of hydrogen production using SCW.

Therefore, the SCW catalytic process is an optimized combination of catalyst (components, manufacturing process, and morphology), reactants, reaction environment, process parameters such as temperature, pressure, and residence time, and reactor configuration. Ding et al. [49] reported an extensive review of supercritical water catalysts and kinetics. The aforementioned authors evaluated several catalysts employed for SCWO of selected model compounds, highlighted the concern of the catalyst stability, activity and mechanical structure within the SCW environment. In their conclusions, the aforementioned authors reported that catalysts improve the oxidation rates of both organic compounds and refractory intermediates, however, the authors pointed out that the harsh SCW environment and variability of sludge characteristics poses a technical challenge for SCWO process development.

Several researchers demonstrated various catalytic SCWO studies aiming to investigate the effect of SCW on the catalyst surface, activity, stability and selectivity. As an example, deactivation of Pt/ZrO_2 and Pt/TiO_2 occurred in a short time [50], partially due to the crystalline growth of platinum particles. Baker et al. [51] and Elliott et al. [36] reported the softening and swelling of Ni/Al_2O_3 catalyst in SCW due to a low physical strength of the catalyst. Foussard et

al. [52] found that lattice oxygen may come from vanadium oxide or from oxides of Mn, Fe, and Ni. Thus, oxygen may participate in the SCW reactions as it is adsorbed on the catalyst surface in the case of SCWO, and as part of the lattice oxygen present in the metal oxides. Tiltscher and Hofmann [53] and Wu et al. [54] reported that the mechanism involved in catalytic SCWO may be interpreted similarly to those describing gas-phase or liquid-phase oxidation. However, special factors such as high concentrations of water and large differences in physicochemical properties between ambient water and SCW can influence the catalytic oxidation pathways, the product distributions, and the catalyst stability.

An extensive review of the catalysts reported in the literature for SCW revealed that most of the catalysts were employed in wet air oxidation processes (WAO). It should be pointed out that for a typical WAO process, the operating pressures range from 20 to 200 bar and temperatures range from 200 to 330°C, respectively. The deactivation of a catalyst is mainly caused by coking, poisoning, and the solid state transformations of catalysts in the gas-phase oxidation case [49, 50, 55- 57].

2.6 Gasification of Model Compounds in SCW

a) Glucose

Sewage sludge typically consists of 41% protein, 25% lipid, 14% carbohydrate, with the rest ash, biodegradable and recalcitrant organic compounds [11]. A better understanding of sewage sludges behavior in SCW requires both extensive experimental and theoretical studies. This has motivated several research groups to study model compounds for both biomass and sewage sludge. As an example, glucose gasification in SCW can be considered as a good model for gasification of more complex cellulosic sludges in SCW. Glucose is a refractory intermediate

formed during the gasification of biomass for the SCWG process. Amin et al. [58] obtained hydrogen-rich gas from the catalytic gasification of glucose in water at 374 °C and 22.1 MPa, mainly through the water-gas shift reaction with a low efficiency (20%) of carbon gasification. This means that as much as 20% of the feed carbon was detected in the gaseous decomposition products, demonstrating the need for higher temperature and active catalysts to improve the gasification efficiency.

As mentioned before, Yu and co-workers [44] were the first to investigate hydrogen production from biomass and waste streams using SCW. The aforementioned authors gasified different glucose concentrations in SCW and reported that 0.1 M glucose was completely converted to hydrogen-rich synthesis gas whereas higher glucose concentrations were not completely gasified at 600 °C, 34.5 MPa, and 34 s reactor residence time. This could be attributed to the reduction in the amount of water present since the reaction was taking place in a SCW medium. The gas yield and composition was found to depend on the condition of the reactor wall and the reactant concentration. The observed results motivated the same group in a subsequent study to employ activated carbon as a catalyst to improve glucose gasification efficiency in SCW [45]. Carbon is interesting because it is very stable in SCW, especially when hydrogen gas is present. At a glucose concentration of 0.1M, the authors reported that the gasification efficiency reached 98% at 600°C and 34 MPa, and decreased sharply to 51% at 500°C while maintaining the same pressure.

Byrd et al. [59] gasified glucose in SCW in the presence of Ru/Al_2O_3 catalyst. Although the aforementioned authors reported yields as high as 12 mol H_2/mol glucose, they employed relatively high temperatures of 700 and 800°C. Thus, for enhancing H_2 yield and selectivity from glucose, the desired catalytic property and the optimum conditions must be determined.

Anderko et al. [8] reported that nickel catalysts are expected to crack tar and promote the water-gas shift reaction, methanation, and hydrogenation reactions. From economic and energy efficiency points of view, high gasification efficiency at low temperature with more hydrogen production is favorable.

Elliott et al. [36] from the Pacific Northwest Laboratory (PNL) conducted crucial studies on the reaction chemistry in a high pressure aqueous environment. They used nickel and ruthenium catalysts for organic waste gasification in sub and supercritical water in a batch reactor for 2 hr running time, at 350°C and 20 MPa. The authors showed that aromatic and aliphatic hydrocarbons can be transformed into hydrogen and methane rich gases using hydrogenation catalysts. The authors also confirmed these results in a continuous reactor with a residence time of less than 10 seconds. In order to enhance the H_2 production yield, metallic catalysts should be examined. Nickel by virtue of its high melting point of 1453°C, its ready availability and low cost is a suitable and reasonable choice for SCWG and SCWO. Generally, glucose, as a model constituent of waste biomass was used in SCW gasification studies. Table 2.3 summarizes some of the literature reported results for SCW gasification and oxidation of glucose in SCW.

Several observations can be made from Table 2.3. First, the effect of catalysts on the production of hydrogen gas was clearly pronounced. These results point to the importance of identifying effective catalysts for the production of a hydrogen rich synthesis gas from waste biomass. Precious metals and activated carbon appear to have a strong influence on the hydrogen production yield even where glucose concentration in the feed was 17wt%. Second, the operating pressure has no influence on the hydrogen yield whereas the increase of residence time led to only slight increases in the hydrogen yield and the gasification of the glucose.

Table 2.3 Some literature reported results for SCW gasification and oxidation of glucose in SCW

Feed	Reactor type & material; Operating parameters & Catalyst	Gas yield (mol/mol)							Observations	References
Glucose	Continuous flow system (Hastelloy C-276 tubing reactor having 9.53 mm o.d., 6.22 mm i.d., and 670 mm functional length. T= 575- 725°C, P= 28MPa, LHSV=6-24hr^{-1}, 16 wt % Ni/AC and AC, Conc 0.3, 0.6, and 0.9 M.	Catalyst	Ni/AC			AC			1-The 16 %wt Ni/AC catalyst gave almost complete gasification efficiency. 2-The H_2 yield increased with increasing temperature from 575 to 725°C. 3-The hydrogen yield obtained with the 16% wt Ni/AC was about 2 times higher than that with the AC only or without catalysts.	[76]
		Conc (M)	0.3	0.6	0.9	0.3	0.6	0.9		
		H_2	1.69	0.88	0.69	2.82	2.45	2		
		CO	0.86	1.2	1.26	0.19	0.29	0.42		
		CO_2	2.4	1.94	1.39	3.48	3.24	2.57		
		CH_4	0.99	0.67	0.51	1.17	1.11	0.96		
Glucose	Continuous flow system (Hastelloy C-276 tubing reactor having 9.53 mm o.d., 6.22 mm i.d., and 670 mm functional length. T= 480- 750°C, P= 28MPa, τ (residence time) = 10-50s, No catalyst, Conc 0.6M.	Temp(C)	480	600	600	750			1-The hydrogen yield increased sharply by increasing temperature over 660°C. 2- Pseudo-first order kinetics were obtained for glucose and COD degradations by assuming a plug-flow and it is discussed in the appended paragraph.	
		Flow rate (g/h)	240	120	360	240				
		τ(s)	35	50	16	19				
		H_2	0.08	2.63	0.52	4.78				
		CO	0.47	0.59	1.3	0.27				
		CO_2	0.4	1.72	0.32	3.52				
		CH_4	0.03	0.71	0.21	1.26				
		Liquid effluent characterization								
		Glucose	82.1	99.9	91.5	100				
		COD	38.6	86.7	62.7	99.8				
Glucose	Batch SS 316 stainless steel tube bomb T= 400-440°C, P= 30-35MPa, τ (residence time)= 10-15 min, ZrO_2 and NaOH catalysts, Conc 0.5 M.	T =400 C, τ = 15 min		No Catalyst	ZrO_2	NaOH			1-The gasification efficiency with NaOH was the highest. 2- Carbon balance not reported because of lack of analysis for liquid compounds.	[27]
		yield (mol %)		2	5	21				
		T =440 C, τ = 10 min		2	5	25				

Third, the oxidant molar ratio (MR) plays an important role in increasing the hydrogen yield. Although none of the above studies reported the optimum MR, it is clearly understood that the hydrogen yield increases with increasing MR to an optimum point expected to be less than unity, beyond which the hydrogen yield starts to decrease. Fourth, the effect of temperature on the hydrogen yield is clearly reported. As the temperature increases, the hydrogen yield increases, mainly because it promotes the water-gas shift reaction in which carbon monoxide reacts with steam to produce hydrogen and carbon dioxide. Furthermore, the increase of temperature increases the degradation of the intermediate compounds which leads to an increase in the gas yield.

b) Proteins

Several reported studies in the literature have dealt with the gasification of lipids, protein, carbohydrates, and lignin as waste biomass model compounds. Thus, the following section pertains to some of these reported studies. Since cellulose and hemicellulose are carbohydrates and lignin includes aromatic rings, several studies have been reported in the literature with model compounds for these categories.

Schmieder et al. [60] studied glucose as the carbohydrate model compound, catechol and vanillin as a lignin model compounds, and glycine as a protein model compound. The experiments were conducted in two batch reactors and a continuous flow reactor. The first batch reactor was an autoclave, designed for a temperature of 700°C and pressure of 1000 bar with a volume of 100 ml, whereas the second batch autoclave was designed for 500°C and P of 500 bar made from Inconel 625 with volume of 1000 ml. The tubular flow reactor was an Inconel 625 with an inner diameter of 8 mm, and a length of 15m. The aforementioned authors employed alkaline KOH as a homogenous catalyst. The main gaseous products were CO_2, CO, H_2, and

CH_4. For catechol, at an operating temperature of 600°C, residence time of 30 seconds, pressure of 200-300 bars, and feed concentration of 0.2 M, as much as 10.5 mol H_2 per mole of feed was formed corresponding to 82% of the theoretical hydrogen formation. This was achieved considering only CO_2 and H_2 as products i.e. only trace amounts of CO and CH_4 were observed. As a protein model compound, vanillin gasification was easier than catechol. In fact, more than 99% destruction efficiency was reported even without added KOH, which can be attributed to the low feed concentration and the higher reaction time. The authors did not report the H_2 yield; however, they employed thermodynamic calculations to improve the understanding of the reaction pathways occurring during gasification and to compare the experimental results with the theoretical predicted ones. Results of the comparison showed that the temperature and pressure trends found experimentally were confirmed theoretically. However, the CH_4 yield predicted was higher than the experimental yield.

c) Lignin

Lignin is one of the three main components of plant biomass, beside cellulose and hemicellulose and poses the most gasification resistant compound [61] due to the abundance of aromatic rings in the lignin structure. Nunouraa et al. [62] reported on the catalytic effect of activated carbon (AC) on the SCWO of phenol. By applying AC as a heterogeneous catalyst, the decomposition rate of phenol was enhanced, and the yield of carbon dioxide increased largely as well as the yield of dimeric compounds, while tarry materials decreased remarkably with the addition of AC.

Kruse et al. [63] studied the gasification of catechol as lignin model compound in SCW for H_2 production. The authors employed a batch autoclave, made from Inconel 625 designed for 500°C and pressure of 500 bar with a volume of 1000 ml, tubular flow reactor (Inconel 625, I.D

8 mm and O.D 15.4mm, length 500mm) and KOH and LiOH as catalysts for their experimental investigation. The effect of two feed concentrations of 0.6 mol/L and 1.2 mol/L, temperatures of 600-700°C as well as pressure range from 200 to 400 bars on the gas product distribution were experimentally studied and discussed. Furthermore, the authors concluded that the increase in temperature from 600 to 700 °C did not influence the catechol gasification since more than 99% of catechol was gasified at 600°C. However, the addition of KOH as catalyst increased the relative yields of H_2 and CO_2 and decreased the relative CO yield. For example, increasing the KOH amount from 0 to 5wt% enhanced the H_2 yield by 40 vol % at a temperature of 500 °C, pressure of 250 bar, and 1 h reaction time. However, the CO yield decreased from 40 vol % at 0 wt% of KOH to 0.7 vol% with 5wt% KOH amount. This was attributed to formation of formates by the addition of alkali salts and LiOH, which subsequently degraded to H_2 and CO_2.

Yoshida et al. [5] studied cellulose, xylan, and lignin mixtures gasification in SCW. They conducted their experiments in a batch reactor made from SS 316 with an O.D of 9.53 mm and an I.D of 6.53 mm with commercial Engelhard 5132P nickel as a catalyst at a temperature of 400°C and pressure of 25 MPa. At a cellulose:xylan:lignin mixture of 1:1:4 on gas formation, the experimental results confirmed the pronounced negative influence of lignin relative to other two compounds, i.e. cellulose and xylan. This was observed by a decrease of 31% in the H_2 yield to a 1.7 mol per gram of reactant. However, the use of equal amounts of cellulose: xylan: lignin mixture of 1:1:1 increased the H_2 yield by 50% to about 2.5 mol per gram reactant. The highest amount of gas of 17 mol of H_2, CO_2, CH_4, and C_2H_6 per gram of reactant was observed in the case at cellulose: xylan: lignin mixture of 4:1:1.

Savage et al. [64] reported a study of non-catalytic gasification of lignin in SCW. The experiments were conducted in a mini batch quartz capillary tube with dimensions of 2mm I.D,

6mm O.D, 18.4 cm length and a volume of 0.58 ml. The operating conditions were residence times from 2.5 to 75 min, a temperature range of 365-725°C, and a pressure of 31 MPa with three feed concentrations of 5.0, 9.0, and 33 wt %. The aforementioned authors compared their results with cellulose gasification in terms of the product gas yield. As a catalyst, a nickel wire was inserted inside the reactor prior to each experiment. In the absence of catalysts, CH_4 and CO_2 were always the major products from SCWG of lignin. However, cellulose formed 1.8 mmol/g of H_2 after 10 min whereas lignin only formed 0.7 mmol/g. The authors also reported that higher temperatures increased the rate of formation of H_2, CO_2, and CH_4 and the rate of consumption of CO, and the biomass loading was an important parameter to control the CH_4/H_2 ratio for SCWG of both lignin and cellulose.

Watanabe et al. [13] reported on the gasification of lignin in the presence of NaOH as a homogenous catalyst and ZrO_2 as a heterogeneous catalyst. A batch 316-SUS stainless steel tube bomb reactor with volume of 6 cm^3 was employed in all experiments. A temperature of 400°C, pressure of 40MPa, feed concentration of 0.5 M, and a residence time range of 15-60 min were used as operating conditions. The authors reported that without catalyst, the yield of H_2 and CO_2 slightly increased with increasing reaction time which indicated that the water gas shift reaction proceeded gradually even without catalyst. However, in the presence of ZrO_2 as catalyst, the yield of H_2 and CO_2 increased with increasing reaction time and the H_2 yield of 4 mole % twice that without catalyst was observed. On the other hand, adding NaOH significantly enhanced the formation of H_2 and CO_2 whereas the CO yield with NaOH was remarkably low at all reaction times, which confirms that the addition of alkali promoted the water gas shift reaction. The aforementioned authors pointed out that the use of base catalysts (ZrO_2 and NaOH) coupled with oxygen to carbon ratio O/C of 1.0 enhanced the decomposition rates of aldehydes and ketones,

which are assumed to be intermediates of lignin decomposition, and eventually increased the H_2 yield.

d) Cellulose

Generally, waste biomass such as sludges is known to have a high fiber content, most of which is cellulose. Thus, cellulose can be considered as a model compound for biomass as well as sludges. Minowa et al. [65] investigated cellulose gasification in near-critical water at 350 °C and 16.5 MPa with a reduced nickel catalyst and reported that 70% of the carbon could be gasified. Osada et al. [66] reported the formation of a high amount of methane in the presence of ruthenium catalyst during the gasification of cellulose and lignin in SCW. Guan et al. [67] investigated the H_2 production from cellulose as a biomass model compound. The aforementioned authors conducted their experiments in a batch autoclave reactor made of 316 SS with a capacity of 140 mL designed to withstand the reaction temperature of 650°C, and pressure of 35MPa. The operating conditions at which experiments were performed were a 20 min residence time, temperature of 450 and 500°C and pressure of 24–26 MPa with K_2CO_3 and $Ca(OH)_2$ selected as the catalysts. The H_2 and CH_4 yields increased by 70% and 40% as the temperature was raised from 500 to 550°C and the pressure was kept at 26 MPa, 14.3 mol/kg H_2 and 4.1 mol/kg CH_4. As temperature increases, CH_4 tends to react with water to form H_2 and CO_2 and the net production of CH_4 decreases. However, the amount of CO decreased dramatically by increasing the amount of K_2CO_3 whereas those of H_2, CH_4 and CO_2 increased at the same time. This is because K_2CO_3 enhanced the water-gas shift reaction which results in higher production of both H_2 and CO_2. A comparison between the catalysts amounts showed that when no catalyst was added, the H_2 yield was 4.4 mol/kg cellulose, but increased to 9.4 mol/kg cellulose and 8.3 mol/kg cellulose with 0.2 g K_2CO_3 and1.6 g $Ca(OH)_2$. However, when K_2CO_3

and $Ca(OH)_2$ were present simultaneously, the H_2 yield was 11.958 mol/kg cellulose which is 2.5 times that without catalyst, and 25% and 45% more than that when K_2CO_3 or $Ca(OH)_2$ was present alone.

In another cellulose study conducted by Hao et al. [68] using a batch autoclave reactor made of 316 SS with a capacity of 140 mL designed to withstand a reaction temperature of 650°C, and pressure of 35MPa. The operating conditions at which experiments were performed were a 20 min residence time, temperature of 450 and 500°C and pressure of 24–26 MPa. The authors selected Ru/C, Pd/C, CeO_2 particles, nano-CeO_2 and nano-$(CeZr)_x O_2$ as a different set of catalysts. The authors compared the partial oxidation technique with gasification in terms of H_2 production. The H_2 yield in gasification experiments was 4.4 mmol per gram of reactant which corresponds to 40 % higher than the partial oxidation experiments. However, a CO yield of 2.8 mmol per gram of reactant in gasification experiments was observed which corresponds to 25% of the CO yield produced during partial oxidation experiments. This implies that catalytic gasification promotes the water-gas shift reaction which consumes CO and produces H_2. Among all the employed catalysts, Ru/C was the most active catalyst in terms of cellulose gasification which was nearly completely gasified. In general, and from the above literature review, the following conclusions can be drawn:

- For catechol, although homogenous catalysts such as alkali seem to enhance hydrogen yield, corrosion is a major drawback [60, 63]. Also, catechol had undergone complete gasification at a temperature of around 600°C and pressure of 34 MPa. This result underlines the importance of optimizing the SCW operating conditions for maximum hydrogen yield coupled with complete gasification of sewage sludge model compounds as catechol represents lignin which is gasification resistant [61]. Yoshida et al. [5]

pointed out that oxidation of cellulose, xylan, and lignin mixture showed the clear negative effect of lignin on hydrogen yield in the product. This emphasizes the role of lignin and other aromatic ring compounds present in some industrial waste streams on the hydrogen production. Savage et al. [64] utilized higher temperatures to test lignin gasification in SCW, and compared their results with those obtained from cellulose gasification. The aforementioned authors confirmed the role of lignin as a control compound in the gasification process governing the effect of gasification rate. Moreover, aldehydes and ketones are believed to be intermediates of lignin gasification in SCW as reprted by Watanabe et al. [13], thus pointing to the necessity of studying these intermediate compounds extensively by employing different catalysts and other SCW variables. This can lead to a better understanding and improvement of lignin gasification in SCW.

- Vanillin can be gasified completely at a relatively low SCW temperature of 500°C [60]. Also, by employing thermodynamic calculations to predict the product distribution, the predicted methane yield was higher than the experimental yield which highlights the need for improvement of the predictive capability of these models.
- In the case of cellulose, Guan et al. [67] reported that the addition of K_2CO_3 doubled the hydrogen yield with no temperature change. The authors also pointed out that by employing both K_2CO_3 and $Ca(OH)_2$ as catalysts, the hydrogen yield increased by about 2 mol/ kg. These results raise an interesting point which is the synergisitic effects of multiple catalysts on the gas yield of the SCW process. Furthermore, no studies coupled the gasification with partial oxidation despite extensive independent evaluation of each. Hao et al. [68] reported partial oxidation and gasification of cellulose and highlighted that

gasification using Ru/C, Pd/C, CeO_2 particles, nano-CeO_2 and nano-$(CeZr)_xO_2$ as catalysts gave higher hydrogen yield. However, the aforementioned authors did not report the oxygen stoichiometric ratio at which partial oxidation experiments were conducted. Also, the authors did not report any experimental results regarding coupled gasification with partial oxidation i.e. supercritical water partial oxidation.

2.7Gasification of Real waste in SCW

Glycerol, which is a byproduct from the bio-ethanol and biodiesel production plants, was also investigated for H_2 production in SCW. This study was conducted by Byrd and co-workers [69] at the University of Auburn, Alabama, USA. The aforementioned authors performed their experiments using a continuous flow system with Inconel 600 tubular reactor having dimensions of 0.5 m long, 0.635 cm, O.D. and 0.304 cm I.D. The operating temperature was in the range of 700-800°C, pressure of 25 MPa, and a residence time of 1-6 seconds. The authors employed 5 wt% Ru/Al_2O_3 as a catalyst, and feed concentration of 5-40 wt % glycerol. It is well known that the desired overall reaction of glycerol for hydrogen production is given by:

$$C_3H_8O_3 + 3H_2O \rightarrow 7H_2 + 3CO_2 \quad (9)$$

Thus, the maximum theoretical H_2 yield that can be obtained is 7 moles. The aforementioned authors reported that the highest H_2 yield of 6.5 mol H_2/mol glycerol was obtained at a feed concentration of 5 wt%, and a temperature of 800°C, with 1 second reactor residence time. The authors also pointed out that the shortest residence time gave the highest hydrogen yield, however at longer residence times, the hydrogen yield dropped sharply with a simultaneous decline in CO_2 yields as well. Furthermore, the increase of the feed concentration was coupled with a decrease in the yield of hydrogen and an accompanying increase in the

methane yield. As the gasification reaction proceeds in the presence of water, less water was present at the higher concentrations rationalizing the drop in the H_2 yield.

With all the previously mentioned attempts to provide a stable, active, and durable catalyst for the catalytic SCW for H_2 production, none of these catalytic processes are in the stage of commercial application. In fact, with this task still has major challenges especially overcoming the problem of deactivation by sulfur compounds that are present in the waste biomass such as sludges. However, the research in this field has also provided new scientific insights into catalytic chemistry in SCW as well as identifying processes that are technically feasible in SCW.

2.8Catalysts activity and stability in SCW

Catalyst stability and long term activity are prerequisites for commercial applications of the SCW process. Peterson et al. [70] and Lambroua et al. [71] reported that the deactivation of a catalyst is mainly caused by coking, poisoning, and the solid state transformations of catalysts during gas-phase oxidation. Coking is the result of carbon deposition on active sites, poisoning is the physical or chemical adsorption of impurities on active sites, and the solid-state transformations are caused by the phase transition.

Savage et al. [72] compared the activity and stability of three different catalysts i.e. bulk MnO_2, bulk TiO_2, and CuO/Al_2O_3 during supercritical water oxidation of phenol. The experiments were conducted in a tubular flow reactor at 400°C. The authors used the BET surface area, X-ray diffraction (XRD), and XPS or electron spectroscopy for chemical analysis (ESCA) techniques to characterize both fresh and spent catalysts. The aforementioned authors highlighted that on a catalyst mass basis, CuO/Al_2O_3 was the most active whereas MnO_2 was the

most active on a surface area basis. On the other hand, CuO/Al_2O_3 was deactivated during the first 12 hours on stream and maintained its activity at longer times. However, the observation of both Cu and Al in the reactor effluent limited the usefulness of CuO/Al_2O_3 in the SCW.

2.9 Catalyst preparation for SCW

The chemical stability of a catalyst is governed by its physical stability which depends on the preparation technique. In SCW, catalyst stability and ability to preserve its characteristics such as crystal structure is of the utmost importance due to the harsh SCW environment. Catalysts are prepared by several techniques such as impregnation, co-precipitation, fused metal oxide, supercritical deposition, and fused alloy. The catalyst preparation method (precipitation, impregnation, sol gel, etc.), type of precursor, calcination conditions, and reduction have a critical impact on the catalyst activity. The impregnation and co-precipitation techniques are the most popular for metal and metal oxides [73, 74].

Kaddouri et al. [75] prepared Co/SiO_2 and $Co/\gamma\text{-}Al_2O_3$ catalysts using a combined incipient wetness and sol-gel method. The aforementioned authors reported that the catalytic performance toward hydrogen production over Co/SiO_2 catalyst was enhanced by the preparation method.

Ihm et al. [76] prepared a 16 wt % Ni/AC catalyst by an incipient wetness method. The authors compared their experiments with prepared catalyst by a control one with only AC. The aforementioned authors reported that AC provided catalytic activity toward methane production at temperatures above 650 °C whereas the Ni/AC catalyst was relatively stable in SCW. A comparison between the fresh and spent catalysts revealed that unlike the AC only, the Ni/AC

catalyst was deactivated. Characterization of the spent catalyst showed that the nickel particles were larger than the fresh one which is due to the crystallite growth of the nickel.

Table 2.4 reports the most used catalyst characterization techniques in examining the catalyst activity and identifying catalytic properties such as bulk metal loading, total surface area, crystalline phase and oxidation state, and phase transformation.

Table 2.4 Catalyst characterization techniques

Property	**Technique**
Surface area and pore volume	Brunauer-Emmett-Teller
Phase transformation	Powder X-ray diffraction (XRD)
Catalyst Reducibility	Temperature-programmed reduction of H_2
Bulk metal loading	Inductive couple Plasma-Atomic Emission spectroscopy (ICP-AES)
Acid and basic site density	Temperature-programmed desorption (TPD) of NH_3 and CO_2
Surface topography	Scanning electron microscopy (SEM)

2.10 Oxidation kinetics in SCW.

Knowledge of reaction kinetics is of great importance since it is used to determine the required reactor volume V, and the residence time τ for the desired conversion X. Considering a reaction of a model compound in SCW that contains only carbon, H and oxygen atoms, the general reaction equation is given by:

$$\text{Organic compound (A)} + \text{oxidant} \rightarrow \text{carbon dioxide} + \text{water} \qquad (10)$$

According to most chemical reaction engineering books, the reaction rate equation of component A is given by:

$$-r_A = (-1/V)\,(dN_A/dt) = -\,(dC_A/dt) = -\,d\,[A]/dt\ [mol/m^3\ s] \quad (11)$$

where r_A is the reaction rate, V is the reactor volume, N_A is the number of moles of component A, and τ is the residence time. The reaction rate constant temperature dependence is represented by Arrhenius's law, $k = k_o \exp(—E/RT)$, where k_o is called the pre-exponential factor and E the activation energy, and R is the universal gas constant. Thus, the global reaction rate for SCW is expressed as follows:

$$-r_A = -\,d\,[A]/dt = k_0 \exp(-E/RT)\,[A]^a\,[O_2]^b\,[H_2O]^c \quad (12)$$

where a, b, and c are the reaction orders of the organic compound, oxygen, and water respectively. The above equation parameters can be obtained by employing multiple linear regressions of experimental data after transforming equation 11 into the following linear form:

$$\ln(-r_A) = \ln k_0 - E/RT + a \ln[A] + b \ln[O_2] + c \ln[H_2O] \quad (13)$$

The approximation of pseudo-first order kinetics has dominated most kinetic equations derived previously in the literature [77- 82]. However, predictions from kinetic models obtained below and above the critical point of water are completely different Li et al. [83]. Furthermore, predictions from kinetic expressions obtained in the same range of operating conditions vary considerably. Therefore, given the complexity of the real waste biomass streams, both batch and continuous flow reactors should be studied extensively to compare gasification and partial oxidation kinetics at supercritical conditions.

A great number of kinetic studies have been performed in batch reactors, flow-through reactors, quartz tube reactors, and optical accessible cells. According to process conditions (i.e., pressure, temperature, oxygen excess), oxidation, hydrolysis or pyrolysis reactions occur.

Different classes of organic compounds have been subjected to SCWO conditions, which include hydrocarbons, nitrogen-containing compounds, sulfur-containing compounds, chlorine- and fluorine-containing compounds, and oxygen-containing compounds [84]. Moreover, and considering the fact that many wastes are complex organic mixtures whose constituents vary widely in their susceptibility to SCW oxidation, the reaction rate predictions using equation 13 may be misleading, especially because of the crucial role of the experimental set-up i.e. the Reynolds numbers in plug flow reactors are often so small that laminar effects might falsify the rates. Thus, the need for kinetic comparison for both batch and continuous flow reactors, as well as the need for the development of more complex models using advanced numerical techniques seems to be unavoidable.

Li et al. [84] reported a generalized kinetic model of organic compounds based on the formation and destruction scheme of rate-controlling intermediate compounds. The aforementioned authors assumed that ethanol, methanol, and acetic acid were the main intermediates as they exhibit the higher activation energy. From the reported concentrations of the three previously mentioned compounds in the literature [79, 85-88], methanol and ethanol concentrations were insignificant compared to acetic acid concentration. Thus, the authors assumed that acetic acid is the rate controlling-intermediate compound in the generalized model. Another factor supporting the author's assumptions is the fact that the pre-exponential factors for methanol and ethanol are considerably higher than that for acetic acid.

Based on the proposed mathematical model reported by Sioya et al. [89] which describes the reaction pathways for thermal decomposition of activated sludges, Li et al. [84] proposed their generalized kinetic model. The generalized model scheme is comprised of tri-angular pathways i.e. the organic components feed **(A)** reacts with oxygen to give the final product **(C)**

as well as an intermediate product (**B)** which further decomposes to give the final product C. The authors suggested that the concentrations of the feed **(A)** and intermediate product (**B)** are expressed either in forms of total organic carbon (TOC) or chemical oxygen demand (COD).

Goto et al. [90] studied the kinetics of destruction of municipal sewage sludge and alcohol distillery wastewater of molasses in SCW. A batch reactor made of stainless steel tube sealed with Swagelok caps (about 4 mL in volume) was employed to perform the experimental work. Hydrogen peroxide (about 30%) was used as an oxidant. Operating conditions of temperatures 400, 450, and 500°C; and estimated a reaction pressure of 30.0 MPa were used. The amount of hydrogen peroxide used was 300% of the stoichiometric demand and the water content of municipal sludge and alcohol distillery wastewater was 96% and 66 % respectively. Since oxygen and water are present in excess, and because the existences of O_2 as one phase in SCW, the reaction rate becomes independent of the oxygen concentration. Thus, the authors assumed that the constants b and c in Equation 12 are equal to zero and a first order reaction with respect to organics was adopted as was extensively reported in the literature.

The reported rate constants by the aforementioned authors were compared with the data reported by Foussard et al. [52] for biological sludge and Shanableh [79] for activated sludge. Furthermore, the activation energy for the sewage sludge decomposition of 76.3 kJ/mol was somewhat comparable to 67 kJ/mol and 54 kJ/mol obtained by the aforementioned authors respectively.

Goto et al. [90] reported another kinetic study pertaining to ammonia decomposition in sewage sludge in SCW using the same experimental technique used for studying the kinetics of destruction of municipal excess sewage sludge and alcohol distillery wastewater of molasses in SCW. However, the amount of hydrogen peroxide (H_2O_2) was 200% of the stoichiometric

requirements. The authors adopted the reaction pathway proposed by (Li 1993) which is the modified reaction pathway reported by Li et al. [84]. The modified pathway was based on the addition of ammonia as a secondary refractive intermediate. The rate constants for ammonia decomposition determined in the study by Goto et al. [90] were compared with those reported by Webley et al. [81] for ammonia decomposition in SCW, when ammonium hydroxide was used as a reactant and oxygen was used as an oxidant. Although the temperature range in the work reported by Webley et al. [81] was higher than those reported by Goto et al. [90], the activation energy of 139 kJ/mol reported by Webley et al was comparable with the activation energy of 157 kJ/mol evaluated in Goto's et al. [90] work. Moreover, the data reported by Webley et al. [81] were for the decomposition rate of ammonia, whereas the data reported by Goto et al. [90] were for the decomposition rate of ammonia that was formed as an intermediate product during the sewage sludge oxidation in SCW.

2.11 Challenges of H_2 Production from Wastes and Potential Future Research

Hydrogen production from waste biomass using supercritical water gasification is a promising technology. In fact, the reported research publications pertaining to this research area have been increasing steadily in the past ten years as the number of publications surpassed fifty papers per year in the last three years compared to a few per year in the late 1980's [43]. However, this technology faces a number of challenges that require more research as summarized by the following points:

- Corrosion, as mentioned earlier, is the most difficult challenge to solve for using SCW for hydrogen production from waste biomass (sludge, manure, industrial wastewater) due to the harsh SCW environment and the corrosive nature of inorganics contained in certain

types of waste biomass. Therefore, SCW unit components have to be constructed from expensive corrosion resistant alloys such as Hastelloy or Titanium. The application and use of the previously mentioned alloys should be limited to the components that are more prone to corrosion such as the reactor and heat exchanger. However, the use of such alloys increases the capital cost which in turn affects the overall process economic viability. The corrosion problem requires more research efforts for discovering new types of alloys that exhibit better corrosion resistance in the SCW environment. Furthermore, exploring the use of coating materials that can withstand the corrosion is of interest, as such materials if provided could add a valuable incentive to SCW technology and makes it more competitive. In other words, the ability of SCW for gasification of organic compounds as well as supported-nanoparticles can be utilized to limit the corrosion problem and provide the required catalyst for gasification. This was clearly demonstrated by Gadhe et al. [92] who generated catalytic Cu nanoparticles hydrothermally in situ and subsequently used the particles to catalyze methanol SCWG.

- The second challenge is pumping, as it is well known that SCW requires high pressures above the water critical pressure. To obtain such high pressures as well as successfully pumping waste biomass containing a considerable amount of biosolids requires a special type of pump.
- The catalyst and its support, which is the heart of the SCW process for hydrogen production, needs to be stable, and exhibit a reasonable activity and selectivity towards hydrogen generation. The catalyst also needs to be regeneratable which corresponds to a significant impact on the capital cost of a SCW plant.

2.12 References

[1] Brunner G. Near and supercritical water. Part II: Oxidative processes. J. of Supercritical Fluids.2009; 47:382–390.

[2] Kritzer P. Corrosion in high-temperature and supercritical water and aqueous solutions: a review. J. of Supercritical Fluids. 2004; 29:1–29.

[3] Kritzer P, Dinjus E. An assessment of supercritical water oxidation (SCWO) Existing problems, possible solutions and new reactor concepts. Chemical Engineering Journal. 2001;83:207–214.

[4] Modell M. Gasification Process. 1978. U.S. Pat. No. 4,113,446 Pat. No. 4, 338, 199, 1982.

[5] Yoshida Y, Dowaki K, Matsumura R, Matsuhashi D, Li Y. Ishitani H. Komiyama H. Comprehensive comparison of efficiency and CO_2 emissions between biomass energy conversion technologies-position of supercritical water gasification in biomass technologies. Biomass & Bioenergy. 2003; 25:257-272.

[6] Bermejo MD, Fdez-Polanco F, Cocero MJ. Transpiring wall reactor for the supercritical water oxidation process: Operational results, modeling and scaling. Ind. Eng.Chem. Res. 2005; 44:3835–3845

[7] Lieball L. Numerical Investigations on a Transpiring Wall Reactor for Supercritical Water Oxidation. 2003; Doctoral Thesis No. 14-911. Zurich, Switzerland: ETH.

[8] Anderko A, Wang P, Rafal M. Electrolyte solutions: From thermodynamic and transport property models to the simulation of industrial processes. Fluid Phase Equilib. 2002; 197:123-142.

[9] Savage PE, Gopalan S, Mizan TI. Reactions at Supercritical Conditions: Application and Fundamentals. AIChE J. 1995; 41:1723–1778.

[10] Youssef E, Chowdhury M, Nakhla G, Charpentier P. Effect of nickel loading on hydrogen production and chemical oxygen demand (COD) destruction from glucose oxidation and gasification in supercritical water. Int. J. Hydrogen Energy. 2009; 35: 5034-5042.

[11] Goto M, Nada T, Kodama A, Hirose T. Kinetic Analysis for Destruction of Municipal Sewage Sludge and Alcohol Distillery Wastewater by Supercritical Water Oxidation. Ind. Eng. Chem. Res. 1999; 38:1863-1865.

[12] Cortright RD, Davda R. Dumesic J. Hydrogen from catalytic reforming of biomass-derived hydrocarbons in liquid water. Nature. 2002; 418: 29.

[13] Watanabe H, Inomata M, Osada T, Sato T, Adschiric K. Catalytic effects of NaOH and ZrO_2 for partial oxidative gasification of n-hexadecane and lignin in supercritical water. Fuel. 2003; 82:545–552.

[14] Rice, S. Richard R. Steeper, and Jason D. Aiken. Water Density Effects on Homogeneous Water-Gas Shift Reaction Kinetics. J. Phys. Chem. 1998; 102: 2673-2678.

[15] Kruse A, Sinag A, and Schwarzkopf V. Formation and degradation pathways of intermediate products formed during the hydropyrolysis of glucose as a model substance for wet biomass in a tubular reactor. Engineering in Life Science. 2003; 3:469–473.

[16] Sasaki, M. Kabyemela, B. Malaluan, R. Hirose, S. Takeda, N. Adschiri, A. Ara, K. Cellulose hydrolysis in subcritical and supercritical water. J of supercritical fluids. 1998; 13:261-268.

[17] Kabyemela BM, Adschiri T, Malaluan RM, Arai K. Glucose and fructose decomposition in subcritical and supercritical water: detailed reaction pathway, mechanisms, and kinetics. Ind Eng Chem Res. 1999; 38:2888–2895.

[18] Onwudili J, Williams P. Subcritical and Supercritical Water Gasification of Cellulose, Starch, Glucose, and Biomass Waste Energy & Fuels. 2006; 20:1259-1265.

[19] Holgate M, Meyer JC, Tester JW. Glucose hydrolysis and oxidation in supercritical water. AIChE Journal. 1995; 41:637–648.

[20] Abdelmoez A, Nakahasi T, Yoshida H. Amino Acid Transformation and Decomposition in Saturated Subcritical Water Conditions. Ind. Eng. Chem. Res. 2007; 46:5286-5294.

[21] Woerner GA. Thermal Decomposition and Reforming of Glucose and Wood at the Critical Conditions of Water. 1976. MS Thesis, Dept. of Chemical Engineering, Mass. Inst. of Technol.

[22] Antal J Jr. Biomass Pyrolysis: A Review of the Literature. Part 1-Carbohydrate Pyrolysis,. Adv. Solar Energy. 1982; 1:61.

[23] Evans R J, Milne TA. Molecular Characterization of the Pyrolysis of Biomass: 1. Fundamentals. Energy & Fuels. 1987; 1:123.

[24] Antal J Jr, Mok W, Richards G. Mechanism of Formation of S-(HydroxymethyI)-2-Furaldehyde from D-Fructose and Sucrose. Carbohydr. Res. 1991; 71.

[25] Sasaki M, Kabyemela B, Malaluan R, Hirose S, Takeda N, Adschiri T, Arai K. Cellulose hydrolysis in subcritical and supercritical water. The Journal of Supercritical Fluids.1997.13; 15: 261-268.

[26] Wahyudiono A, Sasaki M, Goto M. Conversion of biomass model compound under hydrothermal conditions using batch reactor. Fuel. 2009; 88:1656–1664.

[27] Watanabe M, Inomata H, Arai K. Catalytic hydrogen generation from biomass (glucose and cellulose) with ZrO_2 in supercritical water. Biomass & Bioenergy. 2002; 22: 405-410

[28] Onwudili J, Williams P. Hydrothermal reforming of bio-diesel plant waste: Products distribution and characterization. Fuel. 2010; 89: 501-509.

[29] Guo LJ, Lu YJ, Zhang XM, Ji CM, Guan Y, Pei AX. Hydrogen production by biomass gasification in supercritical water: A systematic experimental and analytical study. Catal. Today. 2007; 129:275-286.

[30] Marrone P, Hodes M, Smith K, Tester J. Salt precipitation and scale control in supercritical water oxidation—part B: commercial/full-scale applications. J. of Supercritical Fluids. 2004; 29:289–312.

[31] Schubert M, Johann W, Vogel F. Continuous salt precipitation and separation from supercritical water Part 2: Type 2 salts and mixtures of two salts. J. of Supercritical Fluids. 2010. 113-124.

[33] Bogaerts C, Bettendor A. Electrochemistry and Corrosion of Alloys in High-Temperature Water. EPRIReport NP-4705, Electric Power Research Institute. 1986.

[34] Mitton J H, Yoon J A, Cline H S, Kim N, Latanision R. Corrosion behavior of nickel-based alloys in supercritical water oxidation systems. Industrial & Engineering Chemistry Research. 2000; 39:4689–4696.

[35] Furness DT, Hoggett L A, Judd SJ. Thermochemical treatment of sewage sludge. Water Environ. J. 2000;14:57-65.

[36] Elliott D, Sealock J Jr, Baker E. Chemical Processing in High-pressure Aqueous Environments. 2.Development of Catalysts for Gasification. Ind. Eng. Chem. Res. 1993; 32:1542-1548.

[37] Rulkens W. Sewage Sludge as a Biomass Resource for the Production of Energy: Overview and Assessment of the Various Options. Energy & Fuels. 2007; 22:9-15.

[38] Kosobucki P A, Chmarzyński B B. Sewage Sludge Composting. Polish Journal of Environmental Studies. 2000; 9:243-248.

[39] Ptasinski K.J. Hamelinck C. Kerkhof PM. Exergy analysis of methanol from the sewage sludge process. Energy Conversion and Management. 2002; 43:1445–1457.

[40] Demirbas A. Hydrogen-rich gas from fruit shells via supercritical water extraction. Int. J. Hydrogen Energy. 2004; 29:1237-1243.

[41] Osada M, Sato T, Watanabe M, Shirai M, Arai K. Catalytic gasification of wood biomass in subcritical and supercritical water. Combust. Sci. Technol. 2006; 178:537-552.

[42] Yanik J, Ebale S, Kruse A, Saglam M, Yüksel M. Biomass gasification in supercritical water: Part 1. Effect of the nature of biomass. Fuel. 2007;86:2410-2415.

[43] Savage E P. A perspective on catalysis in sub- and supercritical water. J. of Supercritical Fluids. 2009; 47:407–414.

[44] Yu D, Aihara M, Antal J Jr. Hydrogen Production by Steam Reforming Glucose in Supercritical Water. Energy & Fuels. 1993; 7.

[45] Xu X, Matsumura Y, Stenberg J, Antal J Jr. Carbon-Catalyzed Gasification of Organic Feedstocks in Supercritical Water. Ind. Eng. Chem. Res. 1996; 35.

[46] Antal J Jr, Allen SG, Schulman D, Xu X, Divilio R. Biomass Gasification in Supercritical Water. Ind. Eng. Chem. Res. 2000; 39:4040-4053.

[47] Ding A, Gloyna E. Catalytic Oxidation in Supercritical Water. Ind. Eng. Chem. Res. 1996; 35:3257-3272.

[48] Dunn JB, Urquhart DI, Savage PE. Terephthalic acid synthesis in supercritical water. Adv. Synth. Catal. 2002; 344-385.

[49] Ding Z Y, Abraham MA. Catalytic Supercritical Water Oxidation of Aromatic Compounds: Pathways, Kinetics and Modeling. First International Workshop on Supercritical Water Oxidation. 1995.

[50] Frisch MA, Li L, Gloyna E F. Catalyst Evaluation: Supercritical Water Oxidation Process. Proceedings of 49th Annual Purdue University Industrial Wastewaters Conference. 1994.

[51] Baker E G, Sealock L Jr, Butner RS, Elliott DC, Neuenschwander G G. Catalytic Destruction of Hazardous Organics in Aqueous Wastes: Continuous Reactor System Experiments. Hazard. Waste Hazard. Mat. 1989; 6.

[52] Foussard J N, Debellefontaine H, Besombes-Vailhe J. Efficient elimination of organic liquid wastes: Wet air oxidation. J. Environ. Eng. 1989; 115:367-385.

[53] Tiltscher H, Hofman H. Trends in High Pressure Chemical Reaction Engineering. Chemical Engineering Science. 1987; 42.

[54] Wu B C, Klein M T, Sandler S. Solvent Effects on Reactions in Supercritical Fluids. Ind. Eng. Chem. Res. 1991; 30:822.

[55] Mahajani M, Joshi B. Wet air oxidation. Ind. Eng. Chem. Res. 1995; 34:1.

[56] Adschiri T, Suzuki T, Arai K. Catalytic Reforming of Coal Tar Pitch in Supercritical Fluid. Fuel. 1991; 70.

[57] Baptist-Nguyen S, Subramaniam B. Coking and Activity of Porous Catalysts in Supercritical Reaction Medium. AIChE Journal. 1992; 38.

[58] Amin S, Reid R C, Modell M. Reforming and Decomposition of Glucose in an Aqueous Phase. The Intersociety Conference on Environmental Systems. 1975.

[59] Byrd A, Pant K, Gupta R. Hydrogen Production from Glucose Using Ru/Al_2O_3 Catalyst in Supercritical Water. Ind. Eng. Chem. Res. 2007; 46:3574-35.

[60] Schmieder H J, Abeln N. Boukis E. Dinjus A. Kruse A, Kluth M, Petrich G, Sadri S, Schacht M. Hydrothermal gasification of biomass and organic wastes. J. of Supercritical Fluids. 2000;17:145–153.

[61] DiLeo G, Neff M, Savage P E. Gasification of Guaiacol and Phenol in Supercritical Water. Energy & Fuels. 2007; 21:2340-2345.

[62] Nunouraa G, Lee H, Matsumura Y, Yamamotob K. Modeling of supercritical water oxidation of phenol catalyzed by activated carbon. Chemical Engineering Science. 2002; 57:3061–3071.

[63] Kruse A, Meier D, Rimbrecht P, Schacht M. Gasification of Pyrocatechol in Supercritical Water in the Presence of Potassium Hydroxide. Ind. Eng. Chem. Res. 2000; 39:4842-4848.

[64] Savage P E. Fernando R, Stephanie A, Berger M. Noncatalytic Gasification of Lignin in Supercritical Water. Energy & Fuels. 2008; 22:1328–1334.

[65] Minowa T, Fang Z, Ogi T. Cellulose decomposition in hot-compressed water with alkali or nickel catalyst Journal of Supercritical Fluids. 1998; 13:253-259.

[66] Osada M, Sato T. Watanabe M, Adschiri T, Arai K. Low temperature catalytic gasification of lignin and cellulose with a ruthenium catalyst in supercritical water. Energy & Fuels. 2004; 18:327-333.

[67] Guan Yu, PEI A, Guo L. Hydrogen production by catalytic gasification of cellulose in supercritical water. J. Chem. Eng. China. 2008; 2:176–180.

[68] Hao Yu, Guo L, Zhang X, Guan Y. Hydrogen production from catalytic gasification of cellulose in supercritical water. Chemical Engineering Journal. 2005; 110:57–65.

[69] Byrd A, Pant K, Gupta R. Hydrogen production from glycerol by reforming in supercritical water over Ru/Al_2O_3 catalyst. Fuel. 2008; 87:2956–2960.

[70] Peterson E, Butt J. Activation Deactivation and Poisoning of Catalysts. Academic Press. Proceedings of the 10th European Meeting on Supercritical Fluids: Reactions, Materials and Natural Products Processing. 1988.

[71] Lambroua S Y, Christoua A P, Fotopoulosb F K, Fotib T N, Angelidisb AM. The effects of the use of weak organic acids on the improvement of oxygen storage and release properties of aged commercial three-way catalysts. Applied Catalysis B: Environmental. 2005; 59:1-11.

[72] Savage P E, Yu Y. Catalyst activity, stability, and transformations during oxidation in supercritical water. Applied Catalysis B: Environmental. 2001; 31:123–132.

[73] Aki S N, Ding Z Y, Abraham M A. Catalytic Supercritical Water Oxidation: Stability of Cr_2O_3 Catalyst. AIChE Journal. 1996; 42.

[74] Ding Z, Gloyna E. Catalytic Oxidation in Supercritical Water. Ind. Eng. Chem. Res. 1996; 35:3257-3272.

[75] Kaddouri A, Mazzocchia C. A study of the influence of the synthesis conditions upon the catalytic properties of Co/SiO_2 or Co/Al_2O_3 catalysts used for ethanol steam reforming. Catalysis Communications. 2004; 6:339-345.

[76] In-Gu L, Son-Ki I. Catalytic Gasification of Glucose over Ni/Activated Charcoal in Supercritical Water. Ind. Eng. Chem. Res. 2009; 48:1435–1442.

[77] Lee D S, Li L, Gloyna E. Efficiencyof Hydrogen Peroxide and Oxygen in Supercritical Water Oxidation of Acetic Acid and 2,4-Dichlorophenol. AIChE Meeting. 1990.

[78] Wilmanns E G. Supercritical Water Oxidation of Volatile Acids. MS Thesis, Civil Eng. Dept., Univ. of Texas. 1990.

[79] Shanableh A M. Subcritical and supercritical water oxidation of industrial excess activated sludge. PhD Dissertation, Civil Engineering Department, University of Texas, Austin, Texas. 1990.

[80] Helling R K., Tester J. Oxidation Kinerics of Carbon Monoxide in Supercritical Water. Energy & Fuel. 1987; 1.

[81] Webley P A, Tester J. Fundamental Kinetics and Mechanistics Pathways for Oxidation Reactants in Supercritical Water. SAE Technical Paper Ser. 1988.

[82] Goto M, Nada T, AkioK, Hirose T. Kinetic Analysis for Destruction of Municipal Sewage Sludge and Alcohol Distillery Wastewater by Supercritical Water Oxidation. Ind. Eng. Chem. Res. 1999; 38:1863-1865.

[83] Li L, Chen P, Gloyna E. Kinetic Model for Wet Oxidation of Organic Compounds in Subcritical and Supercritical Water. ACS Symposium Series. 1993; 305.

[84] Li P C, Gloyna E F. Generalized Kinetic Model for Wet Oxidation of Organic Compounds. AIChE Journal. 1991; 37:11.

[85] Taylor J E, Weygandt J C. A Kinetic Study of High Pressure Aqueous Oxidations of Organic Compounds Using Elemental Oxygen. Can. J. Chem. Eng. 1974; 52:1925.

[86] Conditt M K., Sievers E. Microanalysis of Reaction Products in Sealed Tube Wet Air Oxidations by Capillary Gas Chromatograpy. Anal. Chem. 1984; 56.

[87] Keen R, Baillod C. Toxicity to Daphnia of theEnd Products of Wet Oxidation of Phenol and Substituted Phenols. Water Res. 1985; 19:6.

[88] Baillod C R, Faith B, Masi O. Fate of Specific Pollutants During Wet Oxidation and Ozonation,. Environ. Prog. 1982; 1:3.

[89] Takamatsu S, Hashimoto T. Model Identification of Wet Air Oxidation Process Thermai Decomposition. Water Res. 1970; 4:33.

[90] Goto M, Shiramizu D, Kodama A, Hirose T. Kinetic Analysis for Ammonia Decomposition in Supercritical Water Oxidation of Sewage Sludge. Ind. Eng. Chem. Res. 1999; 38:4500-4503.

[92] Gadhe J B, Gupta R. Hydrogen production by methanol reforming in supercritical water: catalysis by in-situ-generated copper nanoparticles. Int. J. Hydrogen Energy. 2007; 32:2374–2381.

CHAPTER 3

Experimental Set-Up

3.1 SCWG Apparatus

Figure 3.1 portrays a schematic diagram of the experimental SCWG setup. Experiments were performed in the main reactor body which was obtained from Autoclave Engineers, Erie, Penna, U.S.A. The reactor was constructed of Hastelloy C-276 with a capacity of 600 ml. The batch reactor allowed for sampling of gas and liquid samples throughout the experiments. The reactor was heated with a 1.5 kW electrical furnace that surrounded its main body supplied by the same manufacturer. The reactor design operating temperature was 343°C rated at 42MPa which is below the critical points of water (373°C, 22.1MPa). However, based on the temperature and pressure ratings of the reactor material, it was possible to reduce the maximum allowable pressure to 34 MPa at temperature of 500°C. This facilitated the operation of the reactor at temperature and pressure of 500°C and 28MPa which achieved gasification at and above the water critical point of 373°C, 22.1MPa. It should be pointed out here that this modification in the reactor operating conditions was performed in accordance with the pressure temperature rating diagrams posted on the manufacturer's web page for the Hastelloy C-276 material.

3.2 Experimental Procedures

The experimental procedure consisted of several steps which started by opening and washing the reactor body thoroughly with distilled water to remove any residue from previous experiments. The catalyst and 70 ml of de-ionized water were added to the reactor, after which it was closed and purged with helium gas at a constant pressure of 0.2 MPa for 20 min to drive away any air and oxygen present in the system. After purging with helium, the outlet valve

(VO1) was closed and the pressure in the reactor increased. The reactor was then heated to the desired temperature, and the pressure was increased accordingly to about 22.8 MPa. After reaching the desired temperature, the reactor was left for 5 min to stabilize. Subsequently, the feed was injected into the reactor by employing a syringe pump (Model 100 DX, Lincoln NE, USA).

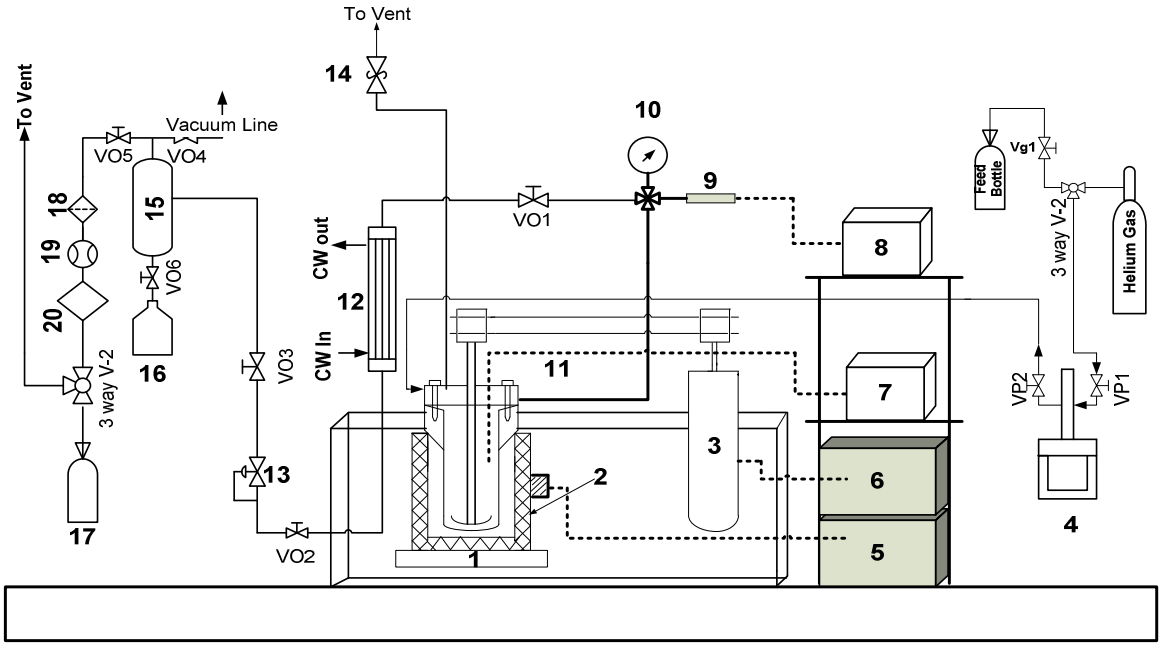

1-Reactor, 2-Heater, 3-Motor, 4-Isco Syringe Pump, 5- Temperature controller, 6- Motor speed controller,7-Temperature reader,8- Pressure reader, 9-Pressure Transducer, 10- Pressure gauge, 11- Thermocouple, 12 Double pipe H/E, 13- Pressure Reducing Valve, 14-Relife Valve , 15- Gas/liquid Separator, 16- Liquid effluent tank, 17-Gas Bag, 18- Line Filter, 19- Mass flow meter, 20- H_2S logger.

Figure 3.1: Schematic diagram of the SCWO batch unit.

As soon as the feed injection was complete, the reaction time (t) was started. Injection of feed solution increased the pressure to about 28MPa. In the experiments where hydrogen peroxide was used i.e. partial oxidation experiments, after 15 min of reaction time, a known amount of hydrogen peroxide was injected into the reactor using the syringe pump. For the manure experiments, the reactor was filled with the feedstock from the start as it was not

possible to inject high solid content hog manure using the syringe pump. After 30 min, the valve (VO1) was opened to allow for effluent gases to pass through the condenser (double pipe H/E), where it were cooled and then depressurized using a high pressure reducing regulator (KHP series Solon, OH, USA). The cooled depressurized effluent passed to a gas liquid separator from which the gases left the separator to pass through an in-line filter to remove any moisture prior to the OMEGA mass flow meter (FMA 1700/1800 series 0–2 L/min, Laval (Quebec), Canada). The mass flow meter was equipped with a totalizer that utilizes a K-factor to relate the mass flow rate of an actual gas to nitrogen, the calibrated reference gas. The actual gas flow rate was calculated by determining the average K-factor for the produced gas by means of the mole fraction of each gas in the stream, as shown by equation (3.1).

$$Avg\ K_{factor} = \frac{1}{K_{ref} \sum y_i K_{factor(i)}} \tag{3.1}$$

where K_{ref} is the K-factor for the reference gas, and y_i is the mole fraction of the individual components. The actual gas flow rate was calculated by (3.2)

$$Q_{total} = Avg\ K_{factor} \times Q_{ref} \tag{3.2}$$

where Q_{total} is the mass flow rate of the actual gas and Q_{ref} is the mass flow rate of the reference gas i.e. nitrogen. After passing through the mass flow meter, the product gases were collected in 3L Tedlar gas sampling bags for subsequent analysis.

3.3 Materials

Glucose experiments: glucose was obtained from Sigma-Aldrich chemical company and used without further purification. Reduced commercial nickel on silica alumina was also obtained from Sigma-Aldrich chemical company (Oakville, Ontario, Canada).

Hydrogen peroxide aqueous solution (50% H_2O_2 solution) was obtained from EMD Chemicals Inc (Gibbstown, NJ, U.S.A). De-ionized water obtained from a compact ultrapure water system (EASY pure LF, Mandel Scientific co, model BDI-D7381).

Oleic acid experiments: oleic acid (99%), 0.5 wt % Ru/Al_2O_3 Pelletilized catalyst, 5% palladium supported on activated carbon, 5% platinum supported on activated carbon, and reduced commercial nickel on silica alumina (63 wt % nickel) catalysts were obtained from Sigma-Aldrich Canada Ltd. (Oakville, Ontario, Canada). KATALCO (high temperature hydrogenation catalyst) and 0.5 wt % Ru/AC (Granular) catalysts were purchased from Alfa Aesar (Ward Hill, MA, USA). 18 m·Ω de-ionized water was obtained using a compact ultrapure water system (EASY pure LF, Mandel Scientific co, model BDI-D7381). An emulsion of oleic acid (0.35M and 28000 mgCOD/L) was prepared using purified water by mechanical mixing and heating. The prepared feed was kept well mixed until delivered to the syringe pump where it was subsequently pressurized and injected to the reactor.

Cysteine experiments: cysteine ($C_3H_7NO_2S$), 0.5 wt % Ru/Al_2O_3 Pelletilized catalyst was obtained from Sigma-Aldrich Canada Ltd. (Oakville, Ontario, Canada), and 0.5 wt % Ru/AC (Granular) catalysts were purchased from Alfa Aesar (Ward Hill, MA, USA). Activated carbon (AC) was purchased from Caledon Laboratories Ltd (Georgetown, Ontario, Canada). De-ionized water (18 m·Ω resistivity) was obtained using a compact ultrapure water system (EASY pure LF, Mandel Scientific co, model BDI-D7381).

Safety Precautions

Due to the possible health risk associated with H_2S gas, all efforts and safety precautions were considered. The first step was to ensure that no H_2S gas leaked through the system as it was tightly closed. The system was equipped with close ventilation through fume hood and the H_2S

concentration in the lab was monitored through Odalog hydrogen sulfide logger obtained from App-Tek Inc (Brandale, Queensland, Australia). The logger has a measuring range of 0-1000 ppm at an accuracy of 1% of the full scale, and equipped with Odalog 3 software for downloading of data in tabular or graphical form to highlight significant variations in recorded hydrogen sulfide levels over time.

Catechol and Starch Co-gasification Experiments: Starch $(C_6H_{10}O_5)_n$, catechol ($C_6H_6O_2$), calcium oxide powder (CaO) with a purity of 99%, and TiO_2 catalyst were obtained from Sigma-Aldrich Canada Ltd. (Oakville, Ontario, Canada). De-ionized water (18 m·Ω resistivity) was obtained using a compact ultrapure water system (EASY pure LF, Mandel Scientific co, model BDI-D7381).

Starch and catechol solutions were individually prepared with concentrations of 9,000, and 18,000 mg/L respectively. Each solution and the mixture of starch and catechol were prepared by using purified water by mechanical mixing and heating. The prepared feed samples were kept well mixed until delivered to the syringe pump where they were subsequently pressurized and injected into the reactor. As shown in Table 3.1, in experiments 1, 2, and 3, starch was gasified alone at 400, 450, and 500°C, and catechol was gasified alone in experiments 4, 5, and 6 at the same temperature levels. Experiments 7, 8, and 9 were performed with different mixtures of starch and catechol.

Table 3.1 Experimental testing conditions.

Exp No.	Time (min)	Temp (°C)	Catalyst	TOC (mg/L)	Starch	Catechol
1	30	400	None	9000	√	None
2	30	450	None	9000	√	None
3	30	500	None	9000	√	None
4	30	400	None	18000	None	√
5	30	450	None	18000	None	√
6	30	500	None	18000	None	√
7	30	500	None	10900	0.8	0.2
8	30	500	None	12100	0.6	0.4
9	30	500	None	14400	0.4	0.6
10	30	500	CaO	14400	(40 % Starch +60 % Catechol)	
11	30	500	TiO_2 (nano-powder)	14400	(40 % Starch +60 % Catechol)	
12	30	500	TiO_2 (nano-powder) + CaO	14400	(40 % Starch +60 % Catechol)	
13	30	500	None (Repeat exp 12)	14400	(40 % Starch +60 % Catechol)	
14	30	400	Opt	14400	(40 % Starch +60 % Catechol)	
15	30	425	Opt	14400	(40 % Starch +60 % Catechol)	
16	30	450	Opt	14400	(40 % Starch +60 % Catechol)	
17	10	400	Opt	14400	(40 % Starch +60 % Catechol)	
18	10	425	Opt	14400	(40 % Starch +60 % Catechol)	
19	10	450	Opt	14400	(40 % Starch +60 % Catechol)	
20	20	400	Opt	14400	(40 % Starch +60 % Catechol)	
21	20	425	Opt	14400	(40 % Starch +60 % Catechol)	
22	20	450	Opt	14400	(40 % Starch +60 % Catechol)	
23	20	500	Opt	14400	(40 % Starch +60 % Catechol)	
24	20	500	Opt	14400	(40 % Starch +60 % Catechol)	

Opt ≡ (TiO_2 (nano-powder) + CaO)

Sequential Gasification and Partial Oxidation Experiments: Hog manure was obtained from a facility in South Western Ontario used as the feed characterized by a total and soluble chemical oxygen demand, Volatile suspended solids, and ammonia. Table 3.2 shows the characteristics of hog manure used in this study. 5% ruthenium supported on alumina and 5%

rutheniums supported on carbon catalysts were purchased from Alfa Aesar (Ward Hill, MA, USA). Alkali NaOH reagent grade and 5% palladium supported on carbon catalysts were obtained from Sigma-Aldrich Canada ltd (Oakville, Ontario, Canada). Activated carbon was purchased from Caledon Laboratories Ltd (Georgetown, Ontario, Canada).

Table 3.2 Hog manure characteristics

characteristic	Conc (mg/L) Ave ± STD	No. of Samples
Total Oxygen Demand (TCOD)	56850 ± 3565	6
Soluble Oxygen Demand (SCOD)	28000 ± 2743	6
Total Suspended Solids (TSS)	24980 ± 1430	6
Volatile Suspended Solids (VSS)	18960 ± 1066	6
Ammonia (NH_4)	2400 ± 90	6
Nitrate	0.7 ± 0.1	6
Sulfate	92 ± 7	3
TKN	4700 + 345	6
Alkalinity	9615 ± 90	6
Volatile Fatty acids (VFAs)	12931 ± 1870	6
Total Phosphorous (PO4-)	5545 ± 622	6

3.4 Gas Analysis

The gas products were analyzed by gas chromatograph (Shimadzu, GC-2014) equipped with a thermal conductivity detector and 120/80 D Hayesep stainless steel Nickel packed column (Grace Davidson) having dimensions of (6.2 m x 3.18 mm). Helium was used as the carrier gas, and the GC was calibrated using a standard gas mixture of known composition containing H_2, CO, CO_2, CH_4, C_2H_4, C_2H_6 supplied by Matheson tri-gas Co (OH, U.S.A), and H_2S standard gas supplied by Concept Controls Inc. (Mississauga, ON, Canada). The analysis was performed

manually using 1ml SGE gas tight syringe (Model number 008100, Reno, NV USA) by collecting the sample from the gas bag. The analysis was performed at least three times for each sample to minimize experimental error, and gas was measured at room temperature and pressure. . For the H_2S analysis during cysteine experiments, the same column was employed with helium as a carrier gas at a flow rate of 30 ml/min. The temperatures of the column and detector were 60 and 140°C, respectively. The analysis was performed manually using 50uL SGE gas tight syringe (Model number 004200, Reno, NV USA).

3.5 Liquid Analysis

The organic content of the process liquid effluent was examined using three independent procedures i.e. Chemical Oxygen Demand (COD), Volatile fatty acids (VFA's), and pH. Total and soluble chemical oxygen demand (TCOD, SCOD) were measured using HACH methods and test kits (HACH Odyssey DR/2500). Individual VFAs were analyzed by a gas chromatograph (Varian 8500) with a flame ionization detector (FID) equipped with a fused silica column (30 m x 0.32 mm).Helium was used as a carrier gas at a flow rate of 5 ml/min. The temperatures of the column and detector were 110, 250°C, respectively. For alcohol measurement, the same instrument with a refractive index detector (RID) was used. pH was measured using OAKTON portable pH meter (Model WD-35615-22). For carbon balance closure requirements, the effluent liquid total organic carbon (TOC) was measured using a Shimadzu TOC-VCPH TOC analyzer. The liquid effluent samples were extracted four times with aliquots of dichloromethane in order to identify components using GC/MS. The extraction was performed by first adjusting the pH to 2 using 0.6M HCl followed by placing the sample in a 300 ml separatory funnel. The extracted samples were left in the separatory funnel for one hour after which the immiscible phases were separated. The organic extract was kept in air tight glass vials for further analysis.

The compounds present in the liquid samples were further identified using a Varian 3400 GC/MS fitted with a 30m long, and 0.32 mm internal diameter DB-5ms capillary column, and a film thickness 0.25 μm. The GC-MS was coupled to a Finnigan MAT 8400 ion-trap detector. The oven temperature was programmed as follows: 45°C (hold for 3 min) and raised at 5°C/ min to 310°C (hold for 3 min); the injector and the detector were operated at 250°C. Compound identification was performed by employing an automatic comparison of the derived ion mass spectra to spectral libraries using HP Chemstation software using similarity indexes (SI) of greater than 75 %.

Oleic acid

Long chain fatty acids (LCFA's), namely, palmitic, myristic, stearic, linoleic, and oleic acid were determined using a calibrated Agilent gas chromatograph equipped with a flame ionization detector (FID) and an HP-5 capillary column 30m long, 0.25mm internal diameter with a film thickness of 0.25 μm. The oven temperature was programmed as follows: 100°C (hold for 2 min) and rose at 10°C/ min to 250°C. The injector and detector were operated at 250°C; while Nitrogen was used as the carrier gas at a flow rate of 1.9 ml/ min and a pressure of 11.2 psi.

Cysteine

For sulfur balance purposes, total dissolved sulfide (S^{2-}) was analyzed by the iodometric titration method (APHA, 1998), and dissolved sulfate (SO_4^{2-}) was measured using ion chromatograph (Model Dionex ICS-3000).

Manure

During hog manure gasification, the experimental procedure was quite different than the regular procedure during model compounds SCW gasification experiments. It consisted of opening and washing the reactor thoroughly with (4:1) acetone-water mixture to collect any residual carbon

from previous experiments. The mixture was used to recover both the catalyst and the unconverted carbon. Two phases were observed in the recovered mixture, the catalyst at the bottom and the treated liquid containing the residual contaminant. The catalyst was then recovered by filtration using 0.45 μm sterile membrane filter (Catalog. No 7141104, Whatman Limited, Maidstone, England). Following the recovery of the solid catalyst, the acetone-water mixture containing the residual contaminant was allowed to evaporate at 105°C for 12 hours in a furnace (Sheldon Manufacturing Inc, Model 1350GM, Cornelius, OR, USA).

After evaporation, the solid of acetone-water mixture was collected, weighed, and then analyzed using thermo-gravimetric analysis technique. The apparatus used for thermo-gravimetric analysis was acquired from THE M&P LAB Co (Model TA SDT Q600, NY, USA). Samples of approximately 20 milligrams were placed in 90μL alumina pans and placed in the apparatus. The samples were run using dual Sample Mode in a Nitrogen atmosphere (100mL/min) at a rate of 20°C/min from room temperature to 800°C. The resulting data was analyzed in the form of weight percent versus temperature. Since carbon burns at temperatures below the 800°C used in the test, the weight of carbon in the sample i.e. the carbon left in the reactor excluding the catalyst and support (which was removed by filtration), was calculated as the initial weight less than the final residual after thermo-gravimetric analysis. Subsequently in order to assess the COD balance, the residual carbon was converted to COD using a factor of 2.7 gCOD/gcarbon. All other analyses (TCOD (total chemical oxygen demand), SCOD (soluble oxygen demand), TSS (total suspended solids), VSS (volatile suspended solids), ammonia, nitrate, sulfate, VFA (volatile fatty acids), glucose, proteins, and pH.) were performed according to standard methods for the examination of water and wastewater (APHA and AWWA, 1992) and the references are as follows:

TSS - Method 2540 D of the standard methods (Standard, 1992)

VSS - Method 2540 E of the standard methods (Standard, 1992)

COD - Method 5220 D of the standard methods (Standard, 1992)

SP - Method 10227 developed by HACH

NH_3 - N - Method 10031 developed by HACH

NO_3^--N - Method 10020 developed by HACH

Protein - Lowry et al., (1951) method with BSA as standard

Glucose - Dubois et al. (1956) method

Volatile fatty acids (VFA's) were analyzed using the following procedure:

The sample was filtered through a 0.45-μm membrane and 1.5 ml of filtered sample was analyzed by a gas chromatograph (Varian 8500) with a flame ionization detector (FID) equipped with a fused silica column (30 m x 0.32 mm).Helium was used as a carrier gas at a flow rate of 5 ml/min. The temperatures of the column and detector were 110, 250°C, respectively. For alcohol measurement, the same instrument with a refractive index detector (RID) was used.

CHAPTER 4

Effect of Nickel Loading on Hydrogen Production and Chemical Oxygen Demand (COD) Destruction from Glucose Oxidation and Gasification in Supercritical Water

4.1 Background

In this chapter, gasification and partial oxidation of glucose was conducted with and without catalysts at various temperatures in supercritical water. The effects of nickel type catalyst, oxidant molar ratio, catalyst support, and the amount of catalyst were investigated. This chapter was published in the International Journal of Hydrogen Energy, and following below is the published version of this work.

4.2 Introduction

With increasing public awareness about the environmental impact of fossil fuels as well as their depletion, hydrogen production from biomass is considered as one of the most effective routes towards a sustainable future. This comes from the fact that the CO_2 produced from gasification is balanced by photosynthesis through biomass growing period. However, the water content of biomass is generally high, in the range of 90 % or even higher, and the thermo-chemical conversion needs a prior drying process which, in turn, consumes a large amount of energy. Supercritical water oxidation (SCWO) is an emerging technology that has been developed to treat hazardous wastewater streams as well as producing green gases such as hydrogen. Supercritical water can dissolve most organic substances and gases and has low viscosity and strong transport ability. Above the critical point of water (374°C, 22.13 MPa) all organic compounds, and oxygen are present in a single, dense fluid phase, minimizing mass-

transfer resistance while providing rapid reaction rates. Gaseous product composition from supercritical water gasification of glucose significantly depends on the reactant concentration [1] and temperature [2, 3, and 4]. In recent decades, there has been a lot of studies carried out on the gasification of wet biomass [1, 3,5,6,7, and 8], and aqueous organic wastes [9,10, and 11] in supercritical water. Enhancement of biomass conversion through oxidation in supercritical water [2, and 12] or partial oxidation [13, 14, and 15] has also been studied.

The catalyst plays an important role in hydrogen production from biomass gasification in supercritical water. Watanabe and co-workers [14] studied the effect of different catalysts on the gasification of biomass model compounds in a batch reactor at a temperature range of 400-440°C and achieved yield ranges of 25-45% of the theoretical. However, Yu and Antal [1] reported that the achievement of 95 % or above in supercritical water requires a reaction temperature above 600°C. Courson et al. [16] and Wang et al. [17] reported that Nickel catalysts are expected to crack tar and promote the water-gas shift, methanation, and hydrogenation reactions. From an economic and energy efficiency point of view, high gasification efficiency at low temperature with enhanced hydrogen production is favorable. Nickel has a higher melting point of 1453°C and is readily available cheap metal which makes it a suitable and reasonable choice for supercritical water gasification and oxidation. Homogeneous catalysts such as KOH and NaOH can easily dissolve in SCWG to produce hydrogen-rich gas, although many cause corrosion of the reactor walls [5]. Minowa et al. [18] reported that reduced nickel catalyst enhanced the gasification of cellulose and the water gas shift reaction in hot compressed water.

In this study, we demonstrate a new approach for introducing hydrogen peroxide as an oxygen source after 15 minutes of reaction time for glucose gasification in supercritical water. Hydrogen peroxide can help to decompose aromatic rings by radical reactions that are not

gasified during supercritical water gasification (SWG) in the first 15 minutes of reaction time [19]. The yield of hydrogen is expected to increase via CO formation by partial oxidation as these intermediate products as well as char and tar are formed during the last 15 minutes of operation in the reactor. In this work, different loadings of nickel on theta(θ) and gamma(γ) alumina catalysts were synthesized via an impregnation method [20] and were tested for supercritical water gasification (SCWG) and supercritical water partial oxidation (SWPO) at a temperature range 400, 450, and 500°C to investigate catalytic ability for hydrogen production.

4.3 Materials and Methods

4.3.1 *Materials*

Glucose was obtained from the Sigma-Aldrich chemical company and used without any further purification. Reduced commercial nickel on silica alumina was also obtained from the Sigma-Aldrich chemical company (Oakville, Ontario, Canada). Hydrogen peroxide aqueous solution (50% H_2O_2 solution) was obtained from EMD Chemicals Inc (Gibbstown, NJ, U.S.A). De-ionized water obtained from a compact ultrapure water system (EASY pure LF, Mandel Scientific co, model BDI-D7381).

4.3.2 *Catalyst preparation*

Catalyst synthesis by incipient wetness impregnation method was described elsewhere [20]. For a typical synthesis, the required metal-salt solution was prepared with pure water of 115 vol % of pore volume of alumina used for catalyst support. All alumina was dipped into the solution at once for uniform metal dispersion. The sample was dried after impregnation at constant rate of temperature rising from room temperature to 60°C for 2 hours. The sample was then placed in a closed beaker for NH_3-H_2O treatment without dissolving for 10 minutes at 60°C. Metal salt anion converts to ammonium salt by amoniacal treatment which increases the activity

and metallic Ni dispersion [21]. The NH_3-H_2O vapor treated catalysts were then dried from 60 to 120°C for 2 hours, and then temperature was elevated up to 250°C for 1.5 hour. In this step most of the ammonium salts removed by sublimation of nitrate. Hydrogen reduction and thermal treatment to 550°C for two hours was done afterwards, in a stream of 10 vol % H_2 diluted with N_2 with a rate of 6 L/h. The rate of temperature increment from room temperature was 3°C /min. The BET (Brunauer-Emmett-Teller) surface area, pore size, and pore volume were determined from nitrogen adsorption- and desorption isotherm data obtained at -196°C Micromeritics ASAP 2010 using N_2 gas. The prepared samples were degassed at 150°C for 5 hours before measurements. Table 4.1 portrays the summary of surface area, pore size and pore volume of gamma (γ) and theta (θ) alumina and synthesized catalysts. The calcination of γ-alumina at 1050°C converts it to θ-alumina, which has a higher stability at high temperature and pressure.

The collapse of some pores during the calcination process results in lowering the surface area and pore volume.

Table 4.1 Physical properties of the synthesized catalysts

Sample	**BET surface area (m^2/g)**	**Average pore size (nm)**	**Micropore volume (cm^3/g)**
γ-alumina	198	8.5	0.42
θ-alumina	57	17.4	0.25
7.5wt%Ni/θ-alumina	51	14.0	0.18
11wt% Ni/θ-alumina	49	15.8	0.19
18wt% Ni/θ-alumina	46	10.2	0.12
63 wt % Ni/silica-alumina commercial catalyst (powder)	190	N/A	N/A

Increasing the Nickel loading decreases the surface area due to some pores blocking by metallic nickel. During the Nickel loading from 7.5 wt% Ni to 11 wt% Ni, the surface area is decreased from 51 m^2/g to 49 m^2/g whereas the average pore size and volume increased. Some inter-crystalline pores formed due to the deposited metallic nickel which contributes to the average pore size and volume. However, further increasing the metallic loading decreased the catalyst surface area, pore size and pore volume, as extra metallic Nickel blocks the pores of catalysts as well as those created by loaded inter-crystalline metallic nickel.

4.3.3 *Gas Analysis*

The gas products were analyzed by gas chromatography (Shimadzu, GC-2014) equipped with a thermal conductivity detector and 120/80 D Hayesep stainless steel Nickel packed column (Grace Davidson) having dimensions of (6.2 m x 3.18 mm). Helium was used as the carrier gas, and the GC was calibrated using a standard gas mixture of known composition containing H_2, CO, CO_2, CH_4, C_2H_4, C_2H_6 supplied by Matheson tri-gas Co (OH, U.S.A), and H_2S standard gas supplied by Concept Controls Inc. (Mississauga, ON, Canada). The analysis was performed manually using 1ml SGE gas tight syringe (Model number 008100, Reno, NV USA) by collecting the sample from the gas bag. The analysis was performed at least three times for each sample to minimize experimental error, and the gas was measured at room temperature and pressure. For the H_2S analysis during cysteine experiments, the same column was employed with helium as a carrier gas at a flow rate of 30 ml/min. The temperatures of the column and detector were 60 and 140°C, respectively. The analysis was performed manually using 50uL SGE gas tight syringe (Model number 004200, Reno, NV USA).

4.3.4 *Liquid Analysis*

The organic content of the process liquid effluent was examined using three independent procedures i.e. Chemical Oxygen Demand (COD), Volatile fatty acids (VFA's), and pH. Total and soluble chemical oxygen demand (TCOD, SCOD) were measured using HACH methods and test kits (HACH Odyssey DR/2500). Individual VFAs were analyzed by a gas chromatograph (Varian 8500) with a flame ionization detector (FID) equipped with a fused silica column (30 m x 0.32 mm). Helium was used as a carrier gas at a flow rate of 5 ml/min. The temperatures of the column and detector were 110, 250°C, respectively. For alcohol measurement, the same instrument with a refractive index detector (RID) was used. pH was measured using OAKTON portable pH meter (Model WD-35615-22). For the carbon balance closure requirements, the effluent liquid total organic carbon (TOC) was measured using a Shimadzu TOC-VCPH TOC analyzer. The liquid effluent samples were extracted four times with aliquots of dichloromethane in order to identify components using GC/MS. The extraction was performed by first adjusting the pH to 2 using 0.6M HCl followed by placing the sample in a 300 ml separatory funnel. The extracted samples were left in the separatory funnel for one hour after which the immiscible phases were separated. The organic extract was kept in air tight glass vials for further analysis.

The compounds present in the liquid samples were further identified using a Varian 3400 GC/MS fitted with a 30m long, and 0.32 mm internal diameter DB-5ms capillary column, and a film thickness 0.25 μm. The GC-MS was coupled to a Finnigan MAT 8400 ion-trap detector. The oven temperature was programmed as follows: 45°C (hold for 3 min) and raised at 5°C/ min to 310°C (hold for 3 min); the injector and the detector were operated at 250°C. Compound identification was performed by employing an automatic comparison of the derived ion mass

spectra to spectral libraries using HP Chemstation software using similarity indexes (SI) of greater than 75 %.

4.3.5 *Yield calculations*

The product gas yield and carbon balance was calculated using the procedure of Xu and Antal [1]. The aforementioned authors calculated the carbon balance as (carbon balance = (total carbon in gas)/ (carbon in feed)) and measured gas yields (yield = (mol of gas species produced)/ (mol of glucose in feed)). The maximum theoretical hydrogen amount that can be produced from glucose ($C_6H_{12}O_6$) following the method proposed by Cortright et al. [22] is 12 moles of H_2 corresponding to 6 CO_2 and 6 CO formed from glucose through partial oxidation. The latter reacts with H_2O to produce another 6 mol H_2 through the water-gas shift reaction. Both equations through which the hydrogen produced are glucose steam reforming reactions:

$$C_6H_{12}O_6 + 6H_2O \rightarrow 6CO_2 + 12H_2 \quad (1)$$

and the water-gas shift reaction

$$CO + H_2O \rightarrow CO_2 + H_2 \quad (2)$$

4.4 Results and discussions

4.4.1 *Effect of Molar Ratio (M.R) and temperature on gas and liquid product distribution*

A series of non-catalytic partial oxidation experiments (A, B, C, and D) were conducted at 400°C at different molar ratios (MR) to optimize the maximum hydrogen yield in the product gas (Figure 4.2a). Runs A1 and F1 which are duplicates of A and F illustrate the reproducibility of the experimental data. The maximum yield of hydrogen was observed at a MR of 0.8 as well as the highest amount of CO (experiment C). This MR of 0.8 was selected because it provided the highest hydrogen and CO yields that could help promote the water-gas shift reaction for more

hydrogen production (equation 4). The CO_2 yield at a MR of 0.8 was higher than 0.5 and 0.7, but lower than 0.9, which is attributed to the availability of oxygen to convert CO to CO_2 by direct oxidation. The optimized MR of 0.8 was selected as a base line for the higher temperatures of 450 and 500°C. The effect of temperature on the partial oxidation without catalyst is depicted in figure 4.2a (experiments E, and F). By increasing the temperature from 400 to 500°C, the hydrogen yield increased from 0.2 to 0.5 mol/mol glucose, which is attributed to the higher conversion at higher temperatures [27]. The CO_2 and CH_4 yields also increased whereas the CO remains almost the same similar to the reported results by Holgate and Tester [2].

Accordingly, 500°C and a MR of 0.8 were selected as the base-line conditions for the catalytic experiments. Based on the work of Lee et al [8], the CO concentration increased and the hydrogen yield decreased at a reaction temperature below 650°C due to the endothermic reforming reaction by the organic acid formation.

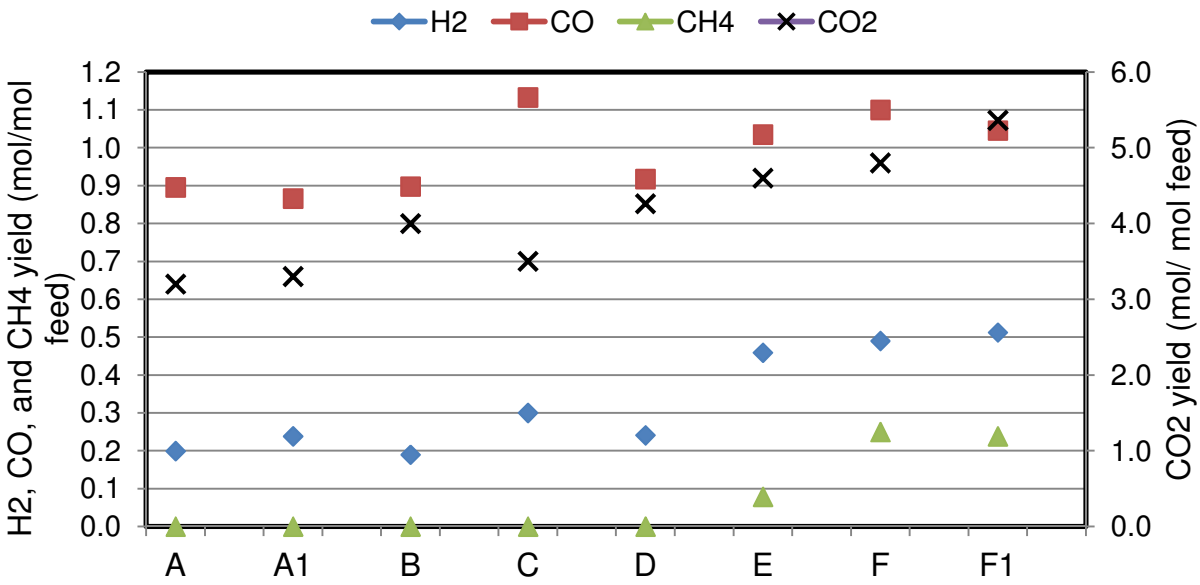

A; T=400°C; MR= 0.7; B; T=400°C; MR= 0.5; C; T= 400°C; MR= 0.55; D; T= 400°C; MR= 0.9; E; T= 450°C; MR= 0.8; F; T= 500°C; MR= 0.8. (A1 is reproducibility, and F1 is F reproducibility

Fig 4.2a Gas yield in the non-catalytic partial oxidation experiments

The COD reduction efficiency was above 90% in all experiments except for experiments A and B where it was 76% and 85%. The lower COD reduction efficiency is explained by the lower MR of 0.5 used and eventually the lack of oxidant.

The main aim of tracking the VFA's is to help identify the intermediate products, facilitate the understanding of reaction mechanisms, and eventually the development of kinetic models required for reactor design. Shanableh et al. [25] reported the formation of acetic acid as one of the residual main intermediates during SCWO and wet air oxidation of organic wastes. Table 4.2 provides the liquid effluent characteristics results. Moreover, the VFA's concentration observed in experiment (B) was more than 2.5 times compared to the other experiments. This is illustrated clearly in Figure 4.2b in which the distribution of VFA's and ethanol is depicted.

Acetic acid was the main component in all experiments with also significant concentrations of propionic acid. Based on the comparison between experiments A, B, C, and D, all of which were run at 400°C but different MR ratios, it is evident that the residual VFA's decrease with increasing MR in the range of 0.5-0.9.

Table 4.2 Liquid effluent characteristics in the non-catalytic partial oxidation experiments.

Experiment	TCOD (mg/L)	SCOD (mg/L)	VFA's (mg/L)	pH	Carbon Gasification efficiency (%)	COD reduction efficiency (%)
A	7942	6360	748	3.2	67	83
A1	7376	6462	717	3.3	69	85
B	11554	11045	2358	3	82	76
C	4836	4734	963	3.2	77	90
D	1680	1527	428	3.3	86	97
E	3512	3003	710	3.2	95	93
F	4479	4428	882	3.3	87	91
F1	4764	4031	779	3.3	102	90

4.4.2 *Effect of M.R and commercial catalyst amount on gas and liquid product distribution*

Experiments (G, H, I, and J) were conducted to investigate the effect of MR and catalyst amount on the product distribution as well as to compare the gas yields between the commercial catalyst and the synthesized one (Figure 4.3). In experiment G, the hydrogen gas yield was almost the same as without catalyst, which is attributed to the potential inhibition of catalyst activity by oxidation of metallic Ni on the catalyst surface. Therefore, the experimental procedure of injecting the hydrogen peroxide (H_2O_2) prior to the feed was manipulated by delaying the injection of the oxidant for 15 minutes (that is, the feed was injected first and after 15 minutes, the oxidant was injected). By using this procedure, catalyst inhibition could be mitigated and potentially more hydrogen could be obtained by oxidizing the intermediate products. This methodology increased the hydrogen yield from 1.1 to 1.5 mol/mol glucose (experiments I, and J).

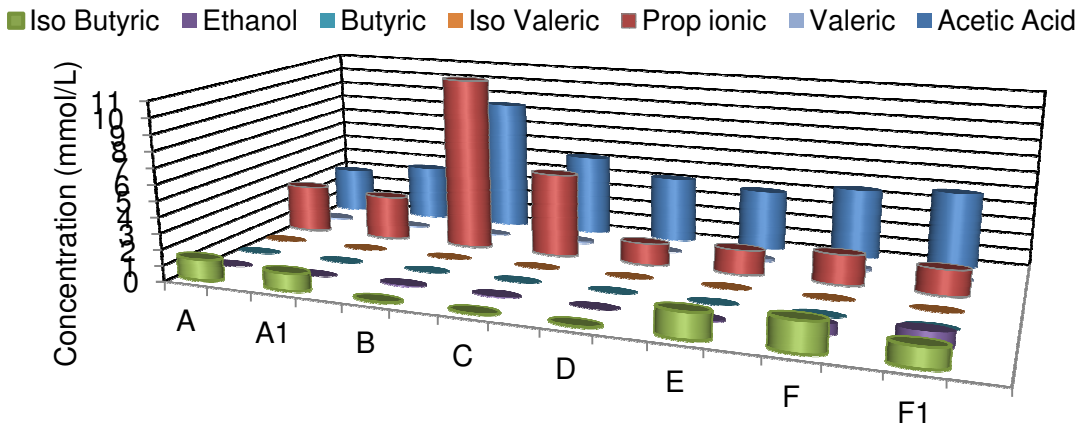

Fig 4.2b VFA's and ethanol concentration distribution in the non-catalytic partial oxidation experiments

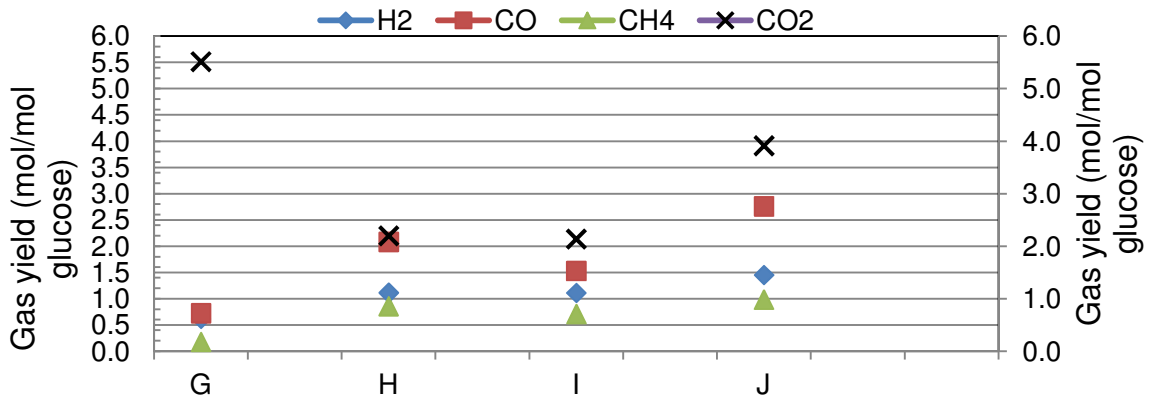

G; MR = 0.8; catalyst amount = 0.5 g; H; MR = 0; catalyst amount = 0.5 g; I; MR = 0; catalyst amount = 1 g; J; MR = 0.8; catalyst amount = 1 g. (H_2O_2 injected after 15 min except experiment G in which H_2O_2 was injected before the feed).

Fig. 4.3 Gas yield with the experiments of commercial Ni/silica alumina catalyst (65 wt % Ni Loading) at 500°C

This partial oxidation of the formed carbon species (tar and char) to form CO by the oxidant; with the CO reacting with the adsorbed methane on the catalyst surface dissociates to produce hydrogen [23]. Carbon monoxide may also undergo the water gas shift reaction catalyzed by Ni to produce more hydrogen. Comparing gasification results using 0.5 and 1 g of catalyst (experiments H and I) showed that the amount of catalyst had no influence on the H_2 fraction in the gaseous products.

The liquid effluent characteristics are reported in Table 4.3. In the presence of metallic catalyst with no oxygen (i.e. MR=0), the COD destruction efficiency was 78 % for both 0.5 g and 1 g of Ni commercial catalyst (experiments H and I). At a MR of 0.8 in experiment (J) the hydrogen yield increased from 1.1 in experiment (I) to 1.5 mol/mol glucose and the COD reduction efficiency increased from 78% to 82%. On the other hand, the reduction of VFA's and TCOD concentration indicates that the presence of oxygen promotes the gasification process. This is confirmed by the higher yield of gases as well as lower liquid effluent TCOD in experiment J compared to I.

Table 4.3 Liquid effluent characteristics in the experiments of commercial Ni/silica alumina catalyst (65 wt %Ni Loading) at 500°C.

Experiment	TCOD (mg/L)	SCOD (mg/L)	VFA's (mg/L)	pH	Carbon Gasification efficiency (%)	COD reduction efficiency (%)
G	2545	2189	729	3.2	107	95
H	10587	9009	5468	3.2	90	78
I	10791	10027	6565	3.2	82	78
J	8467	8755	4538	3.3	109	82

The behavior of individual VFA's was monitored in all experiments (Figure 4.4). In experiment (G), the (H_2O_2) was injected before the feed; thus, the H_2O_2 dissociated and produced oxygen. The very low yield of all VFA's can be attributed to faster the oxidation reaction rates relative to the hydrolysis rate, as confirmed by the higher amounts of acetic and iso-butyric acids produced in the absence of oxygen (MR=0) in experiments (H and I) .

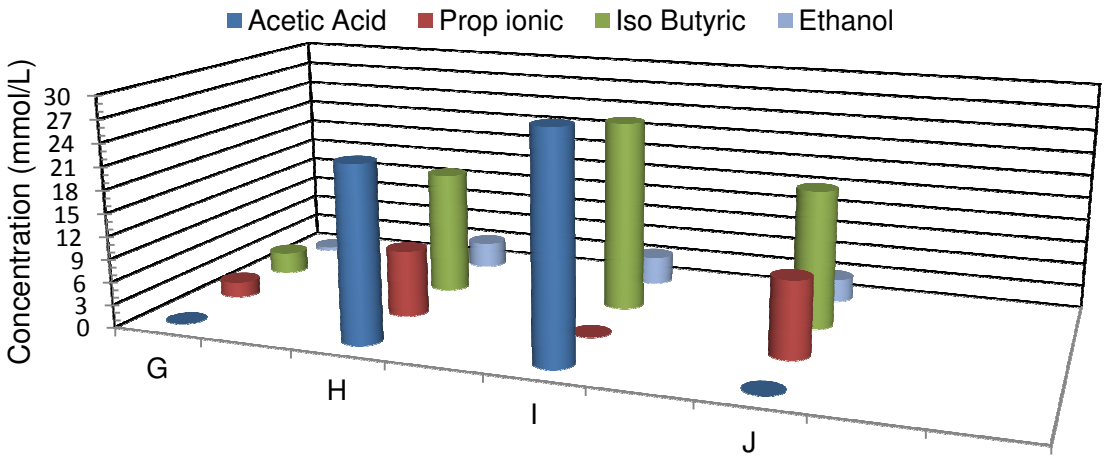

Fig 4.4 VFA's and ethanol concentrations distribution with commercial Ni/silica-alumina catalyst.

The increase in the catalyst mass from 0.5 g in experiment H to 1 g in experiment I led to almost complete disappearance of propionic acid and an increase in the concentration of iso-butyric acid. In experiment (J), the MR of 0.8 decreased the VFA's concentration and increased the gas yield. Meanwhile, Holgate et al [2] found that the stability of intermediate soluble products in glucose hydrolysis and oxidation varied considerably except for acetic acid, propenoic acid, and acetaldehyde. On the basis of the aforementioned reported data, it is hypothesized that the presence of oxidant slightly contributes to the decrease of both TCOD, and VFA's concentration by oxidizing the water soluble intermediates to gases such as H_2, CH_4, and CO.

4.4.3 *Effect of the synthesized catalyst mass and nickel loading on gas and liquid product distribution*

Figure 4.5 portrays the effect of the synthesized metallic Ni/alumina supports on the gas yield. The maximum yield of hydrogen that coincided with the maximum COD reduction efficiency was observed at 11 wt % Ni loading, and the trend of hydrogen yield was similar to that reported for gasification of lignin using Ni/MgO [24] where the H_2 yield increased from 1.9 to 11 % by increasing the amount of nickel deposited on MgO from 5 to 15 wt% Ni/MgO. However, as the amount of deposited nickel increased to 20 wt%, the H_2 yield decreased to 9.3%. To investigate the effect of active metal surface area, the 18 wt% Ni/θ alumina catalyst was crushed to a smaller mesh size and employed in experiment (P), in which the hydrogen yield increased significantly from 0.9 to 1.2 mol/mole glucose.

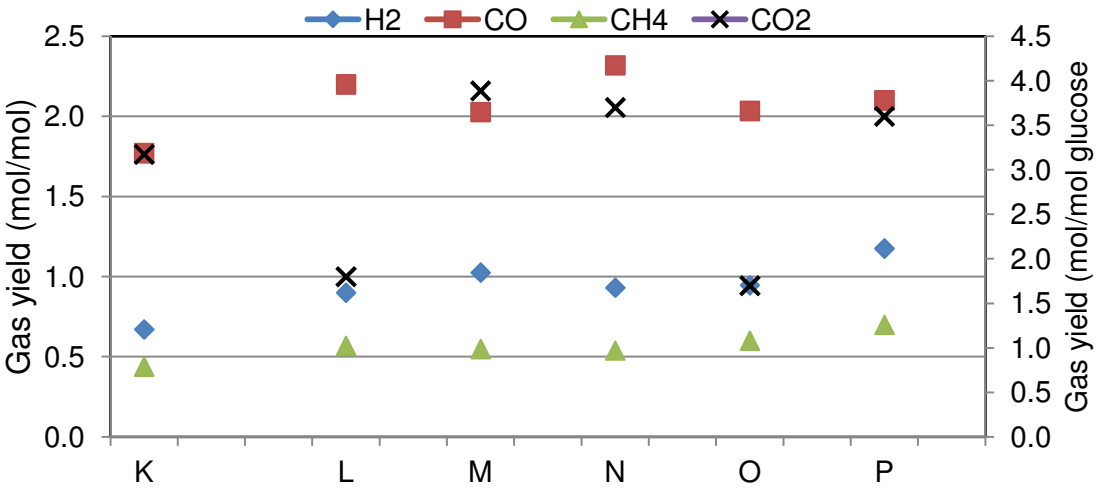

K; MR = 0.8; 0.5 g 7.5 wt% Ni/ θ alumina; L; MR = 0.55; 1.0 g 7.5 wt% Ni/ θ alumina; M; MR = 0.8; 1.0 g 7.5 wt% Ni/ θ alumina; N; MR = 0.8; 1.0 g 7.5 wt% Ni/γ alumina; O; 1.0 g 18 wt% Ni/ θ alumina: P; MR= 0.8;1.0 g crushed 11 wt% Ni/ θ alumina. (H_2O_2 injected after 15 min except experiment K in which H_2O_2 was injected before the feed)

Fig 4.5 Gas yield in the experiments of synthesized Ni/alumina catalyst at 500°C

It was also noted that an increase in Ni loading to 18 wt% (experiment O) resulted in a sharp decrease in CO_2 yield with a slight increase in methane formation. This is possibly because of the reaction of CO_2 with hydrogen to form methane which could have consumed some of the hydrogen and eventually decreased its yield. The effect of catalyst support (experiments M and N) was found to be insignificant. As apparent from Table 3.4, the increase of MR from 0.55 to 0.8 with the presence of 1.0 g 7.5 wt % synthesized Ni/ alumina catalyst increased the COD reduction efficiency sharply from 66% to 88 % (experiments L and N). An increase in the catalyst amount from 0.5 to 1.0 g had no influence on the COD reduction efficiency (experiments K and N). Interestingly, increasing the catalyst surface area increased the hydrogen yield although did not affect any change in the COD destruction efficiency.

Table 4.4 Liquid effluent characteristics in the experiments of synthesized Ni/alumina catalyst at 500°C.

Experiment	TCOD (mg/L)	SCOD (mg/L)	VFA's (mg/L)	pH	Carbon Gasification efficiency (%)	COD reduction efficiency (%)
K	6413	5803	1734	3.4	90	87
L	16783	16583	2725	3.1	75	66
M	5941	6193	2976	3.2	106	88
N	5287	5387	2626	3.2	107	88
O	6420	6273	2917	3.1	95	87
P	4876	4987	2633	3.1	107	90

Based on the reported work of Yu et al [1] and Holgate et al [2], glucose decomposition in SCW has two pathways i.e. both high and low temperature pathway. In the high temperature pathway, glucose reforms and produces CO_2 and H_2. The formation of CO_2 and H_2 comes from the reaction of unstable free radicals with water which is given by Equation 3. The low temperature pathway occurs at temperatures levels from 400 to 600°C which is our temperature range. This pathway proceeds through the formation of acetic acid, propionic acid, and acetaldehyde. The formed intermediates then further decompose to CO_2, CO, H_2, and small amounts of CH_4.The distribution of the individual VFA's reported in Figure 4.6 is in good agreement with the low temperature glucose decomposition pathway. On the other hand, the individual VFA concentrations in experiment (K) were lower than the other experiments, which reveals that the increase in the catalyst mass favors the formation of VFA's and intermediate components.

The free-radical oxidation reaction mechanism adds (OOH) to organic fragments that helps form VFA's [30]. At a MR of 0.8 and 1g catalyst mass (experiments M, N, O, and P), the acetic acid concentration was almost constant at different nickel loadings. Moreover, propionic and iso-butyric acid concentration had insignificant variation in all experiments. Goodwin and Rorrer [33] reported that acetic, butyric, and propionic acids are the major intermediate species obtained for the decomposition of glucose. The presence of CH_4 in the gas products at all conditions supports the conclusion that glucose was being decomposed through acid intermediates [33]. According to Lu et al [6], CH_4 was mainly formed by free radical reactions as glucose is decomposed to gas through acid intermediates.

Comparing experiment L (with commercial catalyst) and M (with synthesized catalyst) at the same temperature, molar ratio, and catalyst mass reveals that the H_2 yield for the commercial catalyst is 50% higher than the synthesized catalyst H_2 yield, albeit with 40% and 50% higher residual COD and VFA. With crushing of the synthesized catalyst, the hydrogen yield increased by 20% to 1.2 mol/mol glucose and thus the commercial catalyst surpassed the synthesized one by only 0.3 mol/mol or 25% of the overall yield.

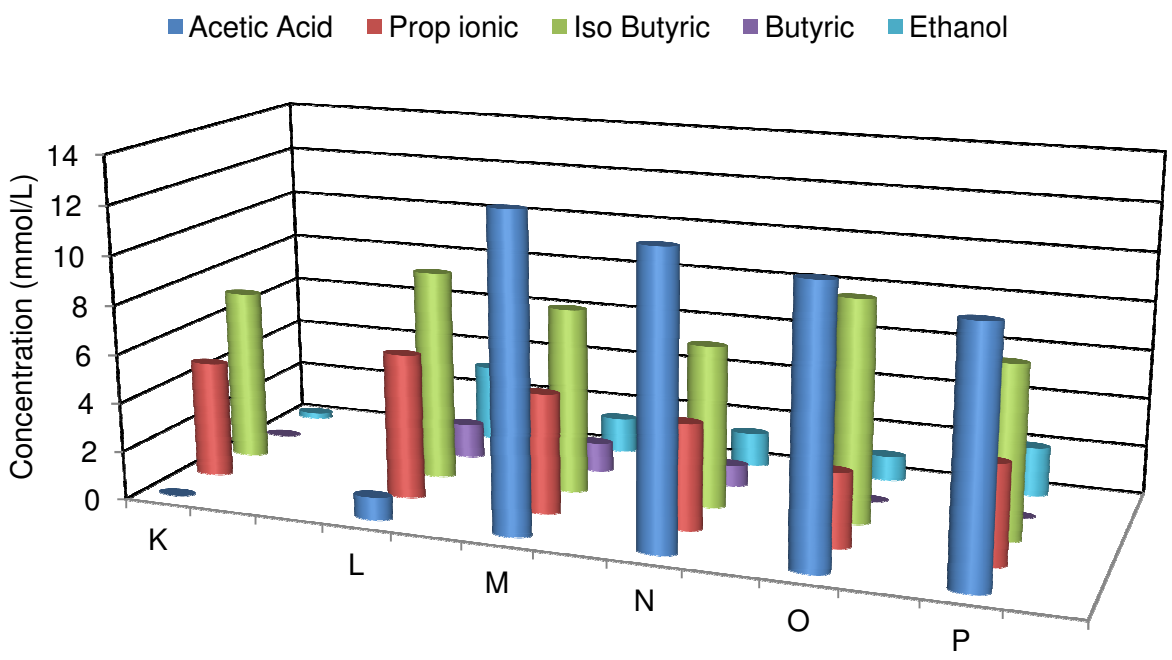

Fig 4.6 VFA's and ethanol concentrations distribution in the experiments of synthesized Ni/alumina catalyst at 500°C.

4.5 References

[1] Yu D A, Antal J Jr. Hydrogen Production by Steam Reforming Glucose in Supercritical Water. Energy & Fuels. 1993; 7: 574.

[2] Holgate H, Tester J. Glucose Hydrolysis and Oxidation in Supercritical water. AIChE J. 1995; 41: 637.

[3] Xu X, Stenberg J, Antal J Jr. Carbon catalyzed Gasification of Organic Feedstocks in Supercritical Water. Ind. Eng. Chem. Res. 1996; 35: 2522.

[4] Lee I, Ihm S K. Gasification of Glucose in Supercritical water. Ind. Eng. Chem. Res. 2002; 41: 1182.

[5] Antal J Jr, Schulman A, Xu X. Biomass Gasification in Supercritical water." Ind. Eng. Chem. Res. 2000; 39: 4040.

[6] Lu Y, Zhang X, Hao M, Yan Q H. Hydrogen production by biomass Gasification in Supercritical water: A parametric study. Int. J. Hydrogen Energy. 2006; 31: 1597.

[7] Furusawa T S, Sugito H, Miura Y, Sato M, Itoh N. Hydrogen production from the Gasification of Lignin with Nickel Catalysts in Supercritical water." Int. J. Hydrogen Energy. 2007; 32: 699.

[8] Lee I, Ihm S K. Catalytic Gasification of Glucose over Ni/Activated Charcoal in Supercritical Water. Ind. Eng. Chem. Res. 2009; 48: 1435.

[9] Blasi B, Galgano A, Meier D, Brodzinski I, Malmros O. Supercritical Gasification of Wastewater from Updraft Wood Gasifiers. Biomass & Bioenergy. 2007; 31: 802.

[10] Yan B W, Hu C H, Xi X, Wu J Z. Hydrogen Generation from Polyvinyl Alcohol-Contaminated Wastewater by a Process of Supercritical Water Gasification." J. Environ. Sci. 2007; 19: 1424.

[11] García Jarana M, Portela J R, Nebot Sanz E, Martínez de la Ossa E J. Supercritical Water Gasification of Industrial Organic wastes." J. Supercrit. Fluids. 2008; **46**: 329.

[12]Calvo L, Vallejo D. Formation of organic acids during the hydrolysis and oxidation of several wastes in sub- and supercritical water." Ind. Eng. Chem. Res. 2002; 41: 6503.

[13]Adschiri T, Sato R, Watanabe M, Arai K. Catalytic Hydrodesulphurization of Dibenzothiophen through Partial Oxidation and Water-Gas Shift reaction in Supercritical Water." Ind. Eng. Chem. Res. 1998; 37: 2634.

[14] Watanabe M, Osada M, Sato T, Adschiri T, Arai K. Catalytic Effects of NaOH and ZrO_2 for partial oxidative gasification of n-hexadecane and lignin in Supercritical Water." Fuel. 2003; 82: 545.

[15]Yoshida T. Partial Oxidative and Catalytic Biomass Gasification in Supercritical Water: A Promising Flow Reactor System." Ind. Eng. Chem. Res. 2004; 43: 4097.

[16] Courson C, Petit C, Kiennemann A. Development of Ni Catalysts of Gas Production from Biomass Gasification: Reactivity in Steam-and dry-Reforming. Catal. Today. 2000; 63: 427.

[17] Wang W, Nader P, Ye Z, Goran O, Andersson A, Ingemar B. Catalytic Hot Gas Cleaning of Fuel Gas from an Air-Blown Pressurized Fluidized-Bed Gasifier. Ind. Eng. Chem. Res. 2000; 39: 2000.

[18] Minowa T, Ogi T. Hydrogen Production from Cellulose in Hot Compressed Water Using Reduced Nickel Catalyst: Production Distribution at Different Reaction Temperatures." J. Chem. Eng. Jpn. 1998; 31: 488

[19] Martino C, Savage P. Supercritical water oxidation kinetics, products, and pathways for CH_3- and CHO- substituted phenols. Ind. Eng. Chem. Res. 1997; 36: 1391.

[20] Choudhury M, Shalabi M, Inui T. Preferential Methanation of CO in a Syngas involving CO_2 at Lower Temperature Range. Applied Catalysis A: General. 2006; 314: 47.

[21] Inui T, Saita Y, Miyake T, Takegami Y. Enhancement of Methanation Activity by Ammonia-water Vapor Treatment at the Stage of Catalyst-metal Salt Supported on a Carrier" Appl. Catal. 1982; 2: 389.

[22] Cortright R, Davda R, Dumesic J A. Hydrogen from catalytic reforming of biomass-derived hydrocarbons in liquid water. Nature. 2002; 418: 964.

[23] Au C, Wan HL. Mechanistic Studies of CH_4/O_2 Conversion over SiO_2-Supported Nickel and Copper Catalysts. J. of Catalysis. 1996; 158: 343.

[24] Sato T F, Ishiyama Y, Sugito H, Miura Y, Sato M, Suzuki N, Itoh N. Effect of Water density on the Gasification of Lignin with Magnesium Oxide Supported Nickel Catalysts in Supercritical Water. Ind. Eng. Chem. Res. 2006; 45: 615.

[25] Shanableh A, Gloyna E. Supercritical Water Oxidations of Wastewater and Sludges. Water Sci. Technol. 1991; 23: 389.

[26] Li L, Chen P, Gloyna E. Generalized Kinetic Model for Wet Oxidation of Organic Compounds. AIChE J. 1991; 37: 11.

[27] Gadhe B, Gupta R. Hydrogen production by methanol reforming in supercritical water: Catalysis by in-situ-generated copper nanoparticles. Int. J. Hydrogen Energy. 2007; 32: 2374-2381.

[28] Oshima Y, Yoshida T. Partial Oxidative and Catalytic Biomass Gasification in Supercritical Water: A Promising Flow Reactor System. Ind. Eng. Chem. Res. 2004**; 43:** 4097-4104.

[29] Shanableh A. Production of useful organic matter from sludge using hydrothermal treatment. Water Res. 1999; 34: 945–951.

[30] Shanableh A. Generalized First-Order Kinetic Model for Biosolids Decomposition and Oxidation during Hydrothermal Treatment. Environ. Sci. Technol. 2005; 39: 355-362.

[31] Yanik J, Ebale S, Kruse A, Saglam M, Yüksel M. Biomass gasification in supercritical water: II. Effect of catalyst. Int. J. Hydrogen Energy. 2008; 33: 4520-4526.

[32] Kabyemela B, Adschiri T, Malaluan R, Arai K. Kinetics of Glucose Epimerization and Decomposition in Subcritical and Supercritical Water. Ind. Eng. Chem. Res. 1997; 36: 1552.

[33] Goodwin K., Rorrer L. Conversion of Glucose to Hydrogen-Rich Gas by Supercritical Water in a Microchannel Reactor. Ind. Eng. Chem. Res. 2008*;* 47*:4106–4114.*

CHAPTER 5

Oleic Acid Gasification over Supported Metal Catalysts in Supercritical Water: Hydrogen Production and Product Distribution

5.1 Background

In this chapter, the feasibility of hydrogen production from oleic acid was investigated. Oleic acid was selected as compound that models the long chain fatty acid (LCFA) because neither lipids nor long chain fatty acids (LCFA) have been explored for hydrogen production using SCW. The effect of different noble metal doped, carbon based catalysts was studied, and the performance of some selected catalysts was also demonstrated. As the knowledge of the reaction mechanism is important for proper catalyst selection and design, the reaction pathways through change of temperature and catalysts were demonstrated and reported.

5.2 Introduction

Hydrogen is considered a promising alternative fuel with its utilization for fuel cells gaining increasing acceptance as the environmental impacts of hydrocarbon fuels become more evident [1, 2]. Hydrogen is a clean fuel as its combustion releases the chemical energy stored in the H-H bond producing water as a by-product. Currently, hydrogen production is almost 48 million metric tons per year globally from non-renewable sources such as fossil fuels [3]. Thus, gasification of waste products is gaining increasing acceptance as a carbon neutral approach to obtain sustainable hydrogen. However, the water content of waste biomass is generally high, in the range of 90 % or higher [1]. Using thermochemical conversion requires prior drying which consumes a large amount of energy due to the high heat capacity of water [1]. Supercritical water gasification (SCWG) technology avoids the need for drying of the waste biomass feed, which

makes it suitable for handling feedstocks that contain high moisture contents. Compared to conventional combustion processes such as incineration, SCWG does not produce NOx compounds due to the significantly lower operating temperatures [4]. Also, thermochemical processes such as steam reforming and pyrolysis produce large amounts of undesirable products including chars and tars (higher hydrocarbons) at the expense of product gases such as H_2 [1,5].

SCWG is an emerging technology that can treat hazardous wastewater streams as well as producing syngas (H_2 & CO). Compared to conventional hydrogen production methods such as bioconversion, the catalytic supercritical water gasification (CSCWG) has proven to be one of the most promising hydrogen production methods for renewable resources [2, 6-8]. SCW can dissolve most organic substances and gases and has low viscosity and strong transportability [2, 4, 5, and 9]. Above the critical point of water (374°C, 22.1 MPa) all organic compounds are present in a single, dense fluid phase, minimizing mass-transfer resistance and accelerating reaction rates [9]. The gaseous product composition of waste biomass model compounds from SCWG significantly depends on the reactant concentration [6] and temperature [4, 10-11].

The extreme operating conditions required for the SCW process i.e. high pressure and temperature reduces its economic attractiveness due to the exotic metals required e.g. Hastelloy. The use of catalysts in the SCW process has been shown to decrease the operating temperatures by reducing the activation energy which would reduce the material cost for the SCW process [12]. Therefore, a proper catalyst design for hydrogen production is vital to enhance the H_2 yield, selectivity, and to reduce the undesirable by-products using CSCWG. Both heterogeneous and homogeneous catalysts (such as NaOH, KOH, activated carbon, metallic catalysts) have been examined. For instance, Watanabe et al. [13] studied the partial oxidative gasification of *n*-hexadecane (*n*-C_{16}) and organosolv-lignin (lignin) using NaOH and ZrO_2 catalysts in a batch

reactor from 400-440°C. They reported that the H_2 yields with zirconia and NaOH were double and quadruple the 4% molar yield without catalyst. Also, Yu et al. [6] reported that the achievement of 95 % carbon gasification and higher in SCW from glucose requires a reaction temperature above 600°C. The decomposition of aromatic compounds in SCW was reported by Osada et al. [7] using the supported noble metal catalysts i.e. ruthenium, rhodium, platinum, and palladium. The aforementioned authors pointed out that lignin is first converted to alkylphenols and formaldehyde through hydrolysis in SCW, after which, the alkylphenols and formaldehyde decompose to gaseous products with the aid of the catalyst. In another study, Osada et al. [8] pointed out that the ruthenium metal particles aggregated during the gasification of coal and waste plastics due to the drastic decrease of the Al_2O_3 support surface area as well as its crystal structure change from γ-Al_2O_3 to α-Al_2O_3. Furthermore, Yamaguchi et al. [14] reported that activated carbon supported noble metal catalysts i.e. ruthenium, rhodium, platinum, palladium, and nickel showed higher H_2 and CO selectivity during the gasification of lignin and woody biomass. According to Cortright et al. [15], H_2 selectivity was evaluated to know how many hydrogen atoms in an organic compound can be taken out as H_2 in the gas phase. Thus, higher selectivity for H_2 and CO is desirable as CO is expected to increase the H_2 yield through the water-gas shift reaction ($CO + H_2O \leftrightharpoons CO_2 + H_2$). The role of gasification using the aforementioned catalysts is primarily to promote the water-gas shift reaction as well as to facilitate the decomposition of intermediates which eventually increases the overall gas yield.

In light of the ever increasing stringent environmental regulations, limited land availability, and a paradigm shift towards resource recovery, sewage sludges (typically 41% proteins, 10-25% lipids, 14% carbohydrates) are becoming increasingly popular feedstocks of interest for SCW processes [16]. Recently, several studies have been carried out on the

gasification of biomass or waste biomass in SCW [6, 11, 17, and 18] and aqueous organic wastes [19 and 20].

Despite the occurrence of lipids and LCFAs in sewage sludge (≈ 25%), neither lipids nor long chain fatty acids (LCFA) have been explored for hydrogen production using SCW. Thus, the overall objective of this study is to demonstrate the feasibility of H_2 production from oleic acid using SCW by examining several commercial heterogeneous catalysts in SCWG. Catalyst selection criteria were mainly based on an extensive literature review, availability of the catalysts, and previous experience with glucose gasification in SCW [21]. Another objective of this study is to characterize the composition and quality of residual liquid products.

5.3 Materials

Oleic acid (99%), 0.5 wt % Ru/Al_2O_3 pelletilized catalyst, 5% palladium supported on activated carbon, 5% platinum supported on activated carbon, and reduced commercial nickel on silica alumina (63 wt % nickel) catalysts were obtained from Sigma-Aldrich Canada Ltd. (Oakville, Ontario, Canada). KATALCO (high temperature hydrogenation catalyst) and 0.5 wt % Ru/AC (granular) catalysts were purchased from Alfa Aesar (Ward Hill, MA, USA). 18 m·Ω de-ionized water was obtained using a compact ultrapure water system (EASY pure LF, Mandel Scientific co, model BDI-D7381). An emulsion of oleic acid (0.35M and 28000 mg_{COD}/L) was prepared using purified water by mechanical mixing and heating. The prepared feed was kept well mixed until delivered to the syringe pump where it was subsequently pressurized and injected into the reactor.

5.4 Data Interpretation

Oleic acid gasification reactions and the relevant processes can be approximated by the following:

Oleic acid reforming to CO and H_2:

$$C_{18}H_{34}O_2 + 16\ H_2O \rightarrow 18CO + 33\ H_2 \quad (1)$$

Water-gas shift reaction:

$$CO + H_2O \leftrightharpoons CO_2 + H_2 \quad (2)$$

Methanation reactions:

$$CO + 3H_2 \rightarrow CH_4 + H_2O \quad (3)$$

$$CO_2 + 4H_2 \rightarrow CH_4 + 2H_2O \quad (4)$$

The calculations of product gas yield and carbon balance were performed as follows:

Gas yield = (mol of gas species produced)/ (mol of oleic acid converted)) (5)

where:

mol of oleic acid converted = moles of oleic acid in the feed – moles of oleic acid in the liquid product (6)

Carbon balance = (moles carbon in the gas+ moles carbon in the liquid) / moles carbon in the feed. (7)

For the purpose of COD balance calculations, the product liquid effluent COD was measured whereas the gaseous product COD was calculated. The COD reduction efficiency, the COD balance, and the carbon gasification efficiency are defined as follows:

$$\text{COD reduction efficiency (\%)} = \{[COD_{initial} - COD_{final}] / [COD_{initial}]\} \times 100 \quad (8)$$

$$\text{COD balance} = [COD_{\text{gas product}} + COD_{\text{liquid product}} + COD_{\text{reactor residual}}] / [COD_{\text{initial}}] \quad (9)$$

Gasification efficiency = carbon in the product gas / carbon in the feed (10)

The procedure for calculating residual COD in the reactor after the end of each experiment was reported elsewhere [21] although generally were found to be insignificant in this work and hence not reported. To ensure experimental reproducibility, two runs were selected randomly and repeated at the exact same conditions, and the overall error was found to be less than 5%.

5.4.1 *Equilibrium Calculations*

Thermodynamic equilibrium calculations were performed using ChemCad software (Chemstations Inc, Houston, TX, USA). The mass and energy balance around the reactor was performed using the Gibbs free energy minimization (GFEM) reactor model. This technique does not consider the reaction pathways and calculates the equilibrium gas composition based on 100% conversion efficiency and the pre-defined product species. The aforementioned product species were selected based on the observed experimental results and include H_2, CH_4, CO, CO_2, ethylene and ethane.

5.4.2 *Liquid Analysis*

Long chain fatty acids (LCFA's), namely, palmitic, myristic, stearic, linoleic, and oleic acid were determined using a calibrated Agilent gas chromatograph equipped with a flame ionization detector (FID) and an HP-5 capillary column 30m long, 0.25mm internal diameter with a film thickness of 0.25 μm. The oven temperature was programmed as follows: 100°C (hold for 2 min) and rose at 10°C/ min to 250°C. The injector and detector were operated at 250°C; while Nitrogen was used as the carrier gas at a flow rate of 1.9 ml/ min and a pressure of 11.2 psi.

5.5 Results

To obtain a synopsis of the expected oleic acid gasification gas yields, Figure 5.1a portrays the calculated theoretical gas yield as mole gas per mole oleic acid fed (using the commercial software ChemCad) as a function of temperature at 28 MPa. Ten wt% oleic acid was used at this is a typical composition for the feed stream of interest corresponding to 28000 mg_{COD}/L. Increasing temperature leads to a sharp increase in the H_2 yield, a dramatic decrease in the CH_4 yield, and a slight increase in the CO yield. The calculated theoretical gas composition with change of the oleic acid feed concentration is portrayed in Figure 5.1b. As the concentration increased from 1 to 30 wt%, the H_2 and CO_2 yields both decreased dramatically, with the H_2 yield giving a sharper decrease. The effect of concentration on the H_2 yield is noticeable at a concentration range from 1 to 5 wt% which coincides with a rapid increase in the CH_4 yield. As will be shown experimentally, the model results were based on a complete oleic acid conversion, which did not go to completion. As such, we reported the gas yield in this work in terms of mole gas/ mole feed and mole gas/mole oleic acid converted.

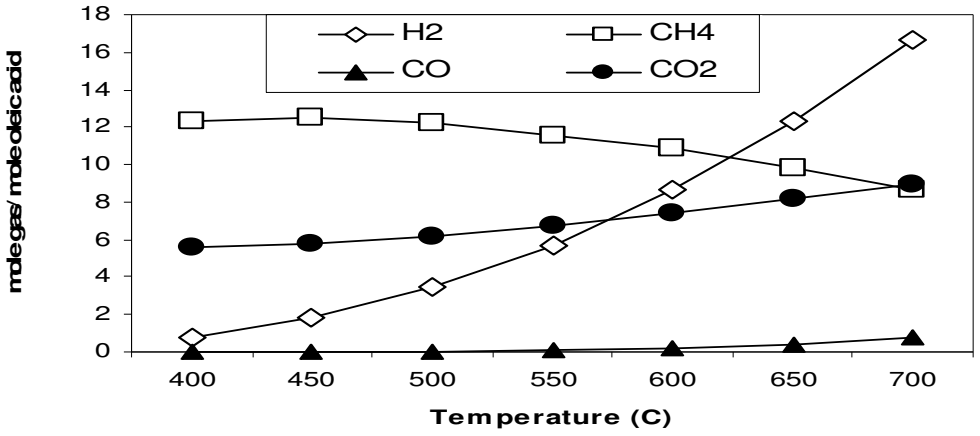

Fig 5.1a. Calculated equilibrium gas yield as a function of temperature at 28MPa, and 10 wt % oleic acid.

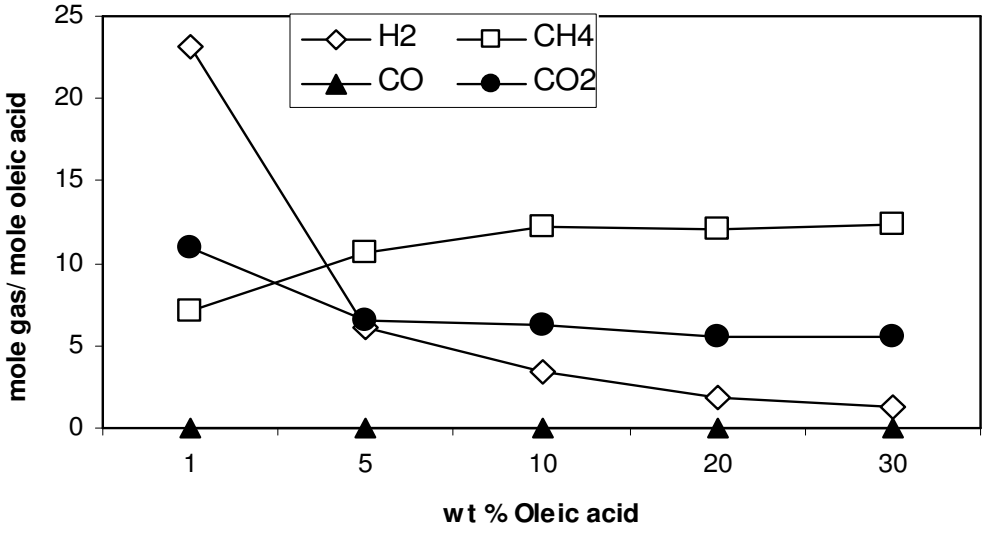

Fig 5.1b. Calculated equilibrium gas yield as a function of concentration at 28MPa, and 500°C.

5.5.1 *Effect of Temperature & Catalysts on the Product Gas*

Figure 5.2a, b, and c shows the distribution of the gaseous product yields measured in SCWG without using a catalyst at the three investigated reactor temperatures of 400, 450, and 500°C. As expected, the total gas product increased significantly with increasing temperature. The product gas composition was mainly composed of H_2, CH_4, CO_2, and a small amount of CO. The total gas volume at a temperature of 400°C was 27% and 8% of the gas volume produced at 450°C and 500°C respectively. Specifically, the H_2 gas yield increased by 48% and 80% as the temperature increased from 400 to 450 and 500°C respectively. However, the experimental H_2 yield was significantly less than that calculated at the three investigated temperatures. In fact, the experimental H_2 yield was 51%, 42%, 59% less than the calculated yield at 400,450, and 500°C respectively. This difference is attributed to the fact that the model calculates the gas composition based on complete conversion of the feed into gaseous products, and as described below; significant residual liquid products are formed which inhibited gas formation. Similar to

the observations with H_2, the observed experimental CH_4 yield was significantly less than the calculated equilibrium at the three investigated temperatures i.e. 400, 450, and 500°C. At 500°C, a dramatic increase in the CH_4 gas yield of 8.5 mol/mol oleic acid converted is observed coupled with a substantial CO yield of 2 mol/mol oleic acid converted compared to 400 and 450°C. It should be pointed out that the amount of CO produced was 0 in all cases except at 500°C where it was 0.2 mol CO/mol feed and 2 mol CO/ mol oleic acid converted.

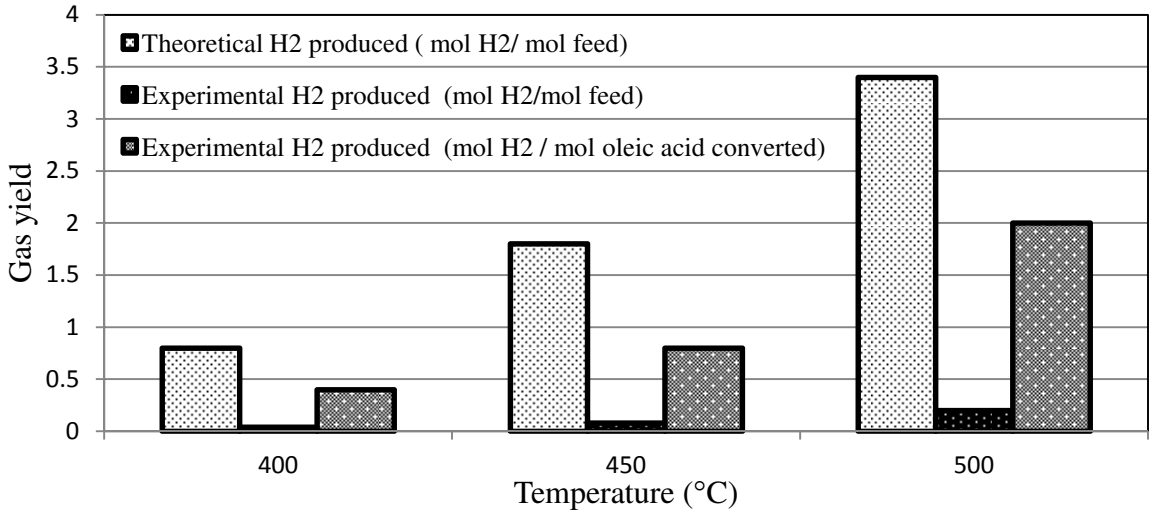

Fig 5.2a. Comparison between the experimental and theoretical H_2 gas yields at three temperatures of 400, 450, and 500 °C.

As oleic acid gasification has not been measured in SCWG, a catalyst screening study was undertaken using several commercially available gasification catalysts. A temperature of 500°C was chosen for catalyst testing to provide the highest gas yield at the maximum vessel pressure/temperature capability.

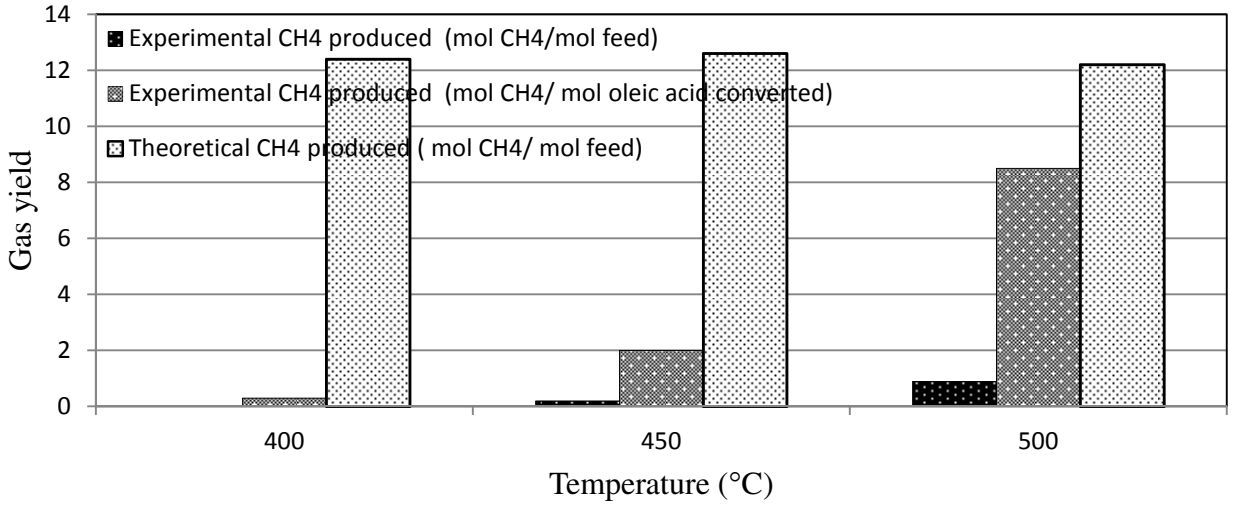

Fig 5.2b. Comparison between the experimental and theoretical CH_4 gas yields at three temperatures of 400, 450, and 500 °C.

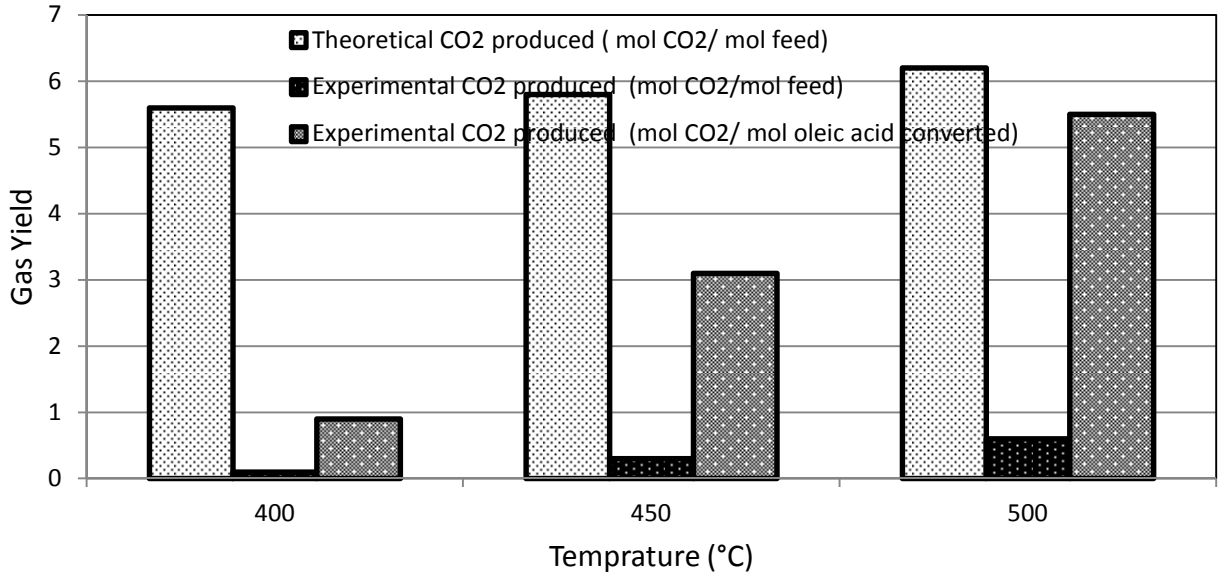

Fig 5.2c. Comparison between the experimental and theoretical CO_2 gas yields at three temperatures of 400, 450, and 500 °C.

As depicted in Figure 5.3a, and b, the use of catalysts enhanced the product gas yield significantly except for the high temperature shift catalyst (KATALCO). For KATALCO, the measured H_2 yield of 2 mol/mol oleic acid converted was the same as without using any catalyst, i.e. 40 % below the equilibrium calculated yield. However, the gas yield increased significantly

using the other catalysts, with the order of H_2 production was following: pelletilized Ru/Al_2O_3 > powder Ni/Silica-alumina > powder Pt/AC > granular Ru/AC > powder Pd/AC > KATALCO. Both the pelletilized Ru/Al_2O_3 and powder Ni/Silica-alumina catalyst surpassed the other catalysts in terms of H_2 yield, giving 15 mol/ mol oleic acid converted which was 4 times higher than that without a catalyst. Based on the moles of oleic acid fed, the H_2 yield for the Ru/Al_2O_3 and Ni/Silica-alumina catalysts was 1.5 mol, which translates to 44% of the theoretical yield. Thus, it is clear that the incorporation of catalyst increased the H_2 production significantly, although still fell short of the maximum theoretically achievable yield. Although the amount of 2 g catalyst was the same in all experiments, it should be pointed out that the Ru metal loading was 0.5 wt% whereas the nickel, Pd, and Pt metal loadings were 63, 5, and 5 wt% respectively.

Figure 5.3a also shows the experimental CH_4 yield at 500°C, with the order using the employed catalysts being as follows: pelletilized Ru/Al_2O_3 > powder Pd/AC > powder Pt/AC > powder Ni/Silica-alumina > granular Ru/AC > KATALCO. Again, and similar to the H_2 yield trend, the pelletilized Ru/Al_2O_3 catalyst showed a higher gasification activity toward CH_4. The CH_4 yield with this catalyst as mol/ mol oleic acid converted was 40% higher than the yield predicted by the equilibrium calculation, and 73%, 41%, 40%, and 61% higher than the CH_4 yield with the KATALCO, powder Pt/AC, powder Pd/AC, and granular Ru/AC catalysts respectively. Furthermore, both the powder Pt/AC and powder Pd/AC catalysts provided the same CH_4 yield experimentally which was also the same as the calculated equilibrium yield.

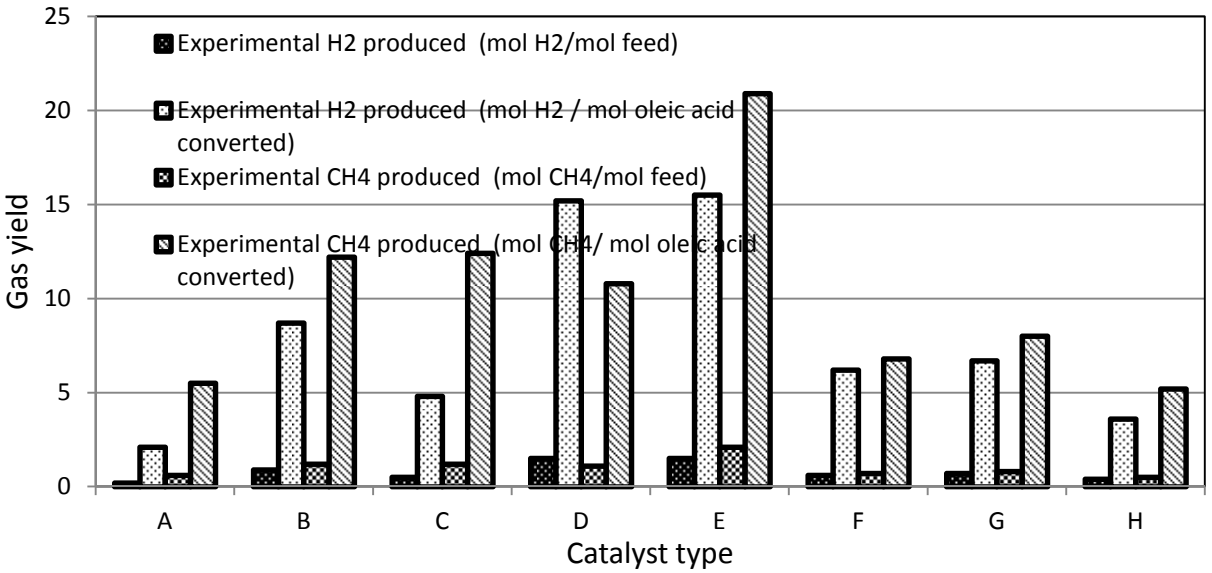

Fig 5.3a. Comparison of calculated H_2 and CH_4 yields related to the measured experimentally in presence of catalysts in mol/ mol feed and mol/ mol oleic acid converted.

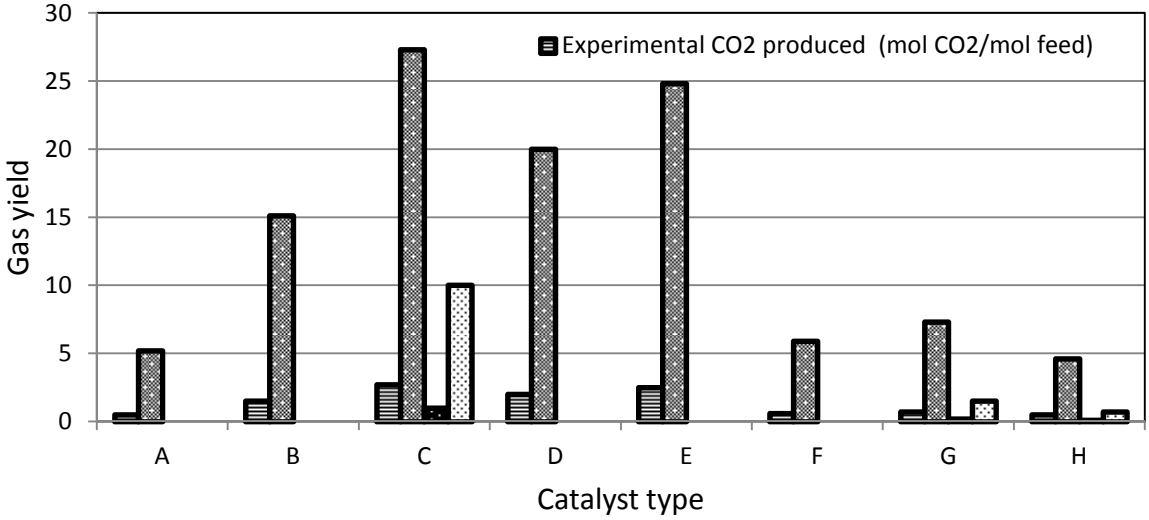

Fig 5.3b. Comparison of calculated CO_2 and CO yields related to the measured experimentally in presence of catalysts in mol/ mol feed and mol/ mol oleic acid converted.
(A; KATALCO, B; Pt/AC, C; Pd/AC, D; Ni/Silica-alumina, E; Ru/Al_2O_3, G; Ru/AC), F is the 2nd run of Ru/Al_2O_3 and H is the 2nd run of Ru/AC. Experimental conditions (0.35 M, 500°C, 28MPa, and 2g catalyst)

The experimental CO and CO_2 yields using all catalysts are reported in Figure 5.3b. The powder Pd/AC catalyst exhibited a different behaviour than other catalysts in achieving the highest CO_2 yield of 27 mol CO_2/ mol oleic acid converted. This observation coincided with a

substantial amount of CO of 10 mol/ mol oleic acid converted. The CO yield was almost zero except when using the powder Pd/AC and granular Ru/AC catalytic experiments, which gave 10 and 1.5 mol/ mol oleic acid converted, respectively. The order of CO_2 yield with the employed catalysts was as follows: powder Pd/AC> pelletilized Ru/Al_2O_3 > powder Ni/Silica-alumina > powder Pt/AC > granular Ru/AC > KATALCO.

5. 5.2 *Effect of Temperature & Catalysts on the Liquid Products*

As described above, significant differences were obtained between the measured and theoretical gaseous yields when using SCWG of oleic acid, necessitating analysis of the residual liquid product characteristics. Table 5.1 provides the chemical oxygen demand (COD), carbon gasification efficiencies and carbon balance results for the three examined temperatures. The COD levels at 400 and 450°C gasification temperatures remained almost the same as the COD in = 28,000 mg/L having values of 19280 and 19020 mg/L, respectively. Although the COD reduction efficiencies were almost the same at 400 and 450 °C i.e. 31% and 32% respectively, the COD reduction efficiency almost doubled to 60% as the temperature increased from 450 to 500°C. At 400°C, the liquid effluent after SCWG was observed as a homogeneous-milky-white-emulsion which became significantly clearer at 450°C and 500°C. In the presence of the high temperature shift catalyst (KATALCO), the residual COD increased slightly to 12050 mg/L over 11220 mg/L obtained with no catalyst at 500°C. However, the presence of the other catalysts enhanced the COD destruction and significantly decreased the residual COD. For example, the residual COD was 1240 mg/L when the Ni/Silica-alumina catalyst was employed which translates to a 90% reduction over that when using no catalyst. In general, the order of COD reduction efficiency was as follows: powder Ni/Silica-alumina > pelletilized Ru/Al_2O_3 > powder Pt/AC > powder Pd/AC > granular Ru/AC > KATALCO.

Comparing the carbon gasification efficiency values of all catalysts in Table 5.1 shows that the efficiency increased for the following catalysts: Ru/Al_2O_3, powder Ni/Silica-alumina, Pd/AC which was 85%, 81%, and 86% respectively.

Based on the COD reduction values, the Ni/Silica-Alumina catalyst gave the best performance with a COD reduction efficiency of 96% followed by Ru/Al_2O_3 and Pt/AC catalysts with COD reduction efficiencies of 86%. The KATALCO catalyst performance was the lowest among all catalysts explored achieving a COD reduction efficiency of 57%, similar to that without a catalyst. Nearly the same extent of decomposition of the liquid product was observed for Pt/AC and Ru/Al_2O_3, with a higher degree of decomposition for Ni/Silica-Alumina and Pd/AC catalysts.

To obtain further insight into the oleic acid conversion, the formation of long chain fatty acids (LCFA) and volatile fatty acids (VFA) after SCWG experiments was measured in the residual liquid fraction using a calibrated and verified GC, with the results provided in Table 5.2. The residual LCFA concentration increased dramatically as the temperature increased from 400 to 450°C. However, when the temperature was further increased to 500°C, a sharp decrease in the LCFA concentrations occurred. At 500°C, the oleic acid conversion was higher than its conversion at 400 and 450°C with a concentration in the residual liquid product of 3 mmol/L and (COD) of 11220 mg/L. From Table 4.2, the LCFA and VFA concentration distribution during the catalytic experiments was significant. For example, the oleic acid concentration during pelletilized Ru/Al_2O_3 catalytic experiment was 40 times higher than the residual liquid concentration when using the Ni/Silica-alumina catalyst.

Table 5.1 Liquid effluent characteristics and carbon gasification efficiency.

Catalyst type	Temp (°C)	COD out (mg/L)	COD Reduction Efficiency (%)	Carbon Gasification Efficiency (%)	COD Balance (%)	Carbon Balance (%)
No Catalyst	400	19280	31	10	77	83
No Catalyst	450	19020	32	25	82	78
No Catalyst	500	11220	60	52	82	80
KATALCO	500	12050	57	51	76	89
Pt/AC (Powder)	500	4060	86	74	80	77
Pd/AC (Powder)	500	7100	75	86	75	94
Ni/Silica-alumina (Powder)	500	1240	96	81	77	82
Ru/Al_2O_3 (Pellets)	500	3800	86	85	97	90
Ru/AC (Granular)	500	7540	73	60	76	81

- COD in 28,000 mg/L (0.35M)

Moreover, the concentrations of stearic, and linoleic acids were significantly higher when using the Ru/Al_2O_3 catalysts than when using the Ni/Silica-alumina catalyst, which was the most active. The residual concentrations of VFAs with the Ni/Silica-alumina catalyst were only 20% of the concentration observed with the Ru/Al_2O_3 catalyst. The most commonly observed VFA was propionic acid while only traces of acetic and butyric acids were observed except when the Ru/AC catalyst was employed. Furthermore, in the thermal decomposition of oleic acid, propionic, stearic, linoleic acids were always found as major carboxylic acid products.

5.5.3 *GC/MS Characterization of Liquid Product from Oleic Acid in SCW*

Table 5.3 reports the gas chromatography/mass spectrometry (GC-MS) results of the residual liquid effluent. Identifying the compounds was performed by employing an automatic comparison of the derived ion mass spectra to NIST or Wiley spectral libraries. At 400°C, the products were composed of carboxylic and saturated fatty acids, fatty acids esters, alkenes, fatty alcohols, *n*-alkanols, and some cyclo-compounds. At 450°C, the distribution of liquid products shifted towards aromatic and cyclo-compounds i.e. isomers of xylene such as m-xylene, p-xylene and o-xylene as well as cyclododecanol. At 500°C, the aforementioned compounds disappeared, with heptanoic and hexanoic acids, cresol, and two ketones being the only observed organics.

When using the Ru/Al_2O_3 and Ru/AC catalysts at 500°C, the organics were composed mainly of: (i) aromatic hydrocarbons such as m, o, and *p*-xylene, toluene, ethylbenzene, naphthalene, methyl naphthalene, and azulene; and (ii) polycyclic hydrocarbons such as indane and indene. It was observed that the Ru/Al_2O_3 catalyst was highly selective for aromatic hydrocarbons since no aliphatic hydrocarbons were detected.

Table 5.2 Concentrations of the LCFAs & VFAs for all experiments.

Catalyst type	T (°C)	LCFA conc (mmol/L)					Concentration (mmol/L)			VFA (mg COD/L)
		Palmitic acid	Myristic acid	Stearic acid	Linoleic acid	Oleic acid	Aceti c acid	propioni c acid	butyric acid	
No Catalyst	400	1	0	0.6	2.1	6.2	0	0	0.1	9.5
No Catalyst	450	8	7	9.4	10.1	13.2	0.1	0.7	0.4	142
No Catalyst	500	1	1	2.2	1.6	3	0	0.0	0.1	17
KATALCO	500	3	3	3.0	2.2	1.9	0.2	0.7	0.1	99.5
Pt/AC (Powder)	500	0	0	0.3	2.5	3.3	0.1	0.7	0.1	94
Pd/AC (Powder)	500	1	0	0.8	2.2	0.5	0.1	0.6	0.1	95
Ni/Silica-alumina (Powder)	500	0	0	0.3	0.2	0.1	0.1	0.0	0.1	17
Ru/Al_2O_3 (Pellets)	500	1	0	4.1	2.0	5.1	0.1	0.6	0.1	85
Ru/AC (Granular)	500	0	0	0.2	0.1	0.2	0.6	0.7	0.1	135

5.5.4 *Catalyst Sustainability & Performance*

In this study, the assessment of catalyst deactivation was limited to an examination of the surface area, gasification efficiency, and liquid quality parameters with Table 5.4 providing the details. Both catalysts Ru/Al_2O_3, and Ru/AC were significantly deactivated from the first run as reflected by a 60 and 50 % reduction in the H_2 yield respectively. A reduction of 70% and 40% in the CH_4 yield was also observed for both Ru/Al_2O_3, and Ru/AC catalysts respectively.

The BET surface areas of both fresh and used catalysts reported in Table 5.4 show a substantial decrease in the surface area of both catalysts after the second run. The BET surface area decreased from 100 m^2/g to 17 m^2/g for the Ru/Al_2O_3 catalyst and from 1069 m^2/g to 220 m^2/g for the Ru/AC catalyst. The GC-MS results in Table 5.3 show that when re-using the Ru/Al_2O_3 catalyst for a second SCWG experiment, the distribution of the compounds was almost the same as with the fresh catalyst. During the second run when using the Ru/AC catalyst, most of the aromatic hydrocarbons detected during the first run (i.e. toluene, ethylbenzene, and substituted benzene compounds), were not detected during the second run.

Table 5.3 Gas chromatography/mass spectrometry (GC-MS) qualitative analysis.

Similarity Index	Temperature (°C)	400	450	500	500	500	500	500
	Catalyst used	N/A	N/A	N/A	Ru/Al_2O_3*	Ru/Al_2O_3#	Ru/AC*	Ru/AC#
72	Heptanoic acid	ND	ND	√	ND	ND	ND	ND
73	2-Pentanone, 3-ethyl-3-methyl-	ND	ND	√	ND	ND	ND	ND
70	Hexanoic acid	ND	ND	√	ND	ND	ND	ND
71	2(3H)-Furanone, dihydro-5-methyl-	ND	ND	√	ND	ND	ND	ND
70	Phenol, 3-methyl- (m-Cresol)	ND	ND	√	ND	ND	ND	ND
74	2-Hexadecanol	√	ND	ND	ND	ND	ND	ND
73	1-Nonene	√	ND	ND	ND	ND	ND	ND
72	4-Nonyne	√	ND	ND	ND	ND	ND	ND
75	Cyclodecane	√	ND	ND	ND	ND	ND	ND
72	2-Undecene	√	ND	ND	ND	ND	ND	ND
72	1-Dodecanol	√	ND	ND	ND	ND	ND	ND
76	8-nonenoic acid	√	√	ND	ND	ND	ND	ND
74	Pentadecanoic acid	√	√	ND	ND	ND	ND	ND
75	Cyclodecene	√	ND	ND	ND	ND	ND	ND
74	Tetradecanal	√	ND	ND	ND	ND	ND	ND
74	1-Tetradecanol	√	√	ND	ND	ND	ND	ND
86	Oxa Cyclohepta Decan-2-one	√	√	ND	ND	ND	ND	ND
91	Hexadecanoic acid (Ethyl, methyl, tetradecyl, and octadecyl esters)	√	ND	ND	ND	ND	ND	ND
72	1,12-Tridecadiene	√	ND	ND	ND	ND	ND	ND
72	Cyclopropene, 1-butyl-2-ethyl-	√	ND	ND	ND	ND	ND	ND
79	Naphthalene, decahydro-	√	ND	ND	ND	ND	ND	ND
73	Cyclopropene, 1-pentyl-2-propyl-	√	ND	ND	ND	ND	ND	ND
73	1-Undecenoic acid	√	ND	ND	ND	ND	ND	ND
75	Ethanol, 2-(9-octadecenyl oxy)-, (Z)-	√	ND	ND	ND	ND	ND	ND
74	12-Heptadecyn-1-ol	√	ND	ND	ND	ND	ND	ND
73	13-Heptadecyn-1-ol	√	ND	ND	ND	ND	ND	ND
75	Heptadecanoic acid	√	ND	ND	ND	ND	ND	ND

84	2(3H)-Furanone, dihydro-5-tetradecyl-	√	ND	ND	ND	ND	ND	ND
80	Octadecanoic acid esters	√	ND	ND	ND	ND	ND	ND
72	Benzene, 1,2-dimethyl- (o-Xylene)	ND	√	ND	√	ND	√	ND
70	p-Xylene	ND	√	ND	√	√	√	ND
73	Cyclododecane	ND	√	ND	ND	ND	ND	ND
73	8-nonenoic acid	√	√	ND	ND	ND	ND	ND
78	Cyclopentadecanol	ND	√	ND	ND	ND	ND	ND
82	Octadecanoic acid methyl ester (Methyl Stearate)	ND	√	ND	ND	ND	ND	ND
74	Dodecanoic acid, 3-hydroxy-	ND	√	ND	ND	ND	ND	ND
73	Isopropyl Myristate	ND	√	ND	ND	ND	ND	ND
74	Toluene	ND	ND	ND	√	√	√	ND
78	Ethylbenzene	ND	ND	ND	√	√	√	ND
79	Benzene, 1,3-dimethyl (m-Xylene)	ND	√	ND	√	√	√	ND
74	Benzene, 1-ethyl-2-methyl	ND	ND	ND	√	√	√	ND
77	Benzocyclopentane (Indane)	ND	ND	ND	√	√	√	ND
73	benzocyclopentadiene (Indene)	ND	ND	ND	√	ND	√	√
70	Naphthalene	ND	ND	ND	√	√	√	√
71	Naphthalene, n-methyl	ND	ND	ND	√	√	√	ND
77	Benzene, 1,2,3-trimethyl	ND	ND	ND	√	√	√	√
75	1H-Indene, 3-methyl-	ND	ND	ND	√	√	√	√
78	Cyclobutene, 2-propenylidene-	ND	ND	ND	ND	√	√	ND
76	Benzene, 1,2,4-trimethyl	ND	ND	ND	√	√	√	ND
80	Benzene, 1-ethenyl-2-methyl-	ND	ND	ND	ND	ND	√	ND
76	Azulene (Isomer of Naphthalene)	ND	ND	ND	√	√	√	√
79	9-Octadecanoic acid (Z)-, tetradecyl ester (oleic acid ester)	ND	ND	ND	ND	ND	ND	√

ND≡ Not Detected, √ ≡ Detected, * ≡ 1st Use, # ≡ 2nd Use

5.6 Discussion

5.6.1 *Effect of Temperature & Catalysts on the Product Gas*

Higher temperatures were found to facilitate higher gas yields during the SCWG of oleic acid as portrayed in Figure 5.2 a, b, and c. At higher temperatures, gaseous products are formed through decomposition via pyrolysis of fatty acids as well as reforming reactions of oleic acid (equation 1) [22]. This is also supported by the oleic acid conversion at 500°C in Table 5.2, which was higher than its conversion at 400 and 450°C. The oleic acid concentration in the residual liquid product at 500°C of 3 mmol/L corresponds to a 23 % and 48 % reduction over those measured at 400 and 450°C respectively.

In order to rationalize the dramatic change in the composition of the product gas in relation to the residual liquid components, we relate the H_2 contribution in the reaction to the formation of liquid compounds. H_2 is usually produced by dehydrogenation of the unsaturated compounds such as olefins and the water-gas shift reaction (equation 2). On the other hand, hydrogen may also be consumed through various other reaction routes including methane formation reactions (reactions 3 &4), stabilization of hydrocarbon radicals, and hydrogenation reactions [23-26].

For example, the presence of stearic acid as a saturated fatty acid in the liquid phase suggests that the hydrogenation of the oleic acid double bond occurred. Hydrogenation requires H_2 to proceed which implies that some of the H_2 produced by other routes was consumed through the hydrogenation reaction route. The observed increase of CH_4 yield at 500°C was significant which implies its formation through either the decomposition of intermediate compounds or through equation 4.

Table 5.4 Used Catalyst surface area and performance.

Catalyst type	Metal Loading	Manufacturer BET Surface Area (Fresh Catalyst),	Measured BET Surface Area (Fresh Catalyst)	Measured BET Surface Area (Used Catalyst)
Ru/Al_2O_3 (Pellets)	0.5 wt% (Ru)	N/A	100 m^2/g	17 m^2/g
Ru/Al_2O_3 (Pellets) 2nd use	0.5 wt% (Ru)	N/A		
Ru/AC (Granular)	0.5 wt% (Ru)	900-1100 m^2/g	1069 m^2/g	220 m^2/g
Ru/AC (Granular) 2nd use	0.5 wt% (Ru)	900-1100 m^2/g		

Catalyst type	LCFA's & VFA's concentration (mmol/L)							VFA (mg COD/L)
	Acetic acid	Propionic acid	butyric acid	Palmitic acid	Stearic acid	Linoleic acid	Oleic acid	
Ru/Al_2O_3 (Pellets)	0.1	0.6	0.1	1	4.1	2.0	5.1	84.7
Ru/Al_2O_3 (Pellets) 2nd use	0.1	0.7	0.1	0	1.8	1.0	2.2	107.9
Ru/AC (Granular)	0.6	0.7	0.1	0	0.2	0.1	0.2	135.4
Ru/AC (Granular) 2nd use	0.2	0.8	0.1	0	0.0	0.1	0.2	122.5

Catalyst type	CODout (mg/L)	COD Reduction Efficiency (%)	Carbon Gasification Efficiency (%)	COD Balance (%)	Carbon Balance (%)
Ru/Al_2O_3 (Pellets)	3800	86	85	97	90
Ru/Al_2O_3 (Pellets) 2nd use	11260	60	44	79	81
Ru/AC (Granular)	7540	73	60	76	81
Ru/AC (Granular) 2nd use	11562	59	37	77	80

This is also supported by the presence of noticeable amounts of CO at 500°C, which suggests that the rate of CO consumption to form either H_2 through equation 2 or CH_4 through equation 3 was minimal. Furthermore, at 400 and 450°C, the residual liquid COD was almost the same whereas the COD at 500°C was about 42% lower than at 400 and 450°C. Approximately, 96% of the increase in the formed gas was from the 42% decrease in the COD. This implies that most of the gas formed at 500°C was through the decomposition of the formed intermediate compounds. Thus, the measured H_2 in the product gas is the difference between the amount of H_2 produced and consumed. The increase in both CO_2 and CO suggests that decarbonylation and decarboxylation of intermediates occurred which is also supported by the remarkable decrease in the concentration of LCFAs and VFAs. Consequently, H_2 concentration in the gas phase increased with the temperature rise which was found to be in a good agreement with the results for sewage sludge gasification in SCW reported by Zhang et al. [27]. The aforementioned authors pointed out that higher temperature facilitates the necessary free-radical reactions required for gas formation. Furthermore, and as reported by Yu et al. [6] who predicted the equilibrium gas composition during glucose gasification in supercritical water, the expected gaseous products at equilibrium are H_2, CH_4, CO_2 with traces of CO. The aforementioned author's equilibrium calculations showed that higher temperatures favored gaseous product formation. The effect of temperature on the gas formation is demonstrated by the performed equilibrium gas composition calculations in this work which is depicted in Figure 4.1a which showed that oleic acid requires temperature above 750°C to liberate the H_2 contained in the oleic acid into the gas phase.

In their gasification experiments with lignin, Yamaguchi et al. [14] reported that the Ru/AC catalyst was the most active for lignin gasification consistent with our observed results

which showed the highest carbon gasification efficiency (%) and COD reduction efficiency (%) of 85% and 86% respectively. Moreover, the CH_4 produced during the experiment with Ru/Al_2O_3 was 75% higher than the powder Pt/AC and powder Pd/AC catalysts, and 95% higher than the powder Ni/Silica-alumina catalyst. This was found to be in a good agreement with the observations of Osada et al. [7 and 8] using Ru as an active metal for methanation reaction as per equations 3 and 4. The negligible CO yield (almost 0 mol/ mol oleic acid converted) with the powder Ni/Silica-alumina, pelletilized Ru/Al_2O_3, powder Pt/AC catalysts suggests the occurrence of the water-gas shift reaction. According to Cortright et al. [15], the C-C bond cleavage occurring on the catalyst surface produces CO and H_2. CO reacts with H_2O to produce H_2 and CO_2 through the water-gas shift reaction. Furthermore, the formation of carbon oxides i.e. CO and CO_2 was through decarbonylation & decarboxylation of oxygenated hydrocarbons such as fatty acids and esters to saturated, unsaturated hydrocarbon, CO, and CO_2 [28]. From Table 4.2, the higher observed oleic acid concentration in the residual liquid product during pelletilized Ru/Al_2O_3 catalytic experiment relative to the other catalysts implies that oleic acid with Ru/Al_2O_3 catalyst was initially converted to product gases as per equation 1 followed by the methanation reaction (equations 3 and 4). On the other hand, the rate of methanation reactions seemed to be slower during Ni/Silica-alumina catalytic experiments as the methane yield was 50% lower than the pelletilized Ru/Al_2O_3 catalytic experiment.

5.6.2 *Effect of Temperature & Catalysts on the Liquid Product*

At the lowest operating temperature of 400°C, the formation of long chain compounds was more favorable at the expense of gasification. This implies that the thermal decomposition of saturated fatty acids and fatty acids esters was minimal. This observation is consistent with Marquevich et al. [29] who conducted steam reforming experiments of sunflower oil, reported

that at temperatures below 450°C, the carbon conversion ratio in the feed to product gas was minimal of less than 5%. The aforementioned authors also pointed out that linoleic, oleic, and stearic acids were identified as the major liquid products indicating that the C-C bond cleavage reaction of the unsaturated fatty acid chains did not take place. This finding is also in good agreement with that reported by Williams and Onwudili [22], who observed that higher temperatures favor the formation of fatty acids, and articulated that the concentration of oleic and palmitic acids in the produced oil from hydrothermal reforming of bio-diesel plant waste increased by 40% and 100% upon increasing the temperature from 380°C to 440°C. Holliday et al [30] pointed out that both saturated acids such as myristic, palmitic, and stearic acids, and free fatty acids such as oleic and linoleic acids were reasonably stable during hydrolysis at temperatures below 300°C.

At 450°C, the liquid products were composed mainly of aromatic and cyclo-compounds. Isomers of xylene i.e. m-xylene, p-xylene and o-xylene as well as cyclododecanol were also observed. The absence of alkenes and the presence of aromatic isomers coupled with increased H_2 production suggest that the aromatization reactions increased with increasing the cracking temperature as a result of dehydrogenation, similar to that reported by Savage [23]. The decrease in the number of saturated fatty acids and fatty acids esters identified is consistent with the corresponding increase in product gas concentrations. This indicates that the thermal decomposition or cracking of the aforementioned compounds was faster as it is also known that the unsaturated acids are thermally unstable and decompose by both thermal and oxidative routes [23 and 29]. As the temperature increased to 500°C, heptanoic and hexanoic acids, cresol, and two ketones were observed, and it is interesting to note that the concentration of LCFAs, VFAs also decreased. This suggests that the thermal decomposition of the aforementioned acids was

very fast, hence minimizing the occurrence of other possible reaction routes. The thermal decomposition of the LCFAs and VFAs was translated into more gaseous products at 500°C which also helps confirm the observed reduction in residual liquid effluent COD.

A similar trend was observed with the VFA distribution, primarily due to decarboxylation and decarbonylation of these carboxylic acids. The absence of *n*-alkanes, *n*-alkenes, and cyclo-compounds suggests that the generation path of the radicals such as RCOO was limited as it is reported that the RCOO radical would be responsible for the presence of *n*-alkanes and *n*-alkenes in the mixture through disproportionation and successive eliminations of ethylene [23, 26, 28, and 29]. In summary, the presence of heptanoic and hexanoic acids, cresol, and two ketones indicates that several intermediate compounds were formed. These intermediates had undergone two possible simultaneous routes; thermal decomposition to product gas through decarboxylation, dehydrogenation and aromatization reactions which facilitate the formation of aromatic hydrocarbons. Eventually, as reported by Marquevich et al. [29], the formation of aromatic hydrocarbons leads to the formation of radicals which conjugated with phenol to form cresols.

On the other hand, it was observed that Ru/Al_2O_3 catalyst was highly selective for aromatic hydrocarbons and no aliphatic hydrocarbon compounds were detected. This observation is contradictory to the one reported by Sai et al. [24] and Katikaneni et al. [25] who studied the catalytic cracking of canola oil to produce hydrocarbon fuels and chemicals. It should be pointed out that the aforementioned authors experimental conditions were significantly different than those employed here i.e. atmospheric pressure and 290- 410°C compared to 28MPa and 500°C in this work. The shift in the product distribution may have resulted from the effect of SCW properties due to high pressure and temperature as well as the catalyst.

The unique presence of aromatic hydrocarbons, namely, xylene, benzene, toluene, and ethylbenzene indicates that the Ru/Al_2O_3 and Ru/AC catalysts facilitate the Diels–Alder addition of ethylene to a conjugated diene. Sarkai et al. [31] reported that the decarboxylation of oleic acid and other LCFA led to the formation of aromatic-cyclic hydrocarbons. When the C-C dehydrogenation takes place, it facilitates more double-bond formation in the hydrocarbon chains which eventually increases the tendency for aromatic hydrocarbon formation. On the other hand, the detection of compounds such as 2-propenylidene-cyclobutene and stearic acid methyl ester during the second run of Ru/Al_2O_3 catalyst indicates that the gasification activity of Ru/Al_2O_3 catalyst towards saturated fatty acids such as stearic, palmitic acids, LCFA esters and oleic acid was diminished. This is also supported by the BET surface area results reported in Table 4 which shows that the Ru/Al_2O_3 catalyst was significantly deactivated during the first run as reflected by the substantial decrease in the gaseous products yield and the observed increase of the residual liquid products COD.

5.6.3 *Catalyst Deactivation*

The stability of the Ru catalyst supports i.e. Al_2O_3 and AC was investigated as their recovery was possible. The investigation focused mainly on the effect of reusing the catalyst on both the gas yield and the residual liquid effluent quality. As reported in Table 5.4, both catalysts i.e. Ru/Al_2O_3, and Ru/AC were significantly deactivated in the first run which is reflected by a substantial reduction in the both the H_2 and CH_4 yields. Osada et al. [8] studied the activity of different Ru supported catalysts; with the catalyst deactivation attributed to the formation of aggregated Ru particles. This aggregation is a result of the drastic decrease of the Al_2O_3 support surface area which occurs due to its crystal structure change from γ-Al_2O_3 to α-Al_2O_3. The aforementioned authors also reported that the Ru/AC had similar activity to Ru/TiO_2 for the first

run, however, the activity of Ru/AC decreased in the second run and the gas yield decreased by 60%. Another observation that corroborates the catalytic deactivation is the reduction in both the COD reduction and carbon gasification efficiencies as reported in Table 5.4. In addition, the deactivation of the catalyst poses a real challenge since the catalyst role in the SCW process is vital from an economic point of view. This raises the question on how the catalyst was deactivated which can be explained by two phenomena, i.e. coke formation and crystal structure change. As reported by Sai et al. [24], who studied the catalytic cracking of fatty acids to produce liquid hydrocarbon fuel using HZSM-5 catalyst at atmospheric pressure, the presence of fatty acids enhances the formation of radicals which leads to coke formation. The aforementioned authors pointed out that the formation of radicals is encouraged by the presence of catalyst as the hydrocarbons formed from fatty acids collide with the catalyst surface and formed radicals. The formed radicals then cracked and formed coke that deposited on the catalyst surface, eventually deactivating it. The second reason could be the instability of the catalyst support which led to changes in its crystal structure as demonstrated by Osada et al. [8].

To provide a better insight, we investigated the distribution of the LCFA's and VFA's in each run in Table 5.4. A substantial decrease in the concentration of stearic, linoleic, palmitic, and oleic acids in the second run was observed when Ru/Al_2O_3 catalyst was employed but no change in the concentration of acetic, propionic, and butyric acid was observed. For the Ru/AC catalyst, the concentration ratio of stearic to oleic acid was 1 mmol/L in the first run and 0 mmol/L in the second run which indicates that the extent of oleic acid decarboxylation reaction decreased drastically in the second run. The absence of palmitic and stearic acids as well as straight-chain paraffins with less than 7 carbon atoms in the second run of Ru/AC catalyst suggests that C-C bond cleavage for saturated oxygenated hydrocarbons takes place prior to the

decarboxylation and decarbonylation reactions. However, the gasification activity or the catalyst ability for C-C bond cleavage decreased from 60% in the first run to 37% in the second run as reflected by the carbon gasification efficiency. Meanwhile, Savage [23] reported that C-C bond cleavage of unsaturated compounds results in the formation of dienes, short-chain fatty acids, and hydrocarbon radicals. The formation of short-chain fatty acids was not observed in this work as the concentrations of these compounds did not increase as shown in Table 5.4. Thus, it is likely that the decarboxylation of fatty acids containing C=C resulted in the formation of long-chain cyclic hydrocarbons through formation of dienes followed by a Diels-Alder addition of diene to other olefins followed by cyclization.

5.6.4 *Possible Reaction Pathways*

Knowledge of the reaction mechanism is important for proper catalyst selection and design. Based on our results and the above discussion, we postulate a reaction scheme for the decomposition of oleic acid in SCW with and without Ru/Al_2O_3 and Ru/AC catalysts as shown in Figure 5.4. The proposed reaction route is based on the main products observed in both the gas and liquid phases during this experimental work and on the literature for steam reforming and thermal cracking of vegetable oils [15, 23-26, and 28-23]. The main possible reactions that occurred through the formation and disappearance of some intermediate compounds as well as the obtained gaseous and liquid final products are reported in Table 5.5a and b.

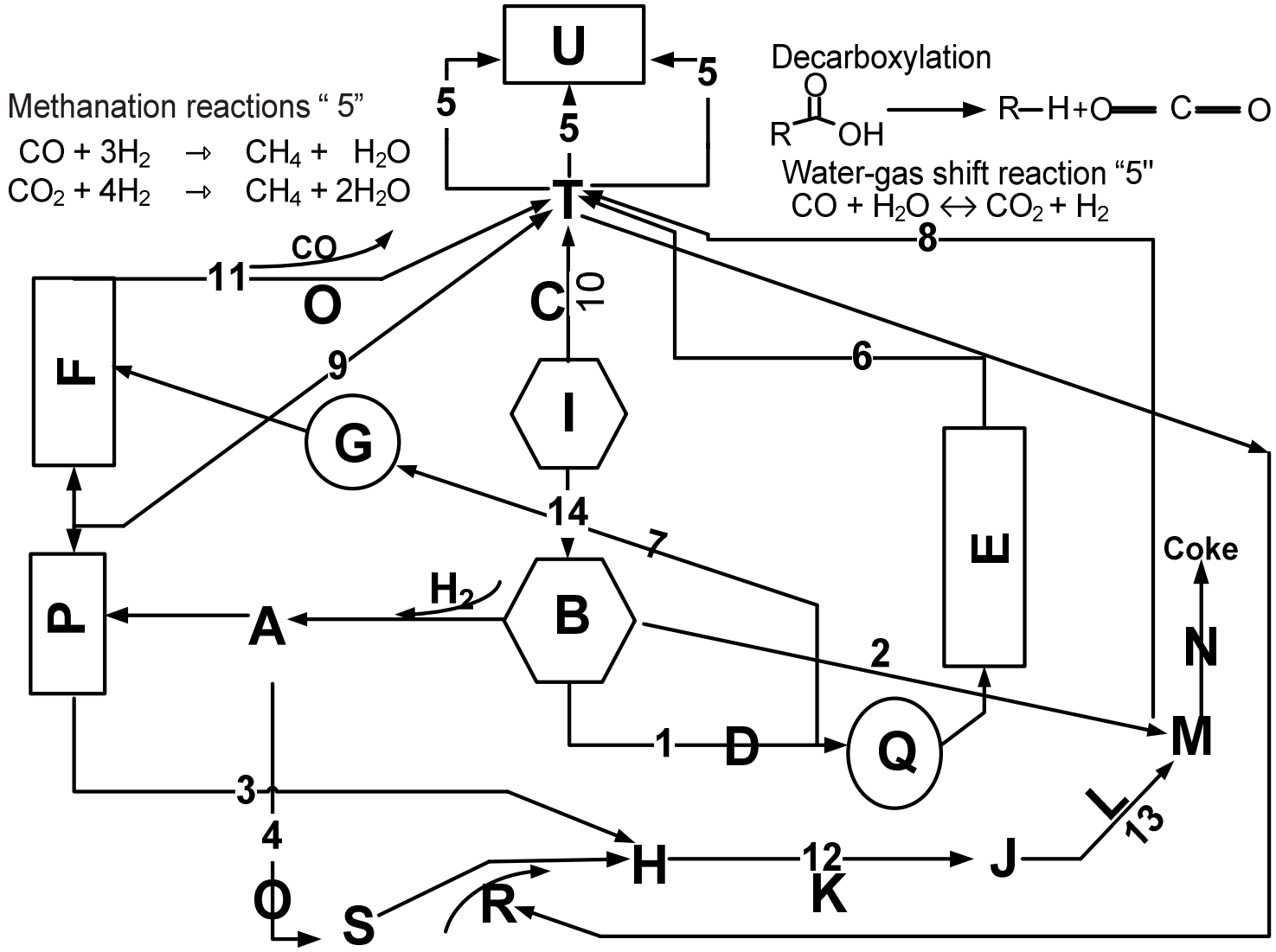

Figure 5.4 A schematic showing the proposed reaction pathways for oleic acid gasification in SCW.

Table 5.5a Product formation main reaction routes

Detected Products	Process No. in Figure 4	Possible formation route
H_2	5,8 and10	Dehydrogenation of the saturated compounds forming olefins, splitting of hydrocarbon molecules into its elements, formation of aromatics, and the water-gas shift reaction
CO_2	1, 4, and 5	Decarboxylation of unsaturated and saturated carboxylic acids
CH_4	9 and 5	Decomposition of formed intermediate compounds such as acetic acid), other possible gasification routes, methanation reactions (equations 3 & 4)
CO	1, 9, and 11	Decarbonylation of fatty acids, fatty acid esters, and other intermediate oxygenated hydrocarbons
LCFAs & VFAs & hydrocarbon radicals	14	Hydrolysis of oleic acid followed by thermal cracking and C-C bond cleavage.
Cyclo-compounds (Indene, Naphthalene, Cyclobutene, 2-propenylidene-, ….)	12	Diels-Alder addition of ethylene to a conjugated diene
Conjugated dienes	7	β-scission of unsaturated free fatty acids and hydrocarbons
Aromatics (Toluene, Ethylbenzene, p-Xylene, ….)	2 and 13	Elimination of hydrogen from Cyclo-compounds

Table 5.5b Examples of some the formed products through the main reaction routes.

A	Fatty acid esters "FA ester" (e.g Hexadecanoic acid (Ethyl, methyl, tetradecyl, and octadecyl esters)
B	LCFA's, Saturated FA, & VFA's
C	Thermal decomposition
D	Decarboxylation & Decarbonylation
E	Ether dehydration & alcohol dehydration
F	Ketones, fatty acids & fatty acid esters
G	C-C cleavage
H	Olefins "alkenes" (e.g Nonene)
I	Oleic acid
J	Cyclo-compounds
K	Diels – Alder "Cyclization"
L	Aromatization
M	Aromatics (e.g toluene, ethylbenzene)
N	Polymerization & Condensation
O	Decarbonylation
P	Unknown Intermediates
Q	R-H, R-OH, CO_2, CO
R	Ethylene
S	"R" CO_2
T	H_2, CO, CO_2, CH_4, and C_2-C_3
U	H_2, CH_4, CO_2, and H_2O

5.7 REFERENCES

[1] Furness DJ, Hoggett LA, Judd SJ. Thermochemical treatment of sewage sludge. Water Environ. J. 2000; 14: 57-65.

[2] Kruse A. Supercritical water gasification. Biofuels, Bioprod. Bioref. 2008; 2: 415–437.

[3] Navarro RM, Pen˜a MA, Fierro JG. Hydrogen Production Reactions from Carbon Feedstocks: Fossil Fuels and Biomass. Chem. Rev. 2007; 107: 3952-3991

[4] Holgate HM, Tester WJ. Glucose Hydrolysis and Oxidation in Supercritical water. AIChE J. 1995; 41: 637.

[5] Savage PE. A perspective on catalysis in sub- and supercritical water. J. of supercritical fluids. 2009; 47: 407-414.

[6] Yu DA, Masahiko A, Antal MJ Jr. Hydrogen Production by Steam Reforming Glucose in Supercritical Water. Energy & Fuels. 1993; 7: 574.

[7] Osada M, Sato O, Watanabe M, Arai K, Shirai M. Catalytic Gasification of Wood Biomass in Subcritical and Supercritical Water. Combust Sci Technol. 2006a; 178: 537–552.

[8] Osada M, Sato O, Watanabe M, Arai K, Shirai M. Stability of Supported Ruthenium Catalysts for Lignin Gasification in Supercritical Water. Energy&Fuels. 2006b; 20: 930– 935.

[9] Gloyna EF, Li L, McBrayer RN. Engineering Aspects of Supercritical Water Oxidation. Water Sci. Technol. 1994; 30: 1–10.

[10] Xu XM, Stenberg YJ, Antal MJ Jr. Carbon catalyzed Gasification of Organic Feedstocks in Supercritical Water. Ind. Eng. Chem. Res. 1996; 35: 2522.

[11] Lee IG K, Ihm SK. Gasification of Glucose in Supercritical water. Ind. Eng. Chem. Res. 2002; 41: 1182.

[12] Sutton D B, Kelleher J R. Review of literature on catalysts for biomass gasification. Fuel Process Technol. 2001; 73: 155.

[13] Watanabe MI, Osada M, Sato T, Adschiri T, Arai K. Catalytic Effects of NaOH and ZrO_2 for partial oxidative gasification of n-hexadecane and lignin in Supercritical Water in Supercritical Water. Fuel. 2003; 82: 545.

[14] Yamaguchi A, Hiyoshi N, Sato O, Bando K, Osada M, Shirai M. Hydrogen Production from Woody Biomass over Supported Metal Catalysts in Supercritical Water. Catalysis Today. 2009; 182: 192–195.

[15] Cortright RD, Davda RR, Dumesic JA. Hydrogen from catalytic reforming of biomass-derived hydrocarbons in liquid water. Nature. 2002; 418: 964-967.

[16] Goto M, Takatsugu N, Akane O, Akio K, Tsutomu H. Kinetic Analysis for Destruction of Municipal Sewage Sludge and Alcohol Distillery Wastewater by Supercritical Water Oxidation. *Ind. Eng. Chem. Res. 1999; 38: 1863*–1865.

[17] Antal MJ Jr. Schulman SD, Xu X. Biomass Gasification in Supercritical water. Ind. Eng. Chem. Res. 2000; 39: 4040.

[18] Lu YJ. Guo L, Ji CM, Zhang XM, Hao XH, Yan QH. Hydrogen production by biomass Gasification in Supercritical water: A parametric study. Int. J. Hydrogen Energy. 2006; 31: 1597.

[19] Blasi Di, Branca C, Galgano A, Meier D, Brodzinski I, Malmros O. Supercritical Gasification of Wastewater from Updraft Wood Gasifiers. Biomass & Bioenergy. 2007; 31: 802.

[20] Yan BW, Hu CS, Xie C, Wu JZ. Hydrogen Generation from Polyvinyl Alcohol-Contaminated Wastewater by a Process of Supercritical Water Gasification. J. Environ. Sci. 2007; 19: 1424.

[21] Youssef AE, Chowdhury BM, Nakhla G, Charpentier P. Effect of nickel loading on hydrogen production and chemical oxygen demand (COD) destruction from glucose oxidation and gasification in supercritical water. Int. J. Hydrogen Energy. 2009; 35: 5034-5042.

[22] Williams PT, Onwudili JA. Hydrothermal reforming of bio-diesel plant waste: Products distribution and characterization. Fuel. 2009; 89: 501-509.

[23] Savage PE. Organic Chemical Reactions in Supercritical Water. Chem. Rev. 1999; 99: 603-621.

[24] Sai P K, Adjaye JD, Bakhshi NN. Catalytic Conversion of Canola Oil to Fuels and Chemicals over Various Cracking Catalysts. The Canadian Journal of Chemical Engineering. 1995; 73: **484 - 497.**

[25] Katikaneni SR, Adjaye JD, Bakhshi NN. Studies on the Catalytic Conversion of Canola Oil to Hydrocarbons: Influence of Hybrid Catalysts and Steam. Energy & Fuels. 1995; 9: 599-609.

[26] Alencar JW, Alves PB, Craveiro AA. Pyrolysis of Tropical Vegetable Oils. J. Agric. Food. Chem. 1983; 31: 1268-1270.

[27] Zhang Q, Shuzhong W, Liang W, Donghai Xu. Catalytic Hydrogen Production from Municipal Sludge in Supercritical Water with Partial Oxidation. Proceeding in International Conference on Power Engineering. October 23-27, 2007, Hangzhou, China.

[28] Chang C, Wan S. China's Motor Fuels from Tung Oil. *Ind. Eng. Chem***.** 1947; *39*: 1543– 1548.

[29] Marquevich M, Coll R, Montane D. Steam Reforming of Sunflower Oil for Hydrogen Production. Ind. Eng. Chem. Res. 2000; 39: 2140-2147.

[30] Holliday R.L, King JW, List GR. Hydrolysis of Vegetable Oils in Sub- and Supercritical Water. Ind. Eng. Chem. Res. 1997; 36: 932-935.

[31] Sarkai T, Nehara D, Kunugi T. In *Industrial and Laboratory Pyrolysis*; Albright, L. F., Ceryness, B. L., Eds.; ACS Symposium Series; American Chemical Society: Washington, DC, 1976; p 32.

[32] Mazaheri H, TeongLee K, Bhatia S, Mohamed A. Subcritical water liquefaction of oil palm fruit press fiber for the production of bio-oil: Effect of catalysts. Bioresource Technology. 2010; 101: 745–75.

CHAPTER 6

Co-gasification of catechol and starch in supercritical water for hydrogen production

6.1 Background

In this chapter, we reported for the first time in the literature the effect of co-gasification of two compounds that model biomass or waste biomass. The experimental results of starch and catechol co-gasification in SCW, as model compounds for carbohydrates, and catechol representing lignin and aromatic compounds were reported. This study also aimed to provide an understanding of the reaction pathways occurring during co-gasification in SCW for future application to waste biomass gasification. Investigating the synergistic/inhibitory effects of co-gasification in the presence of CaO solely as well as in combination with TiO_2 catalyst on the product gas composition was also another objective of this study.

6.2 Introduction

Supercritical water gasification (SCWG) is a promising technique for reforming high moisture content biomass or waste feedstocks (70–95 wt.% water) to alternative and renewable fuels such as Hydrogen (H_2) [1]. Dwindling fossil fuel reserves as well as the negative effects of fossil fuels on the environment from CO_2 emissions has shifted the provided significant importance towards developing alternative energy sources. H_2 is a promising alternative energy form with its use gaining in acceptance, and promoted as one of the cleanest energy vectors. Hydrogen's viability as a clean fuel is greatly enhanced if it is produced from renewable sources such as sewage sludge, manure, or other waste/biomass types which are additionally becoming increasingly expensive to treat due to

new nutrient management disposal laws. However, often these feestocks have a high water content which requires expensive drying steps due to the inherent high heat capacity of water [2].

Supercritical water (SCW) has the advantage of using water directly as the reaction medium which eliminates the need for any expensive subsequent drying steps. SCW has low viscosity, and acts as a non-polar solvent with high diffusivity and excellent transport properties compared to other reforming techniques such as steam reforming [3-6]. SCW exhibits gas-like and liquid-like properties such as low density, high solubility, and high diffusivity which provides for the dissolution of many organic compounds. The dissolution of the organic compounds in SCW facilitates the high mass transfer fluxes that allow for faster reaction rates [7].

Biomass is composed mainly of cellulose, hemi-cellulose, and lignin whereas waste biomass such as municipal sludge and manure are composed of protein, carbohydrates, lipids, and phenolic compounds [3]. H_2 production from biomass and waste biomass using SCW has been the premise of many studies in recent years. Most of these studies were conducted using model compounds to enhance the fundamental understanding of SCW gasification, and to test the feasibility of H_2 production from biomass. For example, Yu et al. [2] gasified glucose as a biomass model compound in SCW at 600°C, 34.5 MPa, and 30 s residence time. The aforementioned authors reported that at glucose concentrations in the range of 0.1M to 0.6 M, there was no tar or char observed and the carbon gasification efficiency (CGE) exceeded 85%. Williams and Onwudili [8] studied the sub and supercritical non-catalytic gasification of glucose, cellulose, starch, and glucose as biomass model compounds at temperature and pressure ranges of 330-380°C and 9.3-22.5MPa

respectively. They demonstrated that the conversion of hydrogen contained in the sample to H_2 gas was greatest for glucose, followed by starch, followed by cellulose. Minowa *et al*. [9 & 10] conducted a series of experiments pertaining to cellulose gasification in SCW at 200-400°C and 8-22MPa, and demonstrated the possibility of H_2 production from cellulose with CGE's up to 70% with the aid of a nickel catalyst. Gasification of catechol as a model compound for lignin in biomass and aromatic compounds in sludges for H_2 production in SCW has also been investigated [3]. Kruse *et al*. [11] studied the effect of the process operating conditions i.e. pressure, temperature, concentration, and reaction time effect on catechol gasification using a continuous flow system with a 500 reactor ml, and compared their experimental results to equilibrium calculations. They reported that increasing temperature increased the H_2 production yield, decreased CH_4 formation with negligible carbon formation; with the pressure effect on the product distribution being negligible. They also investigated the influence of KOH addition as a homogeneous catalyst on the gasification efficiency, and reported that 99% gasification efficiency of catechol was achieved at 600°C and 2-min reaction time or at 700 °C and 1 min reaction time. They also concluded that the presence of KOH facilitated the achieving of the calculated equilibrium gas composition, and the degradation of the aromatic compounds was complete at the experimental conditions employed. Wahyudiono *et al*. [3] studied the decomposition of catechol in SCW as an aromatic and lignin model compound for municipal sludge and biomass at temperatures of 370–420°C and pressures of 25-40 MPa respectively. To identify the hydrolysis products, the aforementioned authors employed GC/MS and HPLC finding that phenol was the main compound identified along with other minor compounds including 2-cyclopentenone, 1, 2-benzenedicarboxylic acid, nonylphenol, 1, 4-

dipropylbenzene, acetophenone, and other benzene and phenol substituted compounds. The authors concluded that the longer reaction time of 240 minutes facilitated the formation of higher molecular weight hydrocarbons with reaction pressure showing negligible effect on the product distribution.

Although these various studies have enhanced the understanding of SCW gasification for H_2 production, the effect of co-gasification of various biomass constituents such as carbohydrates, lipids, lignin, and cellulose on the complex product distribution types needs also to be considered. Co-gasification of model biomass components is required to provide an understanding of the interactions that cannot be deduced from single substrate studies alone. In this chapter, we report the experimental results of starch and catechol co-gasification in SCW, as starch is a model compound for carbohydrates, and catechol represents lignin and aromatic compounds. The rationale for this work is that biomass/ waste biomass typically consists of 14% carbohydrate and 20% aromatic compounds [3]. This study also aims to provide an understanding of the reaction pathways occurring during co-gasification in SCW for future application to waste biomass gasification. Investigating the synergistic/inhibitory effects of co-gasification in the presence of CaO solely as well as in combination with TiO_2 catalyst on the product gas composition is also another objective of this study.

6.3 Materials and Methods

Starch $(C_6H_{10}O_5)_n$, catechol ($C_6H_6O_2$), calcium oxide powder (CaO) with a purity of 99%, and TiO_2 catalyst were obtained from Sigma-Aldrich Canada Ltd. (Oakville, Ontario, Canada). De-ionized water (18 m·Ω resistivity) was obtained using a compact ultrapure

water system (EASY pure LF, Mandel Scientific co, model BDI-D7381). Starch and catechol solutions were individually prepared with concentrations of 9,000, and 18,000 mg/L respectively. Each solution and the mixture of starch and catechol were prepared by using purified water by mechanical mixing and heating.

The prepared feed samples were kept well mixed until delivered to the syringe pump where they were subsequently pressurized and injected into the reactor. As shown in Table 6.1, in experiments 1, 2, and 3, starch was gasified alone at 400, 450, and 500°C, and catechol was gasified alone in experiments 4, 5, and 6 at the same temperature levels. Experiments 7, 8, and 9 were performed with different mixtures of starch and catechol.

6.4 Data Interpretation

The calculations for the product gas yield, and carbon balance were performed as follows:

$$\text{Gas yield} = (\text{ml of gas species produced})/ (\text{g of carbon fed})) \quad (1)$$

and,

$$\text{Carbon balance} = (\text{g carbon in the gas} + \text{g carbon in the liquid}) / \text{g carbon in the feed} \quad (2)$$

The TOC reduction efficiency is defined as follows:

$$\text{TOC reduction efficiency } (\%) = \{[TOC_{initial} - TOC_{final}] / [TOC_{initial}]\} \times 100 \quad (3)$$

In order to obtain the amount of CO_2 released and sequestered by the CaO for experiments 14 to 24 in chapter 3 in Table 3.1, an aqueous solution of HCl was added to the solid residue in the reactor after each experiment to release CO_2 according to the following equation:

$$CaCO_3 + 2HCl \rightarrow CaCl_2 + H_2O + CO_2 \quad (4)$$

The CO_2 released was then collected in a gas bag after passing through the mass flow meter. The collected gas was then analyzed using the aforementioned Shimadzu gas chromatograph (GC). The absorbed CO_2 volume was calculated knowing the total gas volume i.e. helium and CO_2. To ensure experimental reproducibility, two runs (Experiments no. 12 & 13 and 23 & 24) were selected randomly and repeated at the exact same conditions, with the overall error found to be less than 5%.

6.5 Results and Discussion

6.5.1 *Non-catalytic Gasification of Starch & Catechol*

We first examine the effect of temperature (400, 450, and 500°C) on the gasification of individual starch and catechol solutions at a residence time of 30 minutes as shown in Figure 6.1. The gaseous products consisted mainly of H_2, CO_2, CH_4, CO, and small quantities of C_2-C_3 hydrocarbons. As expected, the gaseous product yield increased significantly with increasing temperature for both individual compounds i.e. starch & catechol. For starch, as shown in Figure 6.1a, the H_2 content of the gas tripled from 10 to 30 ml/g carbon fed as the operating temperature increased from 400 to 500°C. A similar increase in CO_2 content of the gas from 26 ml/g carbon fed at 400 °C to 57 ml/g carbon fed at 500°C was observed.

Figure 6.1b shows the gaseous product distribution from catechol gasification at 400, 450, and 500°C. The increase in temperature resulted in increases in the gaseous product, similar to starch gasification. The H_2 and CO_2 yields produced from catechol were significantly lower than that produced from starch. A 50 % lower H_2 yield was produced with catechol corresponding to a yield of 16 ml/g carbon fed compared to 30 ml H_2/g

carbon fed produced from starch, Also, 21 ml/g carbon fed CO_2 was produced at 500°C with catechol compared to 57 ml CO_2/g carbon fed produced from starch at the same temperature and reaction time. The increase in temperature from 400 to 500°C enhanced the thermal decomposition of intermediates as reflected by the significant reduction in the TOC of the process liquid effluent and increase in CO_2 and H_2 content of the produced gas. Furthermore, the increase in temperature drove the water-gas shift reaction ($CO + H_2O \leftrightharpoons CO_2 + H_2$) through which the H_2 increased at the expense of CO, which resulted in a substantial increase of H_2 and significant reduction in CO [12 & 13].

6.5.2 ***Non-catalytic Gasification of Starch & Catechol Mixtures***

We performed gasification of three blended starch and catechol mixtures at 500°C and 30 minutes reaction. Figure 6.2 shows the gaseous product yield for the three investigated starch to catechol ratios. As the starch composition in the feed increased from 40% to 60 %, the H_2 yield decreased 27% from 37 to 29 ml/g carbon fed, and increased by 36% from 29 to 45 ml/g carbon fed as the starch composition increased from 60% to 80%. Similarly, the CO_2 yield decreased by 28 % from 56 to 35 ml/g carbon fed as starch composition in the feed increased from 60% to 80% and increased by 44% from 35 to 62 ml/g carbon fed as the starch composition increased from 60% to 80%.

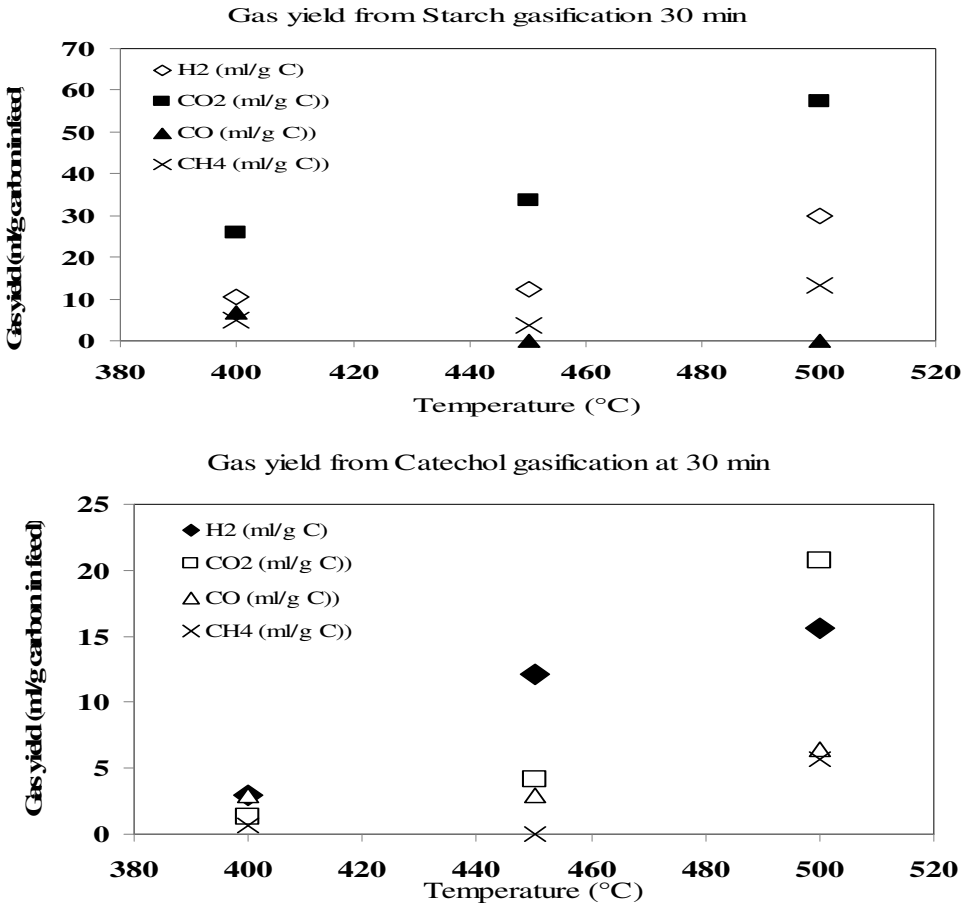

Fig 6.1 Effect of temperature on the gasification of solutions at 30 minutes; a: Starch; b. catechol.

The CO yield remained the same at 6 ml/ g carbon fed at starch composition in the feed of 40% and 60%. There was no apparent correlation between the H_2 yield and the change in the composition. On this basis, we sought to link the H_2 yield to the TOC reduction. Figure 6.2 also shows the distribution of H_2 yield at the three mixtures investigated along with the TOC reduction. The maximum TOC reduction of 61% was observed for 40% starch and 60% catechol, yet, the 80% starch and 20 % catechol mixture blend provided the highest H_2 yield of 44 ml/g carbon fed. Based on the maximum reduction in the TOC of the residual liquid and close to maximum H_2 yield of 37 ml/g

carbon fed, we selected the 40 % starch and 60 % catechol mixture for further catalytic investigations. At the aforementioned mixture blend, the TOC reduction efficiency was 61%. At 80% starch and 20 % catechol mixture blend, a TOC reduction efficiency of 51% was observed compared to 45% at 60% starch and 40% catechol. Furthermore, the value of H_2 yield at 40% starch in the mixture blend was 37 ml/g carbon fed compared to a 44 ml/g carbon fed at 80% starch in the mixture blend which translates to about 15% higher H_2 yield at 80 % starch in the mixture. Thus, the 40 % starch and 60 % catechol mixture was selected for further catalytic gasification at 500°C and 30 min reaction time. The selection was mainly based on the fact that biomass/ waste biomass typically consists of 14% carbohydrate and 20% aromatic compounds which translate to 40% carbohydrate and 60% catechol [3].

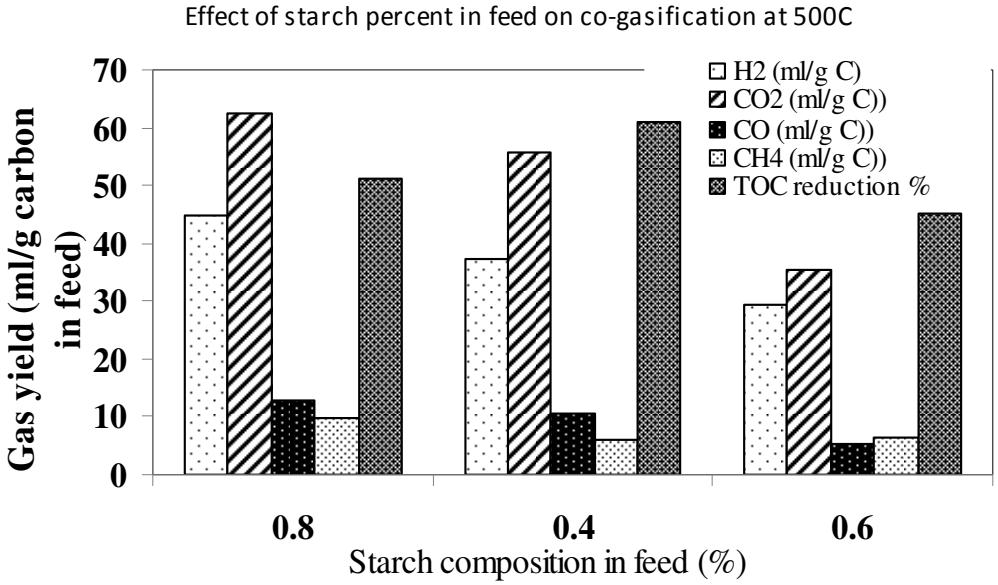

Fig 6.2 Gaseous product yield along with the TOC reduction % at the three different concentration feed blends and 500°C.

6.5.3 *Catalytic Gasification of Starch & Catechol Mixtures*

Figure 6.3 shows the effect of addition of CaO and nano TiO_2 both individually and combined on the gaseous product yield distribution. The control experiment no. 9 was with no addition of catalysts. The enhancement of H_2 yield of 2 ml/g carbon fed through the addition of CaO in experiment 10 was insignificant compared to the 37 ml/g carbon fed obtained in experiment 9. The CO_2 yield in the same experiment decreased remarkably by 90% from 37 to 4 ml/g carbon fed which facilitated the increase of H_2 content in the gas phase to 80%. Theoretically, the addition of CaO would facilitate $Ca(OH)_2$ formation [5 & 14] which serves as a gasification catalyst that enhances the water-gas shift reaction and eventually more H_2 formation. However, the observed H_2 yield in our experiment suggests that $Ca(OH)_2$ formation was minimal and was overruled by the direct and fast reaction of CO_2 with CaO to form $CaCO_3$. Yang and Xi [15] concluded that the effect of steam on CaO carbonation forming $CaCO_3$ was not significant and could not be attributed to the Ca $(OH)_2$ production.

Comparing experiment no. 11 in which TiO_2 was employed as catalyst with no added CaO to the control experiment no. 9 revealed another surprising observation. The use of TiO_2 decreased the H_2 yield from 37 to 33 ml/g carbon fed as well as CO_2 yield from 56 to 38 ml/g carbon fed. This decrease in both H_2 and CO_2 formation was associated with a decrease in the TOC reduction efficiency from 59% to 47%. In experiment no.12, where both TiO_2 and CaO were employed as catalyst and CO_2 sequestration agent respectively, an increase in the H_2 yield coupled with a complete elimination of CO_2, CO, and CH_4 yields to almost zero was observed. The H_2 yield increased by 33% from 37 to 55 ml/g carbon fed compared to the control experiment no.9. The combination of CaO and TiO_2 had a

remarkable effect on gaseous product yields which was corroborated by the TOC reduction efficiency increasing from 47% to 65% as shown in Table 6.1.

It is evident that the catalytic activity of TiO_2 was inhibited as translated by an increase of 40% in the H_2 yield during experiment no.12 in which both CaO and TiO_2 were employed relative to experiment no.11 (TiO_2 only). A possible inhibition route is the formation of cyclo-compounds through cyclo-addition reactions (e.g. Diels- Alder reactions and Huisgen cycloaddition reaction) as it has been reported that the aforementioned compounds are very stable and are precursors of tarry materials and coke that eventually deactivate the TiO_2 [16].

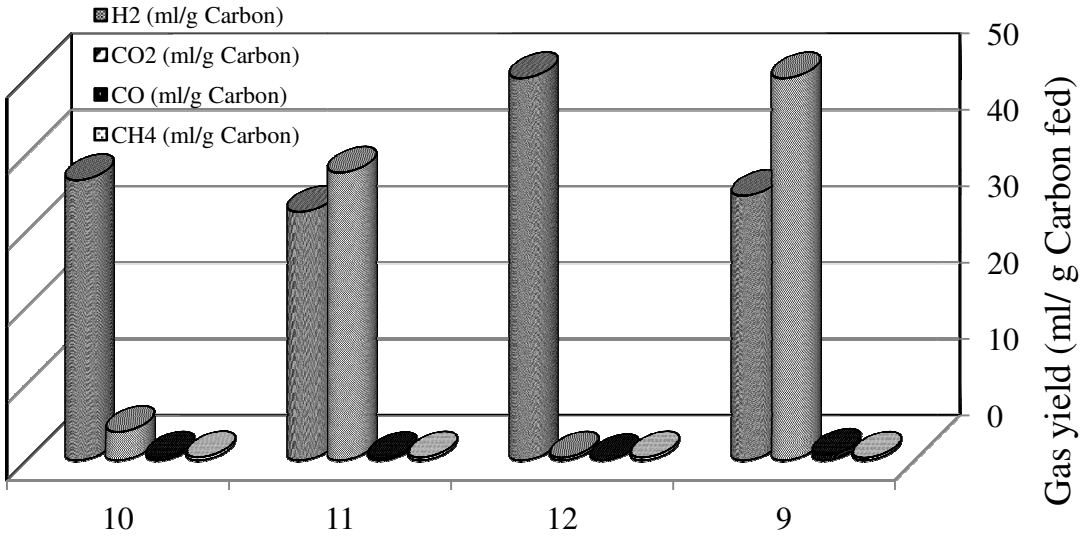

Fig 6.3 Effect of addition of CaO and TiO_2 as catalysts individually and combined on the gaseous product yield distribution (10 ≡ CaO; 11 ≡ TiO_2 (nano-powder); 12 ≡ TiO_2 (nano-powder) + CaO; 9 ≡ none)

The other possible inhibition route is the formation of intermediate cyclo-alkenes that has been observed in our experiments as discussed later in section 6.4.6. These compounds are not easily gasified and considered very stable such as cyclohexene and

cyclo-ketones such as cyclopentanone [6 & 17]. This is also confirmed by the decrease in TOC reduction efficiency to 47 % in experiment no. 11 relative to 65% in experiment 12.

6.5.4 *Effect of Temperature and Residence Time on Catalytic Gasification of Starch & Catechol Mixtures*

Table 6.1 shows the gas yield distribution at the three investigated reaction times of 10, 20, and 30 minutes and at the four studied temperature levels of 400, 425, 450, and 500°C. Increasing the reaction temperature increased the gaseous product yields to a greater extent than that due to the reaction time increase. For example, at 10 mins reaction time, the H_2 yield increased by 40% from 3 to 5.1 ml/g carbon fed at 425°C, to 9.5 ml/g carbon fed at 450°C, and to 41 ml/g carbon fed at 500°C. The same increasing trend was observed for the CO_2 and CH_4 yields, although the increases were less compared to the sharp increase in the H_2 yield at the same conditions. The CO_2 yield increased by 6% from 34 to 37 ml/g carbon fed as the temperature increased from 450 to 500°C and 10 min reaction time whereas the CO yield decreased by 45% from 3 to 1.6 ml/g carbon fed. By increasing the reaction time to 20 min, a similar trend of increasing gaseous product yields at the three investigated temperatures of 400, 425, and 450°C was observed. The increase in the H_2 yield followed a similar trend from 8 to 9.5 ml/g carbon as the temperature increased from 400 to 425°C, and to 12 ml/g carbon fed as the temperature increased from 425 to 450°C. Generally, CO_2 and H_2 were the predominant gases in all experiments and their corresponding concentrations were relatively close. Williams and Onwudili [18] who studied glycerol decomposition in sub and supercritical water reported that higher temperatures facilitated the decomposition of thermally resistant intermediates and led to more gaseous formation at the expense of residual liquid TOC. This observation is

substantiated by the relative constant concentration of CO which decreased only as the temperature increased to 500°C at the three reaction times tested. The decrease in CO concentration was accompanied with a corresponding increase in the other gaseous products including CO_2 and H_2. This implies that the water-gas shift reaction ($CO + H_2O \rightarrow CO_2 + H_2$) contribution to both H_2 and CO_2 formation was more pronounced at 500°C and 30 min reaction time as the CO concentration decreased from 9 ml/g carbon fed at 400 and 450°C (experiments no. 15 & 16) and 30 min reaction time to zero at 500°C. The presence of CaO as CO_2 sequester facilitated the forward direction of the water-gas shift reaction as reported by Han and Harrison [7], who reported that the water-gas shift equilibrium reaction, which is exothermic, is facilitated through the removal of CO_2 where the reaction proceeds in the forward direction. Thus, the temperature increase resulted in increasing gaseous products through thermal decomposition of intermediates and the presence of CaO facilitated the CO_2 sequestration and eventually increased the H_2 yield as a result of the water gas shift reaction.

Table 6.1 Gas yield distribution at three different reaction times of 10, 20, and 30 minutes and at four different temperatures of 400, 425, 450, and 500°C

Experiment No.	Time (min)	Temp (°C)	With CaO & TiO_2				
			H_2 (ml/g Carbon)	CO_2 (ml/g Carbon)	CO (ml/g Carbon)	CH_4 (ml/g Carbon)	Carbon Balance (%)
17	10	400	3.0	17	3.0	0.6	96
18	10	425	5.1	21	2.5	0.5	80
19	10	450	9.5	34	3	1.0	83
23	10	500	41	37	1.6	6	79
24	10	500	40	38	1.6	7	78
20	20	400	8	8	1.5	0.4	89
21	20	425	9.5	21	2.5	0.7	83
22	20	450	12	37	3.0	1.1	80
14	30	400	20	29	8	3	78
15	30	425	23	36	9	4	79
16	30	450	25	44	9	5	77
12	30	500	55	56	0.0	5	78

Table 6.1 also shows the carbon balance based on both the released and measured CO_2. The carbon balance closures were in close proximity and within acceptable ranges given that the unconverted carbon residue in the reactor was not measured because of the difficulty of separating it from the $CaCO_3$. There were small differences of 6%, 11%, and 14% between the carbon balances based on released and measured CO_2 at 400°C and 10, 20, and 30 min reaction time respectively. These differences increased with increasing reaction temperature; for example, the difference in carbon balance closure was 17%, 18%, and 21% at 450°C and 10, 20, and 30 min reaction time respectively compared to the carbon closure of 17% and 36% at 500°C and 10 and 30 min reaction time respectively.

6.5.5 *Effect of Residence Time and Temperature on Liquid Effluent Quality*

Figure 6.4 portrays the characteristics of the liquid effluent in terms of TOC reduction efficiency. The general observation is that increasing the reaction time increases the reduction efficiencies; however, the effect of reaction time was less influential than temperature. For example, the TOC reduction efficiency at 500°C and reaction time of 10 min was 30 % higher than its counterpart at the same reaction time and 400°C. The increase in the TOC reduction efficiency with increasing residence time was found to be in good agreement with the results reported by Williams and Onwudili [8 & 19]. At reaction times of 10 and 20 minutes, the TOC reduction efficiency was in the range of 50% or less even at the maximum operating temperature of 500°C. As the reaction time increased to 30 min, the TOC reduction efficiency was above 50% at the lowest operating temperature of 400°C, and reached as high as 65% at 500°C. This implies that the relatively low TOC reduction

efficiencies obtained at low reaction times were due to the formation of intermediate products which were difficult to gasify.

The impact of reaction time appears to diminish with increasing temperature. For example, a 28% increase in TOC reduction efficiency was achieved by tripling the reaction time from 10 to 30 minutes at 400°C while only 23% increase in TOC reduction efficiency was achieved by tripling the reaction time from 10 to 30 minutes at 425°C. Similar observations were obtained by tripling the reaction time at 450 and 500°C where the TOC reduction efficiency increased by 21% and 19% respectively. At the 30 minutes reaction time the TOC reduction efficiency increased by only 6% as the temperature increased from 450°C to 500°C. This is also mirrored by the comparison of the TOC reduction efficiencies at 20 minutes reaction time where the reduction efficiencies increased by only 4% from a value of 32% at 400°C to value of 36% at 425°C, and by another 6% to a value of 42% as the temperature was raised to 450°C. It has been reported that the initial conversion of organic compounds during SCW gasification process occurs very fast initially and subsequently slows down afterwards [20-21].

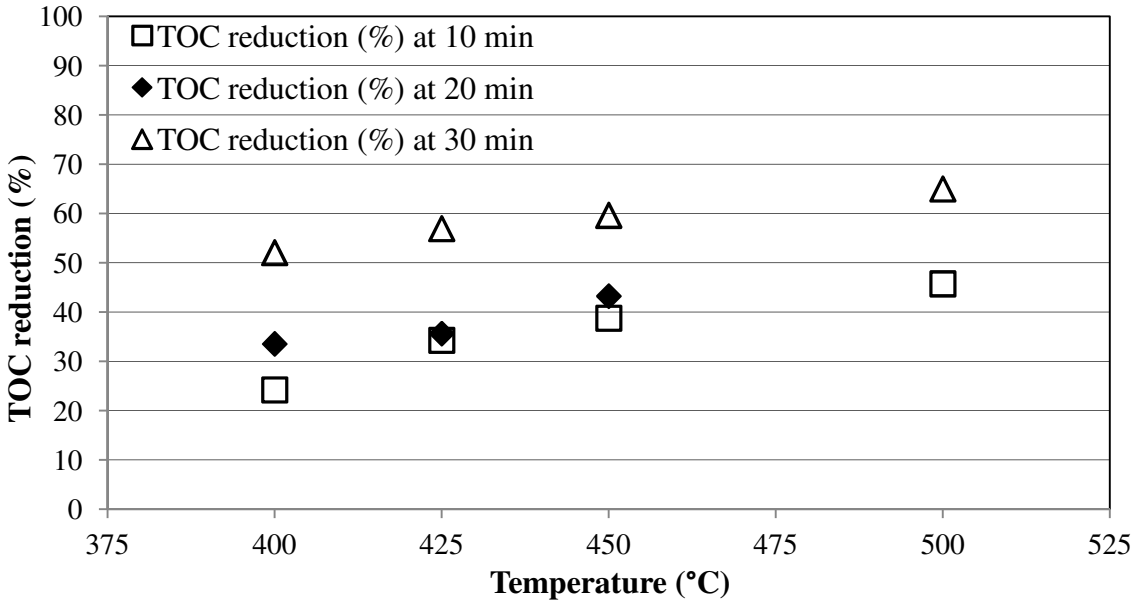

Fig 6.4 Dependence of TOC reduction efficiencies on Reaction Time and Temperature.

6.5.6 *Characterization of the Process Liquid Effluent and Possible Reaction Pathways.*

To obtain a better understanding of the compounds chemical transformation during the co-gasification of starch and catechol in SCW, we performed a qualitative analysis of the process liquid effluent for some selected experiments using gas chromatography/ mass spectrophotometry (GC/MS). An automatic comparison of the derived ion mass spectra to NIST and Wiley spectral libraries was employed for the identification purposes. The selected liquid samples subjected to this analysis originated from experiments 7 to 12 (Table 3.1), and all the reported compounds were identified with similarity indices greater than 80. Table 6.2 reports all the detected products according to the aforementioned criteria i.e. similarity indexes ≥ 80 with total of 33 compounds being reported. The products were mainly composed of aromatic and cyclo-compounds such as cyclobutane, cyclohexene, phenol and its substitutes such as *p, m, o,* cresols. The remaining compounds were of

various structures including ethylene, diethyl ketone, 5-Hydroxymethyl furfural, acetophenone, 5-indanol, and 2-naphthalenol.

At a feed composition ratio of 80 % starch and 20 % catechol, and 40 % starch and 60 % catechol, the detected compounds were mainly cyclo-compounds, phenolic compounds and substituted phenols. Phenol was formed through C-OH bond cleavage as by Wahyudiono *et al*. [3], who reported that catechol decomposition proceeds through the scission of an O–H bond that facilitates the formation of hydroxy-substituted phenoxy radical and H atom, and the H atom then reacts with catechol to form phenol and OH.

Phenol was also formed through the dehydration of furfural whereas the presence of alkyl phenols such as isopropyl phenol, ethylphenol, and cresols confirms the reactions of functional groups e.g. hydroxyl and carbonyl groups with phenolic substitutes forming higher molecular weight compounds. This is supported by the results of Sato *et al.*[20] who confirmed the formation of alkylphenols resulting from the reaction of 2-propanol with phenol at temperature of 400°C and pressure range of 4 to 36 MPa. On the other hand, the presence of furfural and 5-hydroxymethyfurfural (5-HMF) provides evidence that starch decomposition route was through formation of glucose and fructose as reported by Nagamori and Funazukur [22]. During experiments 7 & 9, several cyclo-compounds such as cyclopentanone, cyclohexene, and cyclobutane were detected. The absence of aromatic hydrocarbons and presence of cyclo-ketones, and substituted cyclo-ketones implies that aromatization reactions were limited and cyclo-addition reactions were facilitated through the Diels-Alder reaction and Huisgen cycloaddition reaction. It is also possible that cyclo-compounds were produced through hydrogenation of benzene i.e. cyclohexene and cyclohexane production reactions. The presence of adipic acid confirms the aforementioned

reaction route as cyclohexene is a precursor to adipic acid. The absence of aromatic hydrocarbons reveals that they were consumed through the formation of radicals which conjugated with phenol to form cresols [23].

At a feed composition of 60 % starch and 40 % catechol i.e. experiment no. 8, an interesting observation of the detected compounds distribution was noted. The number of cyclo-compounds decreased whereas the number of phenolic compounds detected remained the same as compared to experiments 7 & 9. This shift indicates that cyclo-compunds could be formed from starch intermediate products such as fructose. This is noteworthy as it is believed that aromatic and cyclo-compounds usually form from the lignin portion in lignocellulosic decomposition in SCW which is also supported by the absence of the 5-HMF as reported by Luijkx *et al*. [24]. The aforementioned authors found that 1, 2, 4-benzenetriol was formed at a high yield of up to 46% from 5-HMF. Experiment no. 10 in which a feed composition of 40 % starch and 60 % catechol was employed along with CaO as CO_2 sequester revealed that the major products identified disappeared. For example, ketones and substituted ketones such as 2-pentanone, 3-pentanone, and 2-butanone were not detected, and the major products were composed of phenol and alkyl-substituted phenols such as cresols. This could be attributed to the reported results by Elliot *et al*. [25], who reported that the carbonate ion reacts with water and forms a hydroxyl ion. The hydroxyl ion liberates phenol and substituted phenols through the cleavage of ether linkages of catechol. On the other hand, the disappearance of cyclo-ketone compounds such as cyclo-pentanone, and cyclo-hexanone suggests that the cyclo-addition reactions were limited. The presence of compounds such as ethylphenol, isopropyl phenol suggests that the C-OH bond cleavage occurred and produced hydroxyl functional group which reacted

with phenol and formed the aforementioned compounds [26]. This is also mirrored by the absence of 5-HMF and conforms to the reported results by Kumar *et al*. [27] who suggested that under alkaline conditions, the formation of 5-HMF is unlikely whereas the formation of substituted phenols is expected.

Experiment no.11 in which nano TiO_2 was employed as a catalyst resulted in the detection of compounds such as cyclobutane, cyclopentanone, cyclopentene-1-one, ethylphenol, isopropyl phenol, and indanol which were not observed in experiment 10 where only CaO was employed. Another interesting observation in experiment 11 is the decrease in the H_2, and CO_2 yields as well as the TOC reduction efficiency. This indicates that the TiO_2 did not facilitate the water gas shift reaction ($CO + H_2O \rightarrow CO_2 + H_2$) and rather, it clearly facilitated the formation of cyclo-ketones, cyclo-alkane, phenols, cresols, and alkyl-phenols. On the other hand, the combination of both TiO_2 and CaO inhibited the formation of the aforementioned compounds except phenol and cresols.

Table 6.2 Gas chromatography/mass spectrometry (GC-MS) qualitative analysis.

Compound No.	Similarity Index	Exp No.	(7)	(9)	(8)	(10)	(11)	(12)
		Catalyst	N/A	N/A	N/A	CaO	TiO_2	TiO_2 + CaO
		Feed Composition (vol %)	Starch 80% & Catechol 20%	Starch 40% & Catechol 60 %	Starch 60% & Catechol 40%	Starch 40% & Catechol 60 %	Starch 40% & Catechol 60 %	Starch 40% & Catechol 60 %
1	97	2-Butanone (Methyl ethyl ketone) C_4H_8O	√	√	√	ND	√	√
2	98	Cyclohexene (C_6H_{10})	√	√	√	√	√	√
3	97	Cyclobutane (C_4H_8)	√	√	√	ND	√	ND
4	97	2-Butanone, 3-methyl- " 2-Pentanone"($C_5H_{10}O$)	ND	√	√	ND	ND	ND
5	95	Diethyl ketone " 3-Pentanone"($C_5H_{10}O$)	ND	√	ND	ND	ND	ND
6	96	Cyclopentanone " Adipic ketone" (C_5H_8O)	ND	√	ND	ND	√	√
7	93	Ethylene (C_2H_4)	√	ND	ND	ND	ND	ND
8	94	Cyclopentanone, 2-methyl- ($C_6H_{10}O$)	ND	√	√	ND	√	ND
9	96	Cyclopentanone (C_5H_8O)	√	ND	√	ND	√	ND
10	83	Cyclopentene-1-acetaldehyde	√	ND	ND	ND	√	ND
11	82	Cyclopenten-1-one (C_5H_6O)	√	√	√	ND	√	ND
12	97	2-Cyclopenten-1-one, 2-methyl (C_6H_8O)	√	√	ND	ND	ND	ND
13	97	2- Cyclohexen-1-one (C_6H_8O)	√	ND	ND	ND	ND	ND
14	93	Benzene, 1,2,4-trimethyl (C_9H_{12})	√	√	ND	ND	√	ND
15	96	2-Furancarboxaldhyde ($C_6H_6O_2$)	√	√	ND	ND	ND	ND
16	97	5-(Hydroxymethyl) furfural ($C_6H_6O_3$)	√	√	ND	ND	ND	ND
17	98	Phenol (C_6H_6O)	√	√	√	√	√	√
18	98	Ethanone, 1-phenyl " Acetophenone" (C_8H_8O)	√	√	√	ND	ND	ND

19	98	*P, m, o* Cresols "Phenol, 2-methyl- (C_7H_8O)	√	√	√	√	√	√
20	92	*Isopropyl phenol ($C_9H_{12}O$)*	ND	√	√	ND	√	ND
21	95	*o*-Ethylphenol ($C_8H_{10}O$)	√	√	√	ND	√	√
22	81	Naphthalene ($C_{10}H_8$)	√	√	ND	ND	ND	ND
23	86	2,2-Bifuran ($C_8H_6O_2$)	√	√	√	ND	ND	ND
24	98	Benzopyran (C_9H_8O)	√	ND	ND	√	√	√
25	85	2-Methyl-5-hydroxybenzofuran "Benzenepropenoic acid" ($C_9H_8O_2$)	√	√	√	ND	ND	ND
26	93	Indene (C_9H_8)	ND	√	ND	ND	ND	ND
27	91	1H-Inden-1-one, 2,3-dihydro-2-methyl- ($C_{10}H_{10}O$)	ND	√	√	ND	ND	ND
28	87	4-Methyl-1-Indanone "Benzene acetaldehyde" ($C_{10}H_{10}O$)	ND	√	√	ND	ND	ND
29	84	Hexamethylbenzene ($C_{12}H_{18}$)	ND	√	ND	ND	ND	ND
30	97	Phenol,2,4-dimethyl- ($C_8H_{10}O$)	ND	ND	√	√	√	√
31	83	Benzene, hexamethyl- ($C_{12}H_{18}$)	ND	ND	√	ND	ND	ND
32	92	2-Naphthalenol ($C_{10}H_8O$)	ND	ND	√	ND	ND	ND
33	89	5-Indanol ($C_9H_{10}O$)	ND	√	ND	ND	√	ND

ND≡ Not Detected, √ ≡ Detected, Temperature 500°C

The unique presence of phenol and cresols in all experiments confirms that they are largely stable under SCW conditions. The inhibition of cyclo-ketones and cyclo-alkane formation in experiment 11 was accompanied by a remarkable increase in the H_2 yield by 33% from 37 to 55 ml/g carbon fed compared to the control experiment 9 which indicates the occurrence of the cracking and dehydrogenation reactions of the cyclo-compounds and their precursors [28].

6.5.7 *Possible Reaction Pathways*

Based on the above discussion, we postulated the possible reaction pathways for co-gasification of starch and catechol in SCW with and without CaO, TiO_2, and the combined CaO + TiO_2 catalysts. Figure 5.5 provides a schematic diagram of the possible reaction pathways based on the experimental results, GC/MS analysis, and the reported results pertaining to carbohydrates, lignin, and phenols decomposition in SCW [3, 10, 20, and 23-29].

The formation of gaseous products was mainly through the direct decomposition of starch, catechol, and intermediates as shown in Figure 6.5 through routes 1, 2, and 3. Examples of the intermediates are glucose, acids, aldehydes and other unknown intermediates that were formed and degraded during each experiment. Phenol formation was from catechol through route 4 as reported by Wahyudiono et al. [3]. The presence of 5-HMF (routes 5, 6, and 7) indicates that starch degradation produced glucose and fructose which has been reported in the literature by Nagamori and Funazukuri [22]. Route 8 suggests the formation of phenol from the furfurals and 5-HMF through a dehydration

reaction. The formation of cyclo-compounds such as cyclohexene and cyclo-hexane was possible through route 10 and 11 where the hydrogenation reaction of aromatic rings such as benzene was facilitated. The production of hydroxyl or carbonyl groups through the C-OH scission of catechol facilitated phenol reaction with alkyl group originated from acids, aldehydes, alcohols (route 12) which translates to the formation of alkyl-phenols. Ketones and substituted ketones were formed through the facilitation of cyclo-addition reactions such as Diels-Alder and Huisgen reactions.

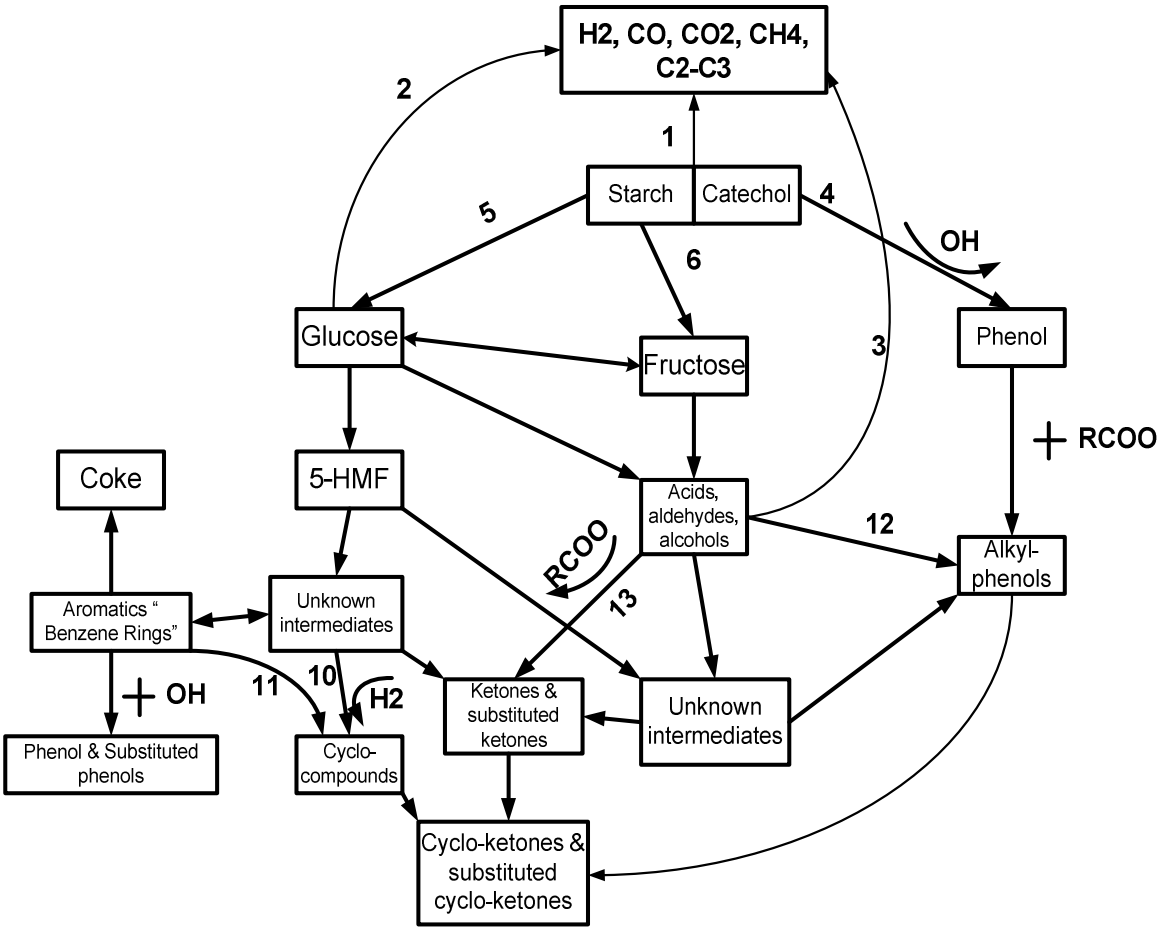

Fig 6.5 Schematic of proposed reaction pathways for starch and catechol co-gasification in SCW.

6.6 References

[1] Sricharoenchaikul, V. Assessment of black liquor gasification in supercritical water. Bioresource Technology. 2009; 100: 638–643.

[2] Yu D, Aihara M, Antal J Jr. Hydrogen Production by Steam Reforming Glucose in Supercritical Water. Energy & Fuels. 1993; 7: 574.

[3]Wahyudiono M, Sasaki M, Goto M. Conversion of biomass model compound under hydrothermal conditions using batch reactor. Fuel. 2009; 88: 1656–1664.

[4] Youssef E, Elbeshbishy E, Hafez H, Nakhla G, Charpentier P. Sequential supercritical water gasification and partial oxidation of hog manure. Int. J. Hydrogen Energy. 2010; 35: 11756-11767.

[5] Wang J, Takarada T. Role of calcium hydroxide in supercritical water gasification of low-rank coal. Energy & Fuels, 2001; 15: 356–362.

[6] Watanabe M, Aizawa Y, Iida T, Nishimura R, Inomata H. Catalytic glucose and fructose conversions with TiO_2 and ZrO_2 in water at 473 K: Relationship between reactivity and acid–base property determined by TPD measurement. Applied Catalysis A: General. 2005; 295: 150-156.

[7] Han C, Harrison P. Simultaneous shift reaction and carbon dioxide separation for the direct production of hydrogen. Chem Eng Sci. 1994; 49: 5875–5883.

[8] Williams P, Onwudili J. Subcritical and Supercritical Water Gasification of Cellulose, Starch, Glucose, and Biomass Waste. Energy & Fuels. 2006; 20: 1259-1265.

[9] Minowa T, Ogi T, Yokoyama S. Hydrogen Production from Wet Cellulose by Low-Temperature Gasification Using a Reduced Nickel Catalyst. Chem. Lett. 1995; 937.

[10] Minowa T, Zhen F, Ogi T. Cellulose decomposition in hot compressed water with alkali or nickel catalyst. J. Supercrit. Fluids. 1998; 13: 253.

[11] Kruse A, Meier D, Rimbrecht P, Schacht M. Gasification of Pyrocatechol in Supercritical Water in the Presence of Potassium Hydroxide. Ind. Eng. Chem. Res. 2000; 39: 4842-4848

[12] Hui J, Youjun Lu, Guo J. Cao C, Zhang X. Hydrogen production by partial oxidative gasification of biomass and its model compounds in supercritical water Int. J. Hydrogen Energy. 2010; 35: 3001-3010.

[13] Antal J Jr, Allen S, Schulman D, Xu X. Biomass Gasification in Supercritical Water. Ind. Eng. Chem. Res. 2000; 39: 4040-4053.

[14] Le-ming C, Zhang R, BI Ji-cheng. Effect of CaO on conversion of lignite to hydrogen-rich gas in supercritical water. Journal of Fuel Chemistry and Technology. 2007; 35: 3.

[15] Yang S, Yunhan X. Steam Catalysis in CaO Carbonation under Low Steam Partial Pressure. Ind. Eng. Chem. Res. 2008; 47: 4043–4048.

[16] Le Besson M, Gallezot P. Stability of ruthenium catalysts supported on TiO_2 or ZrO_2 in catalytic wet air oxidation. Topics in Catalysis. 2005; 33: 1–4.

[17] Béziat J, Besson M, Gallezot P, Durécu S. Catalytic Wet Air Oxidation of Carboxylic Acids on TiO_2-Supported Ruthenium Catalysts. Journal of Catalysis. 1999; 182: 129-135.

[18] Williams P, Onwudili J. Hydrothermal reforming of bio-diesel plant waste: Products distribution and characterization. Fuel . 2010; 89: 501–509.

[19] Williams P, Onwudili J. Composition of Products from the Supercritical Water Gasification of Glucose: A Model Biomass Compound. Ind. Eng. Chem. Res. 2005; 44: 8739-8749.

[20] Sato T, Sekiguchi G, Adschiri T, Arai K. Dealkylation and Rearrangement Kinetics of 2-Isopropylphenol in Supercritical Water. Ind Eng Chem Res. 2002; 41: 3064–3070.

[21] Fang F, Kozinski J. Supercritical water combustion of organic residues from nuclear plants, Combust. Flame. 2001; 124: 255.

[22] Nagamori M, Funazukuri T. Glucose production by hydrolysis of starch under hydrothermal conditions. J. Chem. Technol. Biotechnol. 2004; 79; 229–233.

[23] Marquevich M, Coll R, Montane D. Steam Reforming of Sunflower Oil for Hydrogen Production. Ind. Eng. Chem. Res. 2000; 39: 2140-2147.

[24] Luijkx G, Van Rantwijk D, Van Bekkum H. Hydrothermal formation of 1,2,4-benzenetriol from 5- hydroxymethyl-2-furaldehyde and D-fructose, Carbohydr. Res. 1993; 242: 131–139.

[25] Elliott D, Todd R, Gary G. Chemical Processing in High-Pressure Aqueous Environments; Improved Catalysts for Hydrothermal Gasification. Ind. Eng. Chem. Res. 1993; 32: 1542-1548.

[26] Kruse A. Supercritical water gasification. Biofuels, Bioprod. Bioref. 2008; 2: 415–437.

[27] Kumar S, Kothari U, Kong K, Lee Y, Gupta R. Hydrothermal pretreatment of switchgrass and corn stover for production of ethanol and carbon microspheres. Biomass and Bioenergy. 2011; 35: 956-968.

[28] Savage P. Organic Chemical Reactions in Supercritical Water. Chem. Rev. 1999; 99: 603–622.

[29] Lin Y, Harada M, Suzuki Y, Hatano H. Comparison of pyrolysis products between coal, coal/CaO, and coal/$Ca(OH)_2$ materials. Energy & Fuels. 2003; 17: 602−607.

CHAPTER 7

Fate of Sulfur during Catalytic and Non-catalytic Cysteine Gasification in Supercritical Water for Hydrogen Production

7.1 Background

In this chapter, the fate of sulfur during catalytic and non-catalytic gasification in supercritical water for hydrogen production was investigated and reported for the first time in the literature. Cysteine was selected as a compound that models sulfur-containing constituents of biomass and waste biomass. An experimental investigation was undertaken to characterize and understand the effects of organic sulfur during the SCW gasification of cysteine. Cysteine ($C_3H_7NO_2S$) is α-amino acid and an important structural and functional component of many proteins. Cysteine contains the sulfide group in its structural formula that makes it suitable to represent sewage sludge and waste biomass proteins. The effect of temperature, different noble metal carbon based supported catalysts was studied. Based on the experimental results reported, a schematic diagram of the possible reaction pathways was developed.

7.2 Introduction

Conversion of biomass and waste biomass into fuels has attracted significant attention recently [1-3]. Dwindling reserves of fossil fuels and their negative environmental impacts has shifted the focus toward the development of alternative energy sources. Hydrogen (H_2) is a promising alternative clean energy source. Hydrogen's viability as a

clean fuel is greatly enhanced if it is produced from renewable sources such as sewage sludge, manure, or other waste biomass types. However, these waste/biomass feed streams contain high moisture content (above 85%) [1], and drying or treating this waste biomass is very expensive due to the high energy input required. Supercritical water (SCW) offers the advantage of converting high moisture content waste biomass into useful products such as hydrogen using gasification. SCW exhibits gas-like and liquid-like properties with respect to density, dielectric constant, ionic product, viscosity, diffusivity, electric conductance, and provides the ability to dissolve organic compounds [1-2]. The dissolution of organic compounds in SCW facilitates the high mass transfer fluxes that allow for faster reaction rates.

Hydrogen production using gasification in supercritical water has been the focus of several studies [4-6]. Supercritical water gasification with catalysis is a candidate for utilization of wet biomass at low temperatures [7 & 8]. However, few studies have examined the fate of sulfur during SCW gasification of biomass and waste/biomass. Given that biomass contains as much as 0.5 % by weight sulfur [10], such a study is critical as sulfur is considered to be one of the worst poisons for SCW catalysts; its action resulting predominantly from the blockage of active sites in addition to its adverse environmental impacts [7]. Osada et al. [11] studied the effect of sulfur addition on catalytic gasification of lignin (which does not contain sulfur) in SCW in the presence of ruthenium, rhodium, platinum, and palladium catalysts. Catalytic gasification experiments were conducted in a stainless steel 316 bomb reactor with an internal volume of 6 cm^3 at 400°C and 35 MPa. The aforementioned authors reported that the catalyst screening results showed a decrease in the activity of catalysts in the presence of sulfur, with the ruthenium catalyst having the

highest activity of the employed catalysts. They also reported that lignin gasification occurred at a slower rate in the presence of sulfur as translated by a carbon gasification efficiency of 70% compared to complete carbon gasification in the absence of sulfur. The aforementioned authors also reported that sulfates and sulfides combined with the active metal sites and not with the catalyst support which explained the catalysts activity reduction. Yanagida et al. [12] studied the behavior of inorganic elements in poultry manure in SCW gasification and reported that 79% of the organic sulfur moved to the liquid phase in the form of sulfates and sulfides. Despite the significant focus of research effort on the SCW gasification of biomass and model waste biomass compounds, information on the behavior and effect of sulfur on the gaseous yield distribution is sparse. Volatile organic sulfur and hydrogen sulfide are well known odorous compounds, the fate of which in SCW has been mostly overlooked. Thus, studying cysteine as a model compound containing sulfur could provide an invaluable addition to understand the behavior of sulfur species present in sewage sludges.

In this work, an experimental investigation was undertaken to characterize and understand the effects of organic sulfur during the SCW gasification of cysteine. Cysteine ($C_3H_7NO_2S$) is α-amino acid and an important structural and functional component of many proteins. Cysteine contains the sulfide group in its structural formula that makes it suitable to represent sewage sludge and waste biomass proteins.

7.3 Materials

Cysteine ($C_3H_7NO_2S$), and 0.5 wt % Ru/Al_2O_3 Pelletilized catalyst was obtained from Sigma-Aldrich Canada Ltd. (Oakville, Ontario, Canada), and 0.5 wt % Ru/AC

(Granular) catalysts were purchased from Alfa Aesar (Ward Hill, MA, USA). Activated carbon (AC) was purchased from Caledon Laboratories Ltd (Georgetown, Ontario, Canada). De-ionized water (18 m·Ω resistivity) was obtained using a compact ultrapure water system (EASY pure LF, Mandel Scientific co, model BDI-D7381).

7.4 Safety Precautions

Due to the possible health risk associated with H_2S gas, all efforts and safety precautions were considered. The first step was to ensure that no H_2S gas leaked through the system as it was tightly closed. The system was equipped with close ventilation through a fume-hood and the H_2S concentration in the lab was monitored using an Odalog hydrogen sulfide logger obtained from App-Tek Inc (Brandale, Queensland, Australia). The logger has a measuring range of 0-1000 ppm at an accuracy of 1% of the full scale, and equipped with Odalog 3 software for downloading of data in tabular or graphical form to highlight significant variations in recorded hydrogen sulfide levels over time.

7.5 Data Interpretation

The calculations of gaseous product yields, and sulfur balance were performed as follows:

Gas yield = (moles of gas species produced)/ (moles of cysteine fed)) (1)

and,

Sulfur balance =

(mg sulfur in the gas+ mg sulfur in the liquid)/mg sulfur in the feed (2)

To ensure experimental reproducibility, experiments no. 7 (Table 7.1) was selected randomly and repeated at the exact same conditions as duplicate (experiment no. 8) and the overall discrepancy was found to be less than 10%.

7.6 Results and Discussion

7.6.1 *Effect of Temperature on Gaseous Products Yield.*

Figure 7.1 shows the effect of temperature on the non-catalytic supercritical water gasification of cysteine. Increasing temperature increases the gaseous products except H_2S, and the main products were H_2, CO_2, and CH_4. Hydrogen and CO_2 were the major gases produced as the temperature increased. However, the H_2S yield variation was minimal at the four temperatures tested; for example, the H_2S yield at 400°C was 0.8 mol/ mol feed compared to 0.75 mol/ mol feed at 500°C.

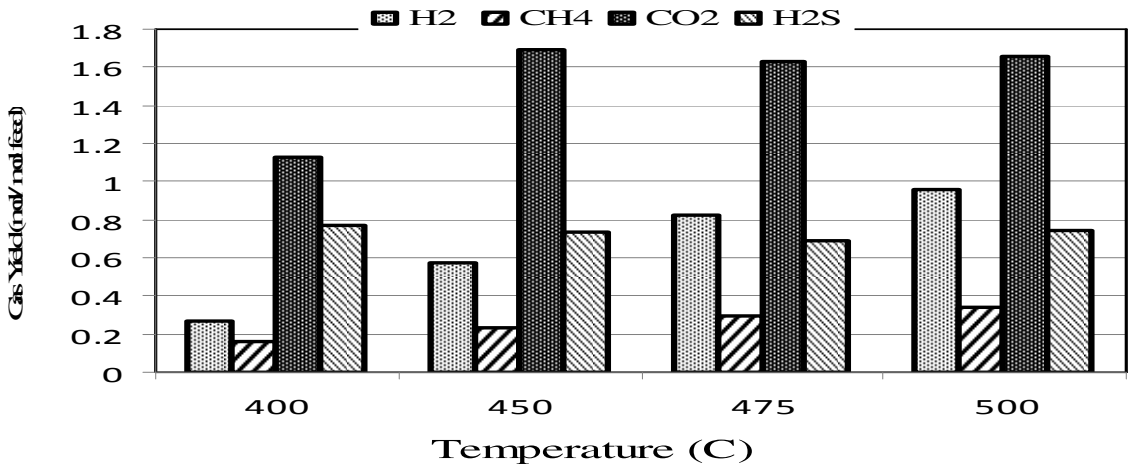

Fig 7.1 The effect of temperature on the non-catalytic supercritical water gasification of cysteine at 28MPa, 30 mins, and 0.25 M.

The maximum hydrogen gas yield of 1 mol/mol feed was achieved at a temperature of 500°C, corresponding to an increase of 0.8 mol/mol feed over the 0.2 mol/mol feed produced at 400°C. However, the trend of increasing H_2 yield with temperature was less pronounced as the temperature increased from 475°C to 500°C i.e. varying from 0.8 to 1 mol / mol feed. The increase in H_2 yield can be attributed to higher cysteine conversion efficiency as well as the degradation of its intermediate products as the temperature increased. The increase in temperature enhanced the thermal decomposition of intermediates facilitating the increase in H_2 content of the produced gas, and potentially the water-gas shift reaction ($CO + H_2O \leftrightharpoons CO_2 + H_2$) through which H_2 increased at the expense of CO [3, 13 and 14]. This s resulted in a substantial increase of H_2 yield and a significant reduction in CO formation as reflected by tripling the H_2 yield from 0.2 to 0.6 mol/mol feed as the temperature increased from 400°C to 450°C and from 0.8 to 1 mol/ mol feed as temperature increased from 475°C to 500°C. The low CO yields helps confirm that the water gas shift reaction was facilitated through which the H_2 yield increases.

7.6.2 *Effect of Catalysts on the Gaseous Products Yield*.

Figure 7.2 shows the distribution of the gaseous product yields measured in SCWG of cysteine using three different catalysts i.e. activated carbon (AC), ruthenium on activated carbon (Ru/AC), and ruthenium on alumina (Ru/Al_2O_3). A temperature of 500°C was selected for catalyst testing to provide the highest gas yield at the maximum vessel pressure/temperature capability. The use of catalysts enhanced the product gas yield significantly when compared with the maximum H_2 yield of 1 mol/mol feed as shown in figure 7.2, with the order of H_2 production following: AC > Ru/AC > Ru/Al_2O_3. The H_2

yields for the aforementioned catalysts i.e. AC, Ru/AC, and Ru/Al_2O_3 of 1.7, 1.6, and 1.5 mol/ mol feed respectively, varied within 10% of one another, and were up to 70% higher than the 1mol/mol feed observed at 500°C without catalyst. Thus, the incorporation of catalyst increased the H_2 production significantly compared to the H_2 yield obtained during the non-catalytic gasification at 500°C. This reveals that the aforementioned catalysts activity was larger than expected since no sulfur poisoning as evidenced by no increase in H_2S and increase in the H_2 was observed.

In fact, a substantial increase in the H_2 gas yield was observed with the examined catalysts and the relatively stable H_2S gas produced which remained at 0.7-0.8 mol/mol feed, close to the levels without catalysts.

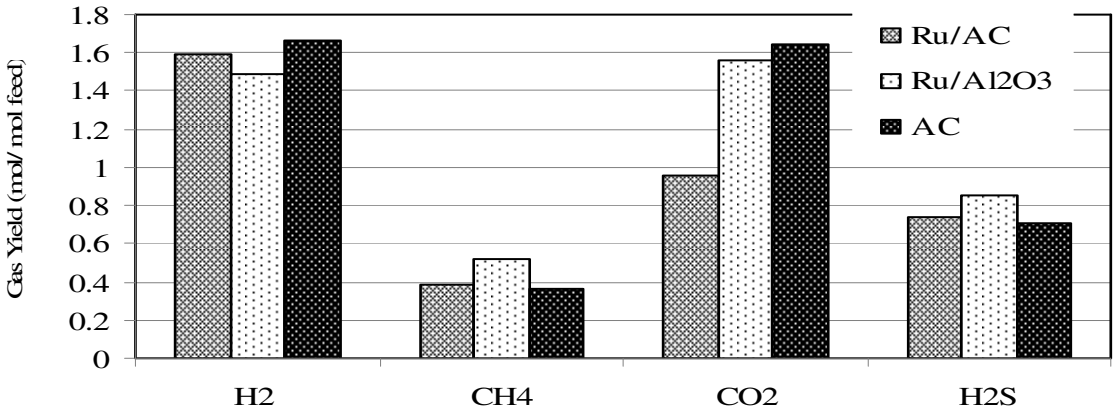

Fig 7.2 Gaseous yields in the catalytic supercritical water gasification of cysteine.

The choice of catalyst did not significantly affect the H_2S gas yield as shown in figure 7.2, with the order of H_2S released as follows: $Ru/Al_2O_3 > Ru/AC > AC$. Clearly, the AC catalyst provided the maximum H_2 yield. The H_2S released ranged from 0.7 to 0.9 mol/mol feed for all 3 catalysts, in close agreement with the 0.7 to 0.9 observed without

catalyst at temperatures of 400 to 500°C. The observation of maximum H_2 production with AC is in good agreement with the findings of Osada et al. [11] who reported that the activity of supported metal catalysts decreased in the presence of sulfur addition in SCW but that the activated carbon remained unaffected. For the Ru/AC catalyst, the CO_2 yield was 70% and 60% lower than that of AC and Ru/Al_2O_3 catalysts respectively. However, the yield of CH_4 for Ru/Al_2O_3 was 25% higher than the yield of Ru/AC and AC.

7.6.3 *Fate of Sulfur in Cysteine*.

The main sulfur-containing compound in the gaseous effluents was H_2S. To track down the sulfur transformations during the SCW gasification of cysteine, analysis of the liquid effluent was conducted. The detected sulfur-containing components in the liquid effluents were sulfide and sulfate. The balance of sulfur was performed for each run to test the reliability of the experiments and analysis. Table 7.1 shows the concentration distribution of sulfur compounds in both the liquid and gas phases, and the typical result of the sulfur balance. The quantity of S from H_2S reported in Table 7.1 was calculated using the measured H_2S in the gas phase and the calculated H_2S concentration in the liquid phase using Henry's law.

The relatively good results of the sulfur balance reported in Table 7.1 indicate that the main sulfur containing compounds in the gaseous and liquid effluents were detected. However, about 20% of sulfur is unaccounted for and could be present as organic sulfur in the liquid phase as evidenced by the presence of Ethanone, 1-3-thienyl (C_6H_6OS) which was not measured.

Table 7.1 The concentration distribution of sulfur compounds in both liquid and gas phases.

Exp.No	Temp (°C)	Catalyst type	mg Sulfide (S^{2-}) in liquid	mg Sulfate (SO_4^{2-}) in liquid	mg Sulfur (from H_2S)	Sulfur balance (%)
1	400	None	12	2	615	79
2	450	None	19	0	582	76
3	475	None	56	3	547	76
4	500	None	47	3	594	81
5	Opt	AC	75	3	561	80
6	Opt	Ru/Al_2O_3	66	4	681	95
7	Opt	Ru/AC	56	3	583	81
8	Opt	Ru/AC*	59	3	572	80

* (duplicate) ; Opt ≡ 500°C

In order to identify the main liquid effluent compounds, we performed a qualitative analysis of the process liquid effluent using gas chromatography/ mass spectrophotometry (GC/MS). Identifying the compounds was performed by employing an automatic comparison of the derived ion mass spectra to NIST or Wiley spectral libraries. Table 7.2 reports the gas chromatography/mass spectrometry (GC-MS) results of the residual liquid effluent. At a similarity indexes of greater than 75%, a total of 16 compounds were reported using the aforementioned selection criteria, and the products were mainly composed of sulfides, cyclo-compounds such as cyclobutane, cyclobutene, phenol and its substitutes such as phenol, and 3,5-dimethyl phenol. The rest of the compounds were of various structures including nitrogen containing compounds such as pyrrole and 2, 3-benzopyrrole.

The results in Table 7.2 showed that the conversion of sulfur contained in cysteine was predominantly to H_2S; for example, only 2% and 3% of the sulfur were present in the form of sulfide and sulfate compared to 98% and 97% in the form of H_2S at temperatures of

400°C and 450°C respectively. However, this percentage distribution of sulfate and sulfide increased to 10% and 9% as the temperature increased to 475°C and 500°C respectively, which indicating that the sulfur conversion depends on the reaction temperature [13 & 14]. The sulfate quantity in the liquid effluent for all experiments was almost the same at around 2-4 mg. However, the sulfides concentration increased as the temperature increased and increased further as the catalysts were introduced. For example, the sulfide quantity in the presence of the AC catalyst and temperature of 500°C was 75 mg which corresponds to an increase of 60% compared to its non-catalytic counterpart at 500°C.

Table 7.2 Gas chromatography/mass spectrometry (GC-MS) qualitative analysis

Compound No.	Similarity Index	Exp No.	(3)	(4)	(5)	(6)	(7)
		Catalyst	N/A	N/A	AC	Ru/Al_2O_3	Ru/AC
		Temperature (°C)	400	500	500	500	500
1	97	Phenol	√	√	√	√	√
2	98	Phenol, 3,5-dimethyl- ($C_8H_{10}O$)	√	√	√	√	√
3	97	Cyclohexene (C_6H_{10})	√	√	√	ND	√
4	97	Cyclobutane (C_4H_8)	ND	√	√	√	ND
5	95	Butanone " ethyl methyl ketone"	√	√	ND	ND	ND
6	96	Pyrrole (C_4H_5N)	ND	√	√	√	√
7	93	Cyclopentanone " Adipic ketone" (C_5H_8O)	√	ND	ND	√	ND
8	94	Acetophenone	ND	√	√	√	√
9	96	Ethanone, 1-3-thienyl (C_6H_6OS)	√	ND	√	√	√
10	83	Cresols (C_7H_8O)	√	ND	ND	√	√
11	82	Diethyl tri-Sulfide ($C_4H_{10}S_3$)	√	√	√	√	√
12	97	Diethyl Sulfide ($C_4H_{10}S_2$)	√	√	√	√	√
13	97	3-Ethyltoluene (C_9H_{12})	√	ND	√	√	ND
14	93	2,3-Benzopyrrole "Indole" (C_8H_7N)	√	√	√	√	√
15	96	Cyclohexen-1-one (C_6H_8O)	√	√	ND	√	√
16	97	2-Cyclopenten-1-one, 2-methyl (C_6H_8O)	√	√	ND	√	ND

Clearly, the presence of diethyl sulfide and diethyl tri-sulfide proves that sulfur present in the liquid was mainly in the form of sulfides and a smaller concentration of sulfates. Based on the above discussion and the experimental results reported that H_2S generation was independent of temperature and catalyst type while the gaseous product yields varied with temperature and catalysts. Figure 7.3 provides a schematic diagram of the possible reaction pathways based on the experimental results and the GC/MS analysis.

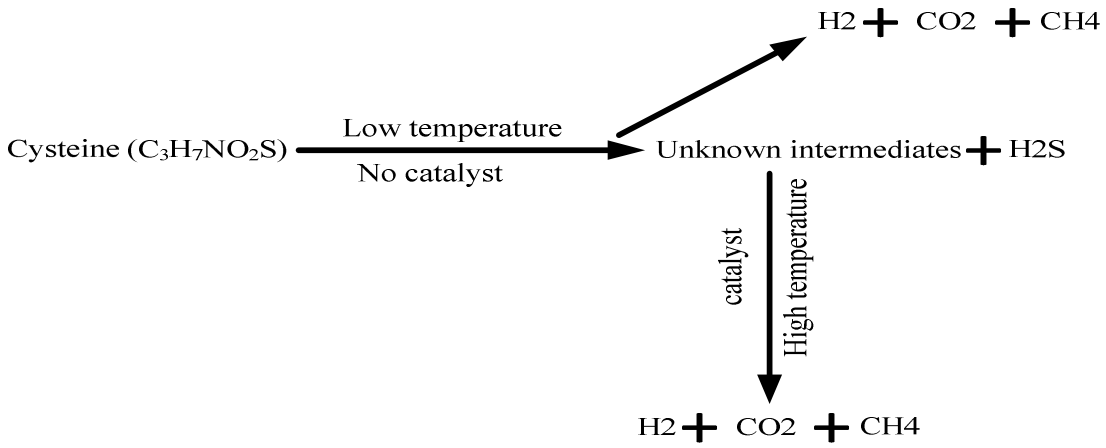

Fig 7.3 Schematic of proposed reaction pathways for cysteine gasification in SCW.

7.7 References

[1] Savage P. Organic chemical reactions in supercritical water. Chem Rev.1999; 2: 603–621.

[2] Kruse A. Supercritical water gasification. Biofuels, Bioprod. Bioref. 2008; 2: 415–437.

[3] Antal J Jr, Allen S, Schulman D, Xu X. Biomass Gasification in Supercritical Water. Ind. Eng. Chem. Res. 2000; 39: 4040-4053.

[4] Guo Y, Wang S, Xu D, Gong Y, Tang X, Zhang J. Hydrogen Production by Catalytic Supercritical Water Gasification of Nitriles. Int. J. Hydrogen Energy. 2010; 35: 4474–4483.

[5] Kruse A, Meier D, Rimbrecht P, Schacht M. Gasification of Pyrocatechol in Supercritical Water in the Presence of Potassium Hydroxide. Ind. Eng. Chem. Res. 2000; 39: 4842-4848.

[6] Minowa T, Ogi T. Hydrogen Production from Cellulose using a Reduced Nickel Catalyst. Catal. Today. 1998; 45: 411.

[7] Osada M, Sato O, Watanabe M, Arai K, Shirai M. Stability of Supported Ruthenium Catalysts for Lignin Gasification in Supercritical Water, Energy & Fuels. 2006; 20: 930–935.

[8] Yamaguchi A, Hiyoshi N, Sato O, Bando K, Osada M, Shirai M. Hydrogen Production from Woody Biomass over Supported Metal Catalysts in Supercritical Water. Catal Today. 2009; 182: 192–195.

[10] Klass D L. Biomass for Renewable Energy, Fuels, and Chemicals; Academic Press: San Diego, CA, 1998; 72-87.

[11] Osada M, Hiyoshi N, Sato O, Arai K, Shirai M. Effect of Sulfur on Catalytic Gasification of Lignin in Supercritical Water. Energy & Fuels. 2007; 21: 1400-1405.

[12] Yanagida T, Minowa T, Nakamura A, Matsumura Y, Noda Y. Behavior of Inorganic Elements in Poultry Manure during Supercritical Water Gasification. Journal of the Japan Institute of Energy. 2007; 86: 731-736.

[13] Wang T, Zhu Xi. Sulfur Transformations during Supercritical Water Oxidation of a Chinese Coal. Fuel. 2003; 82: 2267–2272.

[14] Youssef, A., E, Elbeshbishy, E.; Hafez, H.; Nakhla, G.; Charpentier, P. Sequential Supercritical Water Gasification and Partial Oxidation of Hog Manure for Hydrogen Production. Int J Hydrogen Energy.2010; 35: 11756-11767.

CHAPTER 8

Sequential Supercritical Water Gasification and Partial Oxidation of Hog Manure for Hydrogen Production

8.1 Background

In this chapter, non-catalytic and catalytic gasification of hog manure as real waste biomass was performed in SCW. The effect of reaction time, oxidant molar ratio and different heterogeneous and homogenous catalysts was investigated. while the overall objective of this study is to demonstrate the feasibility of hydrogen production from hog manure using SCW, , the specific goals include:

- Parallel side-by-side assessment of the impact of sequential gasification and partial oxidation relative to the conventional gasification and partial oxidation reaction solely on the fate of ammonia, sulfur, and organics that have not been reported in the literature.
- Evaluate the activity of different commercial heterogeneous and homogenous catalysts including supported activated carbon metallic on the gaseous products as well as on the liquid effluent quality

8.2 Introduction

Conversion of waste biomass to energy is of great interest due to the simultaneous ability for both resource recovery and pollution abatement. Hog manure contains major plant nutrients and organic matter that can be utilized as a potential to produce hydrogen-rich gaseous fuel. Thus, hydrogen production from hog manure may be a solution for cleaner fuel as well as

disposal problems. However, hog manure usually contains a high fraction of water whereas a dry feedstock is required for conventional gasification, as the drying process is an energy-intensive operation due to high heat capacity of water. Supercritical water (SCW) is a promising technology for gasifying waste biomass with high moisture content. SCW is an emerging technology that has been developed to treat hazardous waste streams as well as producing green gases such as hydrogen [9, 18, and 28]. SCW can dissolve most organic substances and gases and has low viscosity and strong transport ability. Above water's supercritical conditions (T>374°C, P>22.1MPa), the density, dielectric constant, and ionic product of water decreases with the SCW acting as a non-polar solvent with high diffusivity and excellent transport properties [9, 11,15, and 19]. This facilitates the dissolution of many non-polar organic compounds and gases in water. The SCW high diffusivity coupled with high solubility of both gases and organic materials provides high mass transfer fluxes which accelerate reactions [22]. Thus, SCWO is considered useful to eliminate a wide range of problematic wastes from a broad variety of industries [19].

The fact that manure has a very high water content (>95% on a wet basis), makes it more suitable for the SCW process than other conventional treatment processes. Furthermore, hog manure due to its high water, solids, and ash content is not amenable to treatment in conventional fossil-type furnaces such as incinerators and gasifiers due to their high energy consumption and plugging [35]. Moreover, sulfur in the waste is converted to sulfur dioxide and trioxides [35] which increases corrosiveness. Biological treatment of hog manure, although technically feasible, requires extremely long hydraulic retention time (HRTs) on the order of days; high energy input, and has a potential for odor generation with a poor response to dynamic loading conditions as well as exhibits sensitivity to toxins [36]. Each of these treatment methods has

shortcomings and therefore may not be the best option for treating organic and toxic wastes [30]. Thus, employing SCW to produce green energy from waste streams such as hog manure has many advantages. Indeed, using SCW as a reaction medium avoids the expensive step of drying. In fact, estimated feedstocks of 30% or higher moisture content are preferable and more economical in SCW [31, 32]. Moreover, the ability of SCWG to achieve higher conversion (over 99%) of the solid particles and high hydrogen production coincident with suppression of char and tar formation [23] renders them very attractive.

Several studies have been reported in the literature on biomass or biomass model compounds gasification for H_2 production using SCW [2, 3, 5-7, 9, 10, 28, 34]. These studies employed both heterogeneous and homogeneous catalysts (such as NaOH, KOH, activated carbon, metallic catalysts). Osada et al. [1, 2, and 3] reported that supported ruthenium, rhodium, platinum, palladium, and nickel catalysts are active in the decomposition of aromatic compounds. The aforementioned authors pointed out that lignin is first converted to alkylphenols and formaldehyde through hydrolysis in supercritical water; the alkylphenols and formaldehyde decompose to gases over the above mentioned catalysts. Osada et al [1] who conducted gasification experiments of biomass, coal and waste plastics in an autoclave at 450°C, 44MPa, and 120 minutes reported that Ruthenium (Ru) metal particles aggregated during the first run because the surface area of the Al_2O_3 support drastically decreased due to its crystal structure change from γ-Al_2O_3 to α-Al_2O_3.

In a recent study, Zhang et al. [8] conducted partial oxidative gasification of municipal sludge (5 wt%) with a NaOH catalyst using a batch type reactor at a temperature ranging of 350-500° C, pressure range 23-28 MPa and residence time from 5 to 40 min. The aforementioned authors reported that municipal sludge can be gasified in supercritical water with no char and tar

at a relatively lower temperature of 500°C than the 700°C required for biomass. Their experimental results on hydrogen production from municipal sludge showed that addition of the base catalyst NaOH coupled with partial oxidation enhanced the hydrogen mole fraction yield from 20% to 40%. The addition of NaOH lowered the decomposition temperature of sludge and promoted the water-gas shift reaction.

Osada et al. [4] who studied the effect of both base (NaOH) and metal zirconium oxide (ZrO_2) catalysts on the partial oxidative gasification of *n*-hexadecane and lignin in SCW reported a doubling of the hydrogen yield from lignin by adding zirconia catalyst at an oxygen-to-carbon ratio of 1.0, and four times higher hydrogen yield upon addition of sodium hydroxide (NaOH). Yamaguchi et al [10] reported that ruthenium, rhodium, platinum, palladium, and nickel noble metal catalysts supported on activated carbon showed higher hydrogen and carbon monoxide selectivity. According to Cortright et al. [21], H_2 selectivity is evaluated to know how many hydrogen atoms in an organic compound can be taken out as H_2 in the gas phase. The role of gasification is to promote the water-gas shift reaction whereas the thermal decomposition of intermediates is enhanced by the partial oxidation reactions. This suggests that the hydrogenation of biomass by employing sequential gasification partial oxidation can enhance the H_2 production rate. Thus, the relevant processes could be approximated by the following general reactions:

Gasification:

$$C_mH_nO_pN_jS_{k\ \{Catalyst\}} \rightarrow CO+CO_2 + H_2 + CH_4 + H_2S + \text{Intermediate products} \quad (1)$$

Partial oxidation:

$$[C_mH_nO_pN_jS_k]_{\{\%O2<1\}} + \text{Intermediate products} \rightarrow CO_2+CO + H_2+ H_2S + \text{other components} \quad (2)$$

Water-gas shift reaction:

$$CO + H_2O \rightarrow \text{active hydrogenating species} \rightarrow CO_2 + H_2 \quad (3)$$

Methanation reactions:

$$CO + 3H_2 \rightarrow CH_4 + H_2O \quad (4)$$

$$CO_2 + 4H_2 \rightarrow CH_4 + 2H_2O \quad (5)$$

The challenges of hog manure stem directly from the high solids content and the odorous compounds i.e. ammonia and sulfur. Furthermore, it is evident from the above literature that even studies on thermal hydrogen production from wastes have focused on the energy recovery aspect without due consideration of residual liquid quality and odorous compounds emissions. Thus, while the overall objective of this study is to demonstrate the feasibility of hydrogen production from hog manure using SCW, the specific goals include:

- Parallel side-by-side assessment of the impact of sequential gasification and partial oxidation relative to the conventional gasification and partial oxidation reaction solely on the fate of ammonia, sulfur, and organics that have not been reported in the literature.
- Evaluate the activity of different commercial heterogeneous and homogenous catalysts including supported activated carbon metallic on the gaseous products as well as on the liquid effluent quality.

8.3 Materials and Methods

Hog manure was obtained from a facility in South Western Ontario used as the feed characterized by a total and soluble chemical oxygen demand, Volatile suspended solids, and ammonia. 5% ruthenium supported on alumina and 5% ruthenium supported on carbon catalysts were purchased from Alfa Aesar (Ward Hill, MA, USA). Alkali NaOH reagent grade and 5% palladium supported on carbon catalysts were obtained from Sigma-Aldrich Canada ltd (Oakville, Ontario, Canada). Activated carbon was purchased from Caledon Laboratories Ltd (Georgetown, Ontario, Canada). The experimental procedures details are explained in chapter 3.

8.4 Data Interpretation

For the purpose of COD balance calculations, the reactor feed, and liquid effluent COD were measured. The gaseous product COD was also calculated. The product gas yield, gas composition, COD reduction efficiency, and COD balance are defined as follows:

$$\text{Gas composition (\%)} = (\text{mol gas product}) / (\text{sum of mol gas product}) \times 100 \quad (6)$$

$$\text{Product gas yield} = \text{gas volume produced (ml)} / \text{COD removed (g)} \quad (7)$$

$$\text{COD reduction efficiency (\%)} = \{[COD_{initial} - COD_{final}] / [COD_{initial}]\} \times 100 \quad (8)$$

$$\text{COD balance} = [COD_{\text{gas product}} + COD_{\text{liquid product}} + COD_{\text{reactor residual}}] / [COD_{\text{in}}] \quad (9)$$

8.5 Results and Discussions

8.5.1 *Effect of residence time and partial oxidation on gas yield from hog manure in SCW*

We first investigated the effect of residence time on the gas yield at a temperature of 500°C, pressure of 28 MPa, oxygen dose (OD) equals to 80% of the theoretical COD required to oxidize all the initial COD, and residence times of 30, 60, and 90 mins. The oxygen dose was optimized in a previous study and was adopted as a base line for catalysts evaluation [5]. Figure 8.1 shows the H_2, CO, and CO_2 yields in the gas stream. As shown in Figure 8.1, the CO yield was always insignificant with the CH_4, and CO_2 yields following 60>30>90 minutes. The H_2 yield at a reaction time of 60 minutes of 5.7 mmol/gCOD removed was higher than the 30 minutes reaction time by an insignificant amount (0.1 mmol/gCOD removed). Thus, since all differences were not substationally significant, we selected the reaction time of 30 minutes as a base line for the subsequent experiments.

However, the yield of methane increased from 4.2 mmol/gCOD removed at 30 minutes to 4.9 mmol/gCOD removed at 60 reaction time which implies acceleration of the methanation reactions as per equations 4 and 5. On the other hand, the absence of CO in the effluent gas in the three experiments implies that the water-gas shift reaction occurred and may be one of the reasons for the enhancement of H_2 production [9, 10]. However, the exact extent of the water-gas shift reaction was not evidently identified since CO_2 could be produced from other reactions or from the thermal decomposition of some intermediates. Another possible way of H_2 formation is the thermal decomposition of the intermediate compounds [8, 28, and 33]. In other words, the presence of oxygen as an oxidant probably contributed to the H_2 formation by oxidizing some of the organic intermediate compounds as reported in our previous study [5].

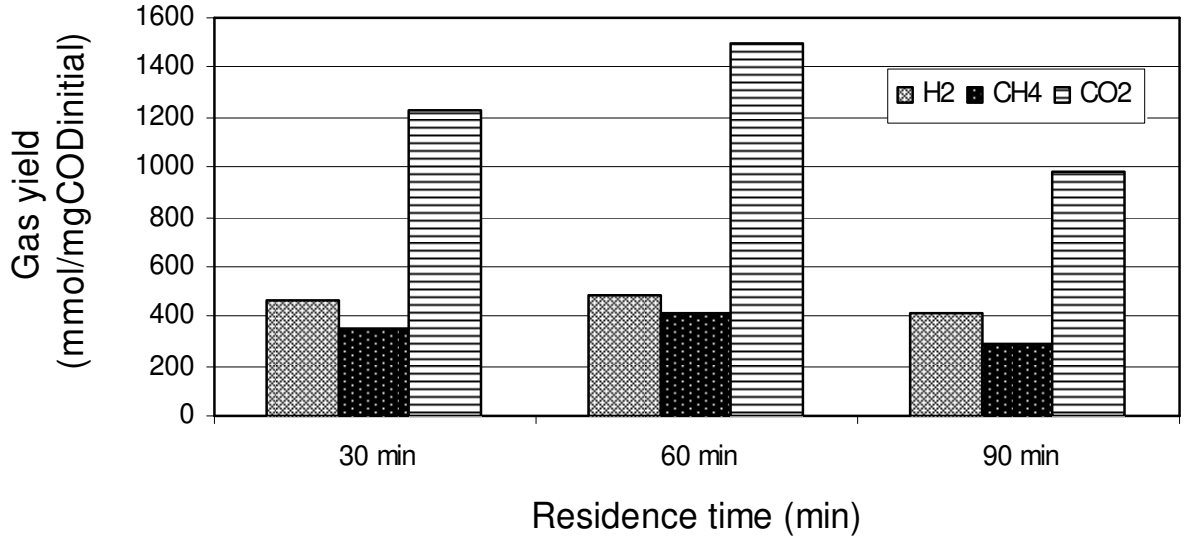

Fig 8.1 Gas yield distribution in partial oxidation experiment at different residence time.

Table 8.1 summarizes the liquid effluent quality for the investigated reaction times. It is apparent that residual ammonia at 90 minutes decreased by 20% to 4180 mg/L relative to 30 and 60 minutes. A COD reduction of 83 %, 85 % and 81 % was achieved at residence times of 30 min, 60 min and 90 min, respectively, and the reduction in COD was found to be independent of

the residence time. The lowest residual COD of 8775 mg/L was observed at the 60 minutes reaction time which was 18% lower than the maximum COD at 90 minutes. This implies that after 60 minutes of reaction, some components were involved in intermediate reactions and formed other liquid components that eventually increased the TCOD and SCOD. The VFAs, ethanol and methanol combined constituted 33 %, 33 % and 24 % of the SCOD at residence times of 30, 60 and 90 minutes, respectively. In all experiments, and as reported in Table 8.1, the TSS and VSS concentrations were less than 300 mg/L which corresponds to destruction of more than 98% of their initial values.

Table 8.1 Liquid effluent characterization in partial oxidation experiments (No Catalyst; MR= 0.8).

Reaction time	30 min	60 min	90 min
Concentration (mg/L)			
Total Oxygen Demand (TCOD)	9740	8775	10740
Soluble Oxygen Demand (SCOD)	6942	6480	8160
Total Suspended Solids (TSS)	540	220	440
Volatile Suspended Solids (VSS)	400	160	360
Total Phosphorous (PO4-)	454	270	302
Volatile Fatty acids (VFA)	2323	2129	1964
Nitrate	15	9	8
Alkalinity	N/A	31030	28890
pH	9.23	9.3	9.21
COD values (mg)			
COD gas product	1775	1725	1559
COD liquid product	974	878	1074
COD reactor residual	2100	2264	2339
COD reduction (%)	83	85	81
COD balance (%)	85.3	85.6	87.4

COD balance calculation sample [COD balance at 30 min = (COD gas product + COD liquid product + COD reactor residual) / {(COD of the feed) X sample volume}], sample volume was 100ml or 0.1 L in all experiments.

8.5.2 *Effect of catalysts on gas yield from hog manure in SCW*

The effect of different catalysts on SCW gasification of hog manure was investigated by using 2.5 grams of catalyst for each experiment, and eliminating the oxygen addition. Figure 8.2 shows the product gas distribution for each catalyst. The major components of the product gas yield in all experiments were CO_2, H_2, and CH_4. However, trace amounts of CO was detected only in the case when NaOH was used as catalyst. The negligible CO yield (almost 0 mmol/gCOD removed) during the Pd/AC, Ru/Al_2O_3, Ru/AC, and AC catalytic experiments was found to be in good agreement with the obtained results for AC catalyst by Antal and Xu [9, 29]. Furthermore, Elliott and Sealock [33] selected the rate of CO disappearance as a measure of the water-gas shift reaction rate in preference to the rate of CO_2 or H_2 increase. It was noticed that the H_2/CO_2 yield ratio equaled to 1.2 in the case when NaOH was used as a catalyst. The higher than unity H_2/CO_2 yield ratio implies that the CO_2 was not completely recovered since CO_2 tends to dissolve in alkaline solutions (NaOH in this case). Zhang et al [8] reported that alkali salts increase the reaction rate of the water-gas shift reaction, and ultimately the reaction of CO with water to produce H_2 and CO_2 as per equation 3.

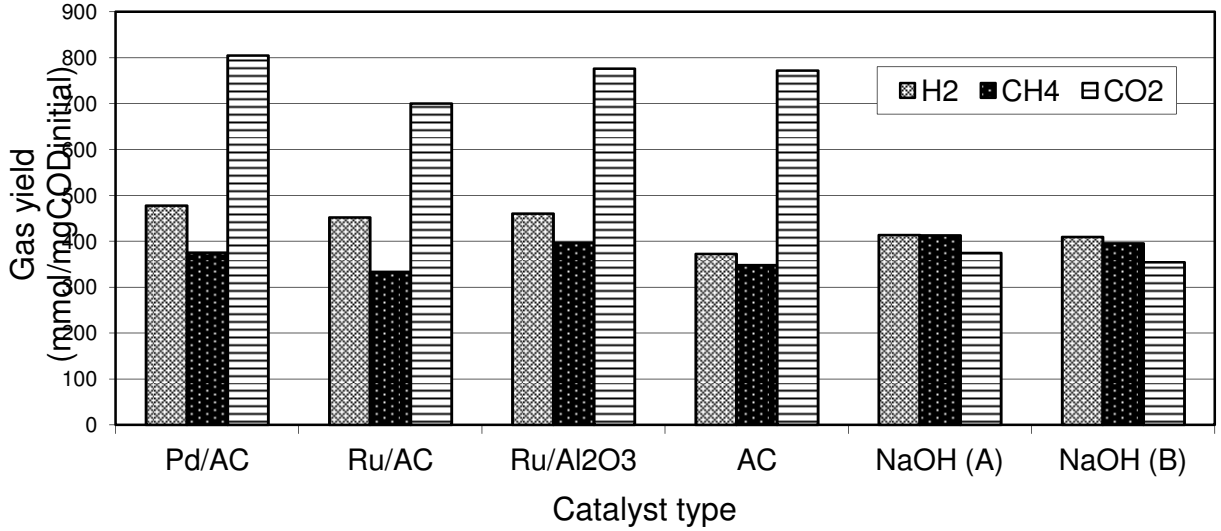

Fig 8.2 Gas yield distribution with different metal supported catalysts

As apparent from Figure 8.2, the Pd/AC catalyst produced the highest H_2 yield followed by Ru/Al_2O_3 catalyst. Yamaguchi et al. [10] reported that the selectivity and yield of H_2 was the highest with Pd/C catalyst whereas the Ru/C catalyst was the most active for lignin gasification. However, and as shown in Table 8.2, the COD reduction efficiency with the Pd/AC catalyst was lower than with the Ru/Al_2O_3 and Ru/AC catalysts since the Ruthenium metal surface is known to promote the methanation hydrogen-consuming reactions [10] as per equations (4 & 5).

Table 8.2 Liquid effluent characterization in gasification experiments.

Catalyst	Pd/AC	Ru/Al_2O_3	Ru/AC	AC	NaOH (A)	NaOH (B)
Concentration (mg/L)						
Total Oxygen Demand (TCOD)	22000	20100	18660	19460	11140	10760
Soluble Oxygen Demand (SCOD)	21500	15200	16920	11720	9050	8940
Total Suspended Solids (TSS)	900	840	1600	420	900	840
Volatile Suspended Solids (VSS)	800	720	580	360	800	720
Total Phosphorous (PO4-)	519	387	513	309	427	453
Volatile Fatty acids (VFAs)	1846	2610	1071	1692	2296	2048
Nitrate	26	7	6	0	0	0
Alkalinity	23450	28160	35000	10130	27450	N/A
pH	9.37	9.27	9.46	9.57	9.88	9.83
COD values (mg)						
COD gas product	1734	2020	1793	2804	3348	3222
COD liquid product	2200	2010	1866	1946	1114	1076
COD reactor residual	1127	560.3	1469	892	1141	1158
COD reduction (%)	61	65	71	66	81	81
COD Balance (%)	89	80.7	90.2	99.2	98.6	96

Experiment B is the duplicate of experiment A

Furthermore, the COD removal efficiency in the absence of oxygen was retarded in all the experiments to less than 70 %, except for the experiments where NaOH was used as a catalyst where a COD removal efficiency of 81 % was achieved comparable to what was observed with partial oxidation. As discussed later, the Pd/AC catalyst affected the highest removal of ammonia as well as the lower H_2S concentration in the gas, which coupled with

highest H_2 yield, rationalizes the retention of Pd/AC for subsequent sequential gasification partial oxidation testing.

8.5.3 *Effect of partial oxidation and catalyst on gas yield from hog manure in SCW*

We studied the effect of two different oxygen doses (OD) of 60% and 80% of the theoretical COD required to destroy all the initial COD on the product gas yield in the presence of Pd/AC catalyst. Figure 8.3 reports the product gas yield in mmol/gCOD removed. At an (OD) of 60%, 3 mmol CH_4/gCOD removed and 3.5 mmol H_2/gCOD removed was produced comparing to 3 mmol CH_4/gCOD removed and 5 mmol CH_4/gCOD removed at an (OD) of 80% was employed.

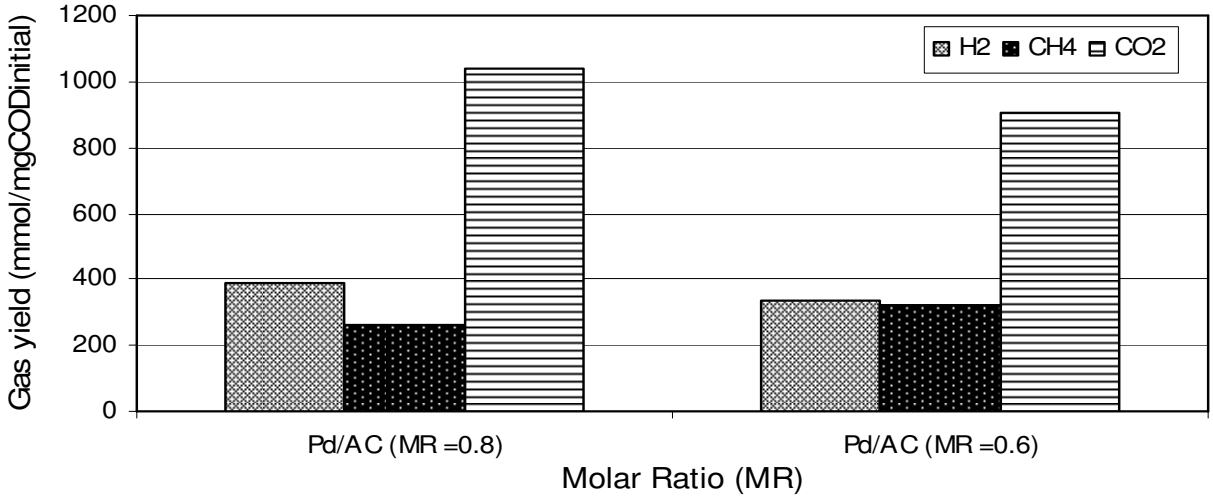

Fig 8.3 Gas yield distribution at gasification followed by partial oxidation experiments.

These results indicated that at an (OD) of 60%, the methanation reaction proceeded and consumed part of the produced H_2 to form CH_4 which was also confirmed by the lower CO_2 yield of 11mmol/gCOD removed compared to the 14mmol/gCOD removed at an (OD) of 80%, [7, 33]. The lower CO_2 yield at an (OD) of 60%, could be also attributed to the lack of oxygen

which affects the formation of CO_2 through direct oxidation of CO to CO_2. Furthermore, and according to Cortright et al [21], the H_2/CO_2 yield ratio of 1.0 at an (OD) of 60% suggests that CO was consumed through the water-gas shift reaction to form H_2 prior to the introduction of hydrogen peroxide (H_2O_2) to the reactor as an oxygen source. This is also supported by Zhang et al [8], who reported that the improvement of H_2 yield in the presence of catalyst in the reactor is explained by the production of CO by partial oxidation followed by the water-gas shift reaction.

On the other hand, Table 8.3, showing the main liquid products in the sequential gasification partial oxidation experiments, indicates that COD removal efficiencies at an (OD) of 60% and 80% were comparable at 79 % and 81% respectively whereas the COD balance closures were 94% and 89% respectively, with COD balance closure of 94% and 89%. In all experiments, the liquid effluent collected from the gas-liquid separator was characterized by a dark brown color with a burnt smell.

Table 8.3 Liquid effluent characterization in sequential gasification and partial oxidation experiments

MR	0.8	0.6
Catalyst	Pd/AC	Pd/AC
Concentration (mg/L)		
Total Oxygen Demand (TCOD)	11920	10800
Soluble Oxygen Demand (SCOD)	7400	8800
Total Suspended Solids (TSS)	820	860
Volatile Suspended Solids (VSS)	700	600
Total Phosphorous (PO4-)	489	504
Volatile Fatty acids (VFAs)	1700	1891
Nitrate	8	14
Alkalinity	10127	26050
pH	9.24	9.31
COD values (mg)		
COD gas product	1330	1424
COD liquid product	1192	1080
COD reactor residual	2802	2573
COD reduction (%)	79	81
COD Balance (%)	94	89

8.5.4 *Fate of VFA's, Ethanol, and Methanol*

Identifying the intermediate products could help understanding the reaction mechanisms and eventually the development of kinetic models required for reactor design. Shanableh et al. [14, 16, and 17] reported the formation of acetic acid as one of the main intermediates during SCWO and wet air oxidation of organic wastes. Jomaa [16] reported that high molecular weight volatile fatty acids (VFAs) generated at lower temperatures were replaced by lower molecular weight VFAs as the reaction temperature and residence time increased. Acetic acid was found to accumulate as the major organic intermediate byproduct during hydrothermal oxidation of biosolids and many other organic feedstocks prior to complete oxidation [14, 19, and 20]. However, in our experiments the trend was quite different; acetic acid was the major component in the initial feed prior to any experiment (Figure 8.4a) with propionic and iso-butyric acids found at smaller concentrations as well as negligible ethanol and methanol concentrations. Figure 8.4 b, c and d portray the concentration distributions of the VFA's, methanol, and ethanol measured in the liquid effluent for all three steps of this study i.e. partial oxidation, gasification, and sequential gasification partial oxidation. Careful observation of the graphs concludes that ethanol exhibits more resistant behavior towards gasification and oxidation in SCW than acetic acid. In their global kinetic model development, Li et al. [19] reported that methanol, ethanol, and acetic acid were intermediates in the wet air oxidation (WAO) reactions.

However, the aforementioned authors assumed that the amounts of ethanol and methanol formed in WAO were usually negligible as compared to acetic acid. Thus, the authors assumed that acetic acid is the rate controlling step for WAO of organic compounds. Furthermore, and for wastewater containing nitrogenous compounds only, Li et al. [19] proposed a variation of the generalized model, assuming ammonia as a rate-controlling intermediate. The results reported in

this study demonstrate that contrary to the literature ethanol, as it evident from the reported results, is the key intermediate rate-controlling step. Thus, one can conclude that during SCW gasification for H_2 production, the global reaction kinetic should be investigated thoroughly i.e. a kinetic model for H_2 production from waste streams should be based on different rate-controlling steps.

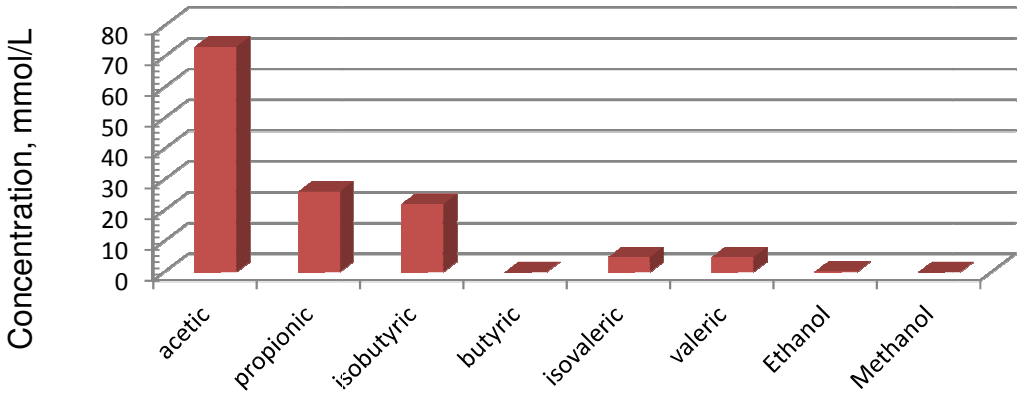

Fig 8.4-a Feed VFA's and alcohols

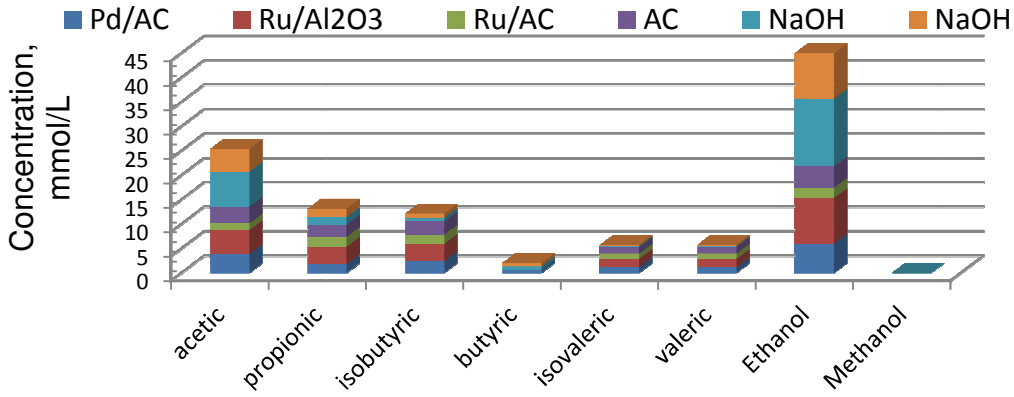

Fig 8.4b. Distribution of VFAs in all catalytic experiments at an MR=0

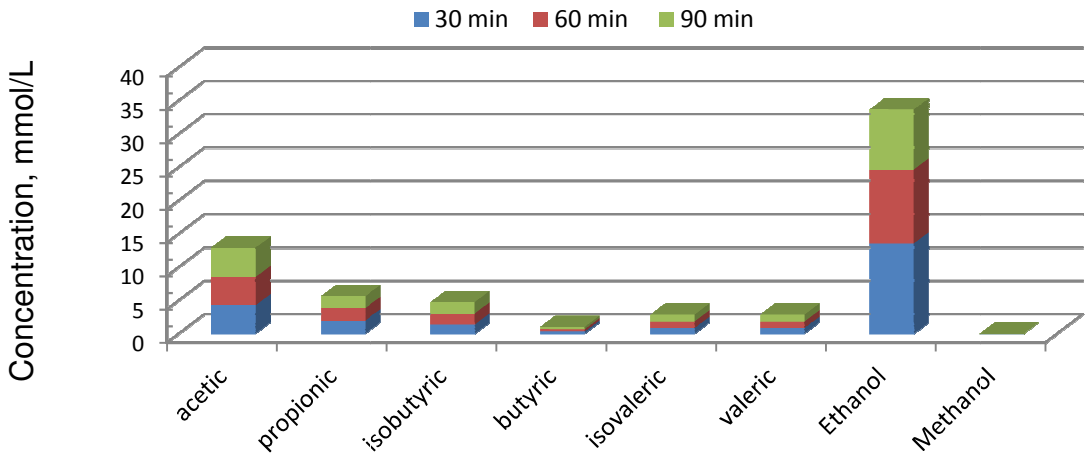

Fig8.4c. Distribution of VFAs in the non-catalytic partial oxidation experiments at an MR=0.8

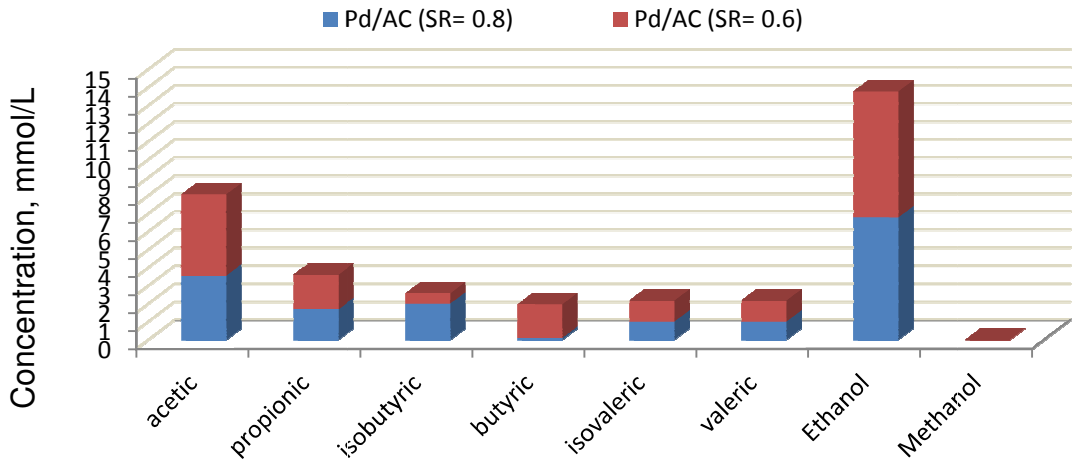

Fig 8.4d. Distribution of VFAs in the sequential gasification partial oxidation experiments with Pd/AC catalyst and an MR=0.8

Fig 8.4 Distribution of VFA's and alcohols in the liquid effluent for each experimental category as (mmol/L)

8.5.5 *Fate of Ammonia*

Table 8.4 depicting the initial and final ammonia concentrations, clearly emphasizes that for all test conditions excluding sequential gasification partial-oxidation, liquid phase ammonia concentrations increased from 2400 mg/L to as high as 5030 mg/L. Comparing the Total

Kjeldahl Nitrogen (TKN) of hog manure presented in the feed of about 5000 mg/L on average with ammonia results during partial oxidation (Table 8.4) clearly indicates that all soluble and particulate organic nitrogen was ammonified at the utilized reaction conditions. However, incomplete ammonification of organic nitrogen was observed for all catalysts investigated during gasification. Thus, the increase of ammonia concentration in the liquid effluent in our partial oxidation oxygen dose of 80% of the required theoretical and residence times of 30, 60, and 90 min) and gasification solely (in presence of catalyst and OD= 0 experiments may be attributed to the hydrolysis of nitrogen-containing organic compounds in subcritical water [12, 13]. In addition, nitrogen-containing compounds in waste streams produce ammonia as intermediate hydrolysate [24]. In the case of sequential gasification partial oxidation, a 36 % reduction of the initial ammonia was observed at the two oxygen doses (OD of 60% and 80%). This suggests that ammonia was oxidized with the aid of both Pd/AC catalyst and oxygen although we cannot presently speculate on the ammonia oxidation mechanism.

Table 8.4 Ammonia concentration distribution in all experiments.

Experiment	MR	Ammonia concentration (mg/L)
Feed	N/A	2400
30 min	0.8	4950
60 min	0.8	5030
90 min	0.8	4180
Pd/AC	0	3875
Ru/Al_2O_3	0	3222
Ru/AC	0	3880
AC	0	2600
NaOH	0	2970
NaOH	0	2910
Pd/AC	0.8	1534
Pd/AC	0.6	1532

Webley and co-workers [11 and 25] who determined the oxidation kinetics of ammonia and ammonia-methanol mixtures at 700 °C, 25 MPa by oxygen in a packed and unpacked tubular reactor, reported ammonia conversions of 10% in unpacked tubular reactors, and 40% in a packed reactor. Goto et al [34] reported that the oxidation of ammonia is the slowest reaction for complete decomposition of wastes into elemental N_2, CO_2, and water. Furthermore, and according to Takahashi [13], nitrogen present in organic compounds is generally converted to N_2 or N_2O with N_2O detected at temperatures ranging from 560°C to 640°C. Moreover, Cocero et al. [15] reported that the temperature range of 570- 600°C is the optimal range to reduce the nitrogenous products with NOx observed above 943°C. However, ammonia is fairly persistent to decomposition at low temperatures, and starts to degrade only above 600°C.

8.5.6 *Fate of hydrogen sulfide (H2S) and sulfate*

The main sulfur-containing compound in the gaseous effluents for all experiments was H_2S. Osada et al [2] reported that the conversion of sulfur was dependent on the oxidant, catalyst, and the reaction temperature. Since we conducted our experiments at a constant temperature of 500°C, we attempted to track the effect of both the oxidant and catalyst on the H_2S and sulfate formation. From the data portrayed in Figure 8.5, the order of H_2S concentration emitted as gas with the used catalysts was as follows: NaOH > AC > Ru/AC > Ru/Al_2O_3 > Pd/AC. Thus, the use of metallic Pd/AC catalyst along with the oxidant i.e. sequential gasification partial oxidation suppressed the formation of H_2S to values of 130 and 123 ppm at OD of 60% and 80% respectively.

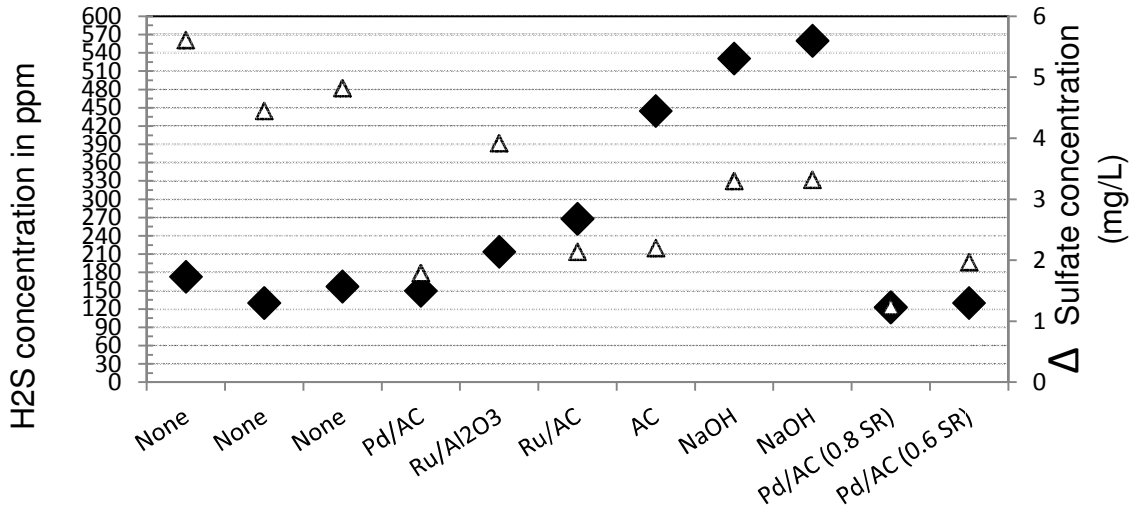

Fig 8.5 Distribution of hydrogen sulfide and sulfate concentration in all experiments

Moreover, the highest H_2S concentration of 560 ppm in the product gas was measured when NaOH was used as a catalyst which was almost double the concentration compared to the other type of metallic catalysts employed. On the other hand, as portrayed in Figure 8.4, residual sulfate concentration in the liquid phase were of 2-6 mg/L reflecting sulfate removal efficiencies of 93% to 98%. Sequential gasification partial oxidation achieved the lowest liquid phase sulfate concentration of about 2mg/L. Nevertheless, in the sequential gasification partial oxidation experiments, a decrease of OD from 80% to 60% showed insignificant effect on H_2S concentration as reflected by a 5% increase in H_2S and a significant effect of 19% decrease in the residual liquid phase sulfate concentration. The use of Pd/AC catalyst without oxidant (OD=0) gave almost the same results as the experiments with oxidant which indicates that the role of the oxidant was less important than the role of the Pd/AC catalyst.

Based on the total gas volumes observed in the experiments, the percentages of the initial sulfate consumed, emitted as H_2S gas in each experiment are reported in Table 8.5. Clearly, the Pd/AC catalyst emitted the least amount of H_2S under both gasification and sequential gasification partial oxidation of 12-15 % of the sulfate consumed.

Alkali NaOH and AC catalysts were the highest contributors to H_2S by emitting 40% of the sulfate consumed. The concurrence of the highest liquid phase sulfate concentration and the lowest H_2S content of the gas in the case of partial oxidation coupled with the significant difference between sulfates consumed and H_2S produced suggest that the sulfur in the hog manure may have undergone other reactions, such as formation of thiosulfites, and thiosulfates [26]. This is supported by results of Yanagida et al [27] who reported that sulfur in liquid effluent from poultry manure existed mainly in the forms of SO_4^{2-} and $S_4O_3^{2-}$.

Table 8.5 Percentage of sulfate consumed emitted as H_2S gas.

Experiment	MR	%
30 min	0.8	22
60 min	0.8	19
90 min	0.8	17
Pd/AC	0	15
Ru/Al_2O_3	0	22
Ru/AC	0	24
AC	0	40
NaOH	0	40
NaOH	0	38
Pd/AC	0.8	13
Pd/AC	0.6	12

8.6 References

[1] Osada M, Sato T, Watanabe M, Arai K, Shirai M. Stability of Supported Ruthenium Catalysts for Lignin Gasification in Supercritical Water. Energy & Fuels. 2006; 20: 930–935.

[2] Osada M, Sato T, Watanabe M, Arai K, Shirai M. Catalytic Gasification of Wood Biomass in Subcritical and Supercritical Water. Combust Sci Technol.2006; 178: 537–552.

[3] Osada M, Sato T, Watanabe M, Arai K, Shirai M. Effect of Sulfur on Catalytic Gasification of Lignin in Supercritical Water, Energy & Fuels.2007; 72: 1854–1858.

[4] Watanabe M, Inomata H, Osada M, Sato T, Adschiri T, Arai K. Catalytic effects of NaOH and ZrO_2 for partial oxidative gasification of n-hexadecane and lignin in supercritical water. Fuel.2003; 82: 545–552.

[5] Youssef E, Chowdhury M, Nakhla G, Charpentier P. Effect of nickel loading on hydrogen production and chemical oxygen demand (COD) destruction from glucose oxidation and gasification in supercritical water, Int J Hydrogen Energy. 2009; 35: 5034-5042.

[6] Furusawa T, Sato T, Sugito S, Miura Y, Ishiyama Y, Sato M, Itoh N, Suzuki N. Hydrogen production from the gasification of lignin with nickel catalysts in supercritical water. Int J Hydrogen Energy. 2002; 32: 699-704.

[7] Sinag A, Kruse A, Schwarzkopf V. Key compounds of the hydropyrolysis of glucose in supercritical water in the presence of K_2CO_3, Ind. Eng Chem Res.2003; 42: 3516–3521.

[8] Zhang Q, Wang S, Wang W, Liang L, Xu D. Catalytic Hydrogen Production from Municipal Sludge in Supercritical Water with Partial Oxidation. Proceeding in International Conference on Power Engineering October 2007; 23-27, Hangzhou, China.

[9] Xu X, Antal J Jr. Gasification of Sewage Sludge and other Biomass for Hydrogen Production in Supercritical Water. Environ Prog. 1998;17: 215.

[10] Yamaguchi A, Hiyoshi N, Sato T, Bando K, Osada M, Shirai M. Hydrogen Production from Woody Biomass over Supported Metal Catalysts in Supercritical Water, Catalysis Today.2009; 182: 192–195.

[11] Webley P, Tester J, Holgate H. Oxidation Kinetics of Ammonia and Ammonia-Methanol Mixtures in Supercritical Water in the Temperature Range 530-700 °C at 246 bar. Ind. Eng.Chem Res.1991; 30: 1745-1754.

[12] Killilea W, Swallow K, Hong G. The Fate of Nitrogen in Supercritical-Water Oxidation. J Supercrit Fluids. 1992; 5: 72-78.

[13] Takahashi Y. Water oxidation waste management system for CELSS- The state of art. boi. Sci in space.1989; 1: 45-54.

[14] Shanableh A, Gloyna E. Supercritical Water Oxidations of Wastewater and Sludges. Water Sci Technol. 1991; 23: 389.

[15] Cocero M, Alonso E, Torıo R, Vallelado D, Fdz-Polanco F. Supercritical Water Oxidation in a Pilot Plant of Nitrogenous Compounds: 2-Propanol Mixtures in the Temperature Range 500-750°C, Ind. Eng. Chem. Res.2000; 39: 3707-3716.

[16] Shanableh A, Jomaa S. Production and transformation of volatile fatty acids from sludge subjected to hydrothermal treatment, Water Sci Technol. 2001; 44: 129-135.

[17] Shanableh A. Production of useful organic matter from sludge using hydrothermal treatment, Water Res.2000; 34: 945-951.

[18] Portela R, Nebot E, de la Ossa M, Generalized kinetic models for supercritical water oxidation of cutting oil wastes. J. Supercrit Fluids. 2001; 21: 135–145.

[19] Li L, Chen P, Gloyna E. Kinetic model for wet oxidation of organic compounds in subcritical and supercritical water. In: Supercritical Fluid Engineering Science. ACS Symp; 1993: 514.13.

[20] Meyer J, Marrone P, Tester J. Acetic Acid Oxidation and Hydrolysis in Supercritical Water. AIChE Journal. 2004; 41: 2108-2121.

[21] Cortright R, Davda R, Dumesic J. Hydrogen from catalytic reforming of biomass-derived hydrocarbons in liquid water. Nature. 2002; 418: 964-967.

[22] Akiya N, Savage P. Roles of water for chemical reactions in high-temperature Water, Chem. Rev. 2003; 102: 2725–2750.

[23] Calzavara Y, Dubien C, Boissonnet G, Sarrade S. Evaluation of biomass gasification in supercritical water process for hydrogen production. Energy Conversion & Management. 2005; 46: 615-6731.

[24] Ploeger J, Mock A, Tester J. Cooxidation of ammonia and ethanol in supercritical water, part 1: Experimental results. AIChE Journal. 2007; 53: 941-947.

[25] Helling R, Tester J. Oxidation of simple compounds and mixtures in supercritical water: carbon monoxide, ammonia, and ethanol. Env. Sci. Technol. 1998; 22: 1319–1324.

[26] Wang T, Zhu X. Sulfur transformations during supercritical water oxidation of a Chinese coal. Fuel. 2003; 83: 2267–2272.

[27] Yanagida T, Minowa T, Nakamura A, Matsumura Y, Noda Y. Behavior of Inorganic Elements in Poultry Manure during Supercritical Water Gasification. Journal of the Japan Institute of Energy. 2008; 87: 731-736.

[28] Yu D, Xu X, Aihara M, Antal J Jr. Hydrogen Production by Steam Reforming Glucose in Supercritical Water, Energy & Fuels.1993; 7: 574-577.

[29] Xu X, Matsumura Y, Stenberg J, Antal J Jr. Carbon-Catalyzed Gasification of Organic Feedstocks in Supercritical Water, Ind. Eng. Chem. Res.1996; 35: 2522-2530.

[30] Gasafi E, Meyer L, Schebek L. Exergetic Efficiency and Options for Improving Sewage Sludge Gasification in Supercritical Water, Int. J. Energy Res.2007; 31: 346–363.

[31] Sudhir N, Aki K, Abraham M. An Economic Evaluation of Catalytic Supercritical Water Oxidation: Comparison with Alternative Waste Treatment Technologies. Enviro Prog.1998; 17: 246 - 255.

[32] Savage P. A Perspective on Catalysis in sub and Supercritical Water. J. Supercrit. Fluids.2009; 47: 407–414.

[33] Elliott C, Sealock J. Aqueous Catalyst Systems for the Water-gas Shift Reaction. 1. Comparative Catalyst Studies. Ind. Eng. Chem. Res. 1983; 22: 426-431.

[34] Guo Y, Wang S, Xu X, Gong Y, Tang X, Zhang J. Hydrogen Production by Catalytic Supercritical Water Gasification of Nitriles. Int J Hydrogen Energy. 2010; 35: 4474- 4483.

[35] Buckley J, Schwarz P. Renewable Energy from Gasification of Manure: An Innovative Technology in Search of Fertile Policy. Enviro Monit & Asses. 2003; 84: 111–127.

[36] Bernet N, Beline F. Challenges and innovations on biological treatment of livestock effluents. Bioresource Technology.2009; 100: 5431-5436.

CHAPTER 9

Summary, Conclusions and Future Work

9.1 Summary and Conclusions

Employing biomass and waste biomass as a renewable source of energy has attracted more attention and being stimulated strongly by governments recently. This thesis is dedicated to the subject of supercritical water gasification (SCWG) of waste biomass for hydrogen production. A large part of the work is related to the postulation and development of biomass reaction pathway, a subject that has not been considered sufficiently. Previous research efforts were focused mainly on the testing of different catalysts and varying the process parameters including temperature, pressure, and reaction time to enhance the hydrogen production yield. To enable a proper catalyst selection, design and to achieve the desired H_2 yield, more knowledge is required concerning the understanding of the biomass feedstocks reaction chemistry and behavior.

The literature review of Chapter 2 revealed that the information needed for process design catalyst selection, is insufficient. It is first of all important to recognize that biomass is a natural material with always differing features, which makes it very difficult to reproduce decomposition measurements. Despite all the experimental results and model compounds employed in the literature, the related product selectivity and the proper catalyst type can still not be predicted very well. Thus, the main conclusion from the literature review of chapter 2 is that the biomass reaction chemistry is needed. From the literature it also appeared that the relation between the process conditions and the precise composition and yield of the products, either

being permanent gases or liquid water soluble products, has never been investigated systematically in a single research work.

This thesis presented the supercritical water gasification (SCWG) and partial oxidation (SCWPO) results of several compounds. The aforementioned compounds were chosen to model complex biomass materials and compared to gain understanding of biomass reaction chemistry that can help predict their behavior during SCWG and SCWPO. Understanding biomass reaction chemistry is needed for the optimum catalyst design and selection. Giving the complexity of biomass composition and reactions, this work was able to provide the base line for understanding the aforementioned reaction chemistry. This was achieved through the development and postulation of the reaction pathway for oleic acid, cysteine, and the Co-gasification of carbohydrate i.e. starch and lignin i.e. catechol model compounds. Furthermore, the data provided here within this work is considered very valuable addition to the literature as the data pertaining to SCW gasification is scarce in the literature.

Therefore, supercritical water gasification of waste biomass model compounds is performed in this work based on the fact that sewage sludge mainly consisted of lipids (about 10%), proteins (about 40%), carbohydrates, and lignin (about 17%). Catalytic and non-catalytic supercritical water gasification of waste biomass and biomass model compounds was investigated in a 600 ml batch reactor at 28MPa and temperature range of 400-500°C. The sequential gasification partial oxidation technique of glucose in Chapter 4 was introduced in this work and performed in the presence of different metallic Ni loadings (7.5, 11, 18 wt%) on different catalyst supports (θ-Al_2O_3 and γ-Al_2O_3) in supercritical water at three temperature levels, *viz.*, 400, 450, and 500°C. The hydrogen yield was relatively insensitive on the pellet

catalyst at nickel loading above 11 wt% as well as the different catalyst supports which was the main finding of the work pertained to glucose.

As a model compound for lipids, the catalytic supercritical water gasification of oleic acid in presence of several commercial catalysts was investigated for hydrogen production in Chapter 5. When studying the various catalysts, the order of H_2 production was as follows: pelletilized Ru/Al_2O_3 > powder Ni/Silica-alumina > powder Pt/AC > granular Ru/AC > powder Pd/AC > KATALCO. Ruthenium catalyst favored the methane formation reaction which consumed part of the H_2 produced and eventually decreased the H_2 yield. Both catalysts Ru/Al_2O_3, and Ru/AC were significantly deactivated in the first run as reflected by 60% and 50 % reduction in the H_2 yield in the 2^{nd} run respectively.

In Chapter 6, the co-gasification of starch and catechol as model compounds of carbohydrates and lignins respectively was performed in SCW. Co-gasification of model biomass components is required to provide an understanding of the interactions that cannot be deduced from single substrate studies alone. Experiments were performed in the presence of CaO, TiO_2, and the combined CaO + TiO_2 catalysts. The enhancement of H_2 yield through the addition of CaO was insignificant, and the CO_2 yield decreased remarkably by 90% which facilitated the increase of H_2 content in the gas phase to 80%. It was found that the use of TiO_2 as sole catalyst facilitated the formation of cyclo-compounds such as cyclohexene, cyclobutane, and cyclopentanone which inhibited gaseous production formation as evidenced by decreasing the H_2 yield from 37 to 33 ml/g carbon fed and the CO_2 yield from 56 to 38 ml/g carbon fed. The combination of CaO and TiO_2 had a remarkable effect on the gaseous products yield and was corroborated by the TOC reduction efficiency increasing from 47% to 59%. Characterization of

the process liquid effluent revealed that phenol, substituted phenols and cresols were the main compounds formed, and were very stable during this process.

Despite significant focus of research effort on the SCW gasification of biomass and model waste biomass compounds, information on the behavior and effect of sulfur on the gaseous yield distribution is sparse. Volatile organic sulfur and hydrogen sulfide are well known odorous compounds, the fate of which in SCW has been mostly overlooked. Thus, studying cysteine could provide an invaluable addition and knowledge to understand the behavior of sulfur species present in sewage sludges. Chapter 7 provides the catalytic supercritical water gasification (CSCWG) of cysteine (0.25M) for hydrogen production study in the presence of two ruthenium catalysts, namely, Ru/Al_2O_3, Ru/AC and AC. Results showed that AC catalyst surpassed the other two catalysts (Ru/Al_2O_3 and Ru/AC) in terms of H_2 yield of 1.7 versus 1.6, and 1.5 mol/ mol feed respectively. The main sulfur-containing compound in the gaseous effluents in all experiments was H_2S. It was found that the formation of H_2S was neither dependent on the temperature nor the catalyst and the detected sulfur-containing component in liquid effluent was mainly sulfide.

The last chapter of this thesis i.e. Chapter 8 contains the demonstration feasibility of hydrogen and methane production using sequential gasification partial oxidation. In this work, the catalytic and non-catalytic hydrogen production from hog manure using supercritical water partial oxidation, gasification, and sequential gasification partial oxidation was investigated in a batch reactor at a temperature of 500°C, and pressure of 28 MPa using several metallic catalysts. It was found that the order of H_2 production in catalytic gasification follows Pd/AC > Ru/Al_2O_3 > Ru/AC > AC > NaOH, whereas the order of chemical oxygen demand (COD) reduction

efficiency was the following NaOH > Ru/AC > AC > Ru/Al_2O_3 > Pd/AC. Also, the following can be concluded:

- Sequential gasification and partial oxidation is better than each one individually from an environmental point of view as it produced the lowest ammonia concentration of 1534 mg/L, the lowest effluent COD concentration in liquid phase, and the lowest H_2S concentration of 130 ppm in the gas phase.
- Of all employed catalysts, Pd/AC was the best as it provided the highest H_2 yield as well as the lowest H_2S concentration in the gas phase.

Generally, supercritical water gasification technique presented in this thesis can be applied to environment friendly waste treatment, production of hydrogen from the waste. However, future investigation into higher temperature and using continuous flow system would be invaluable from practical point of view.

9.2 Technology Limitation

Several major challenges face this technology due to underestimation of the main SCW problems which hinder its widespread industrial application. Although laboratory experiments resulted in a considerable number of SCWO reactor concepts and process designs as well as several compounds that model biomass have been described in literature. The technology still faces considerable challenges, despite its successful demonstration in this work.

Because of the nature of SCW environment (T = 600 °C, P = 300 bar), not only high pressure (mechanical load) and temperature (thermal load) conditions but also a very corrosive aqueous environment, corrosion rates are considerably high. In addition to reactor plugging, the corrosion of the SCW reactor and components is the main technical problem pertaining to SCW systems. At SCW conditions, heteroatoms are converted to the corresponding acids and the

reactive ions lead to corrosion. For example, chloride is the most important corrosive species in SCWO processes. Therefore, the reactor design also needs to account for material fatigue resulting from temperature cycles, loads exerted by thermal shock, and the weakening of material through corrosion.

Experimental investigations on SCWG are tedious, expensive and time consuming. Time to heat-up and cool-down the reactor has never been controlled in our experimental work. Liquid effluent by-products resulting from the non-converted biomass and tars from undesired reaction products are two major challenges in SCWG, although char formation was insignificant compared to other technologies such as pyrolysis. Tar usually formed by pyrolysis of organic molecules leading to severe corrosion problems, and pluging continuous reactors after several hours of running at the expense of the amount of hydrogen production.

The need to produce a tar-free product gas and avoid the formation of undesired products from the gasification of biomass, the removal of tars, and the reduction of the methane have been the main focus areas of several literature studies. However, the criteria for the catalyst are fundamentally the same and may be summarized as follows:

- The catalysts must be effective in the removal of tars.
- The catalysts should be resistant to deactivation as a result of carbon fouling and sintering.
- The catalysts should be easily regenerated, strong, and inexpensive.

Adding to the above criteria, in the case of hydrogen production using supercritical water the catalyst should give reasonable hydrogen yield. An important objective of catalytic SCWO studies is to identify catalysts that are both stable and active in SCW. However, most catalysts are deactivated during SCW gasification. The deactivation of a catalyst is mainly caused by

coking, poisoning, and the solid state transformations of catalysts in the gas-phase oxidation case. In other words, the SCW catalytic process needs optimized combination of catalysts (components, manufacturing process, and morphology), reactants, reaction environment, process parameters such as temperature, pressure, and residence time, and reactor configuration.

9.3 Future Work

Generally, supercritical water gasification technique presented in this thesis can be applied to environment friendly waste treatment, production of hydrogen from the waste. However, future investigation into higher temperature and using continuous flow system would be invaluable from practical point of view.

- The work presented in this thesis should be expanded to explore and investigate other compounds that model biomass and waste biomass. A more detailed investigation into the role of lignin monomers, fatty acids and triglycerides is needed to enhance and broaden the understanding the reaction chemistry of the SCWG for biomass model compounds.
- The observation of catalyst deactivation during this work stimulates the need for future detailed catalyst deactivation study. As part of the SCWG process, catalyst deactivation study can provide hints on the proper catalyst selection criterion for designing SCWG process. Conducting detailed characterization of fresh and spent catalysts to determine the effect of SCW on catalysts and to explore the exact cause of deactivation.
- A possible catalyst synthesizing technique is through SCW using the constructed SCW batch reactor unit. This route or technique can provide a catalyst with good properties that can sustain the harsh SCW conditions i.e. high pressure and high temperature.

- The evaluation of the catalyst should be performed in the developed continuous system with a few seconds residence time for evaluation of practical industrial viability.

Appendices

Appendix A1: Elsevier Policy on reprinting published material.

Authors publishing in Elsevier journals retain wide rights to continue to use their works to support scientific advancement, teaching and scholarly communication. An author can, without asking permission, do the following after publication of the author's article in an Elsevier-published journal:

- Make copies (print or electronic) of the author's article for personal use or the author's own classroom teaching.
- Make copies of the article and distribute them (including via email) to known research colleagues for their personal use but not for commercial purposes as described below.
- Present the article at a meeting or conference and distribute copies of the article to attendees.
- Allow the author's employer to use the article in full or in part.
- Retain patent and trademark rights and rights to any process or procedure described in the article.
- **Include the article in full or in part in a thesis or dissertation.**
- Use the article in full or in part in a printed compilation of the author's, such as collected writings and lecture notes.
- Use the article in full or in part to prepare other derivative works, including expanding the article to book-length form, with each such work to include full acknowledgment of the article's original publication in the Elsevier journal.

Appendix A2: SCW Process Description

Generally, SCW research is conducted in either batch or continuous flow reactors. Batch reactor systems are easy to construct but require longer heating periods, residence times and it is usually difficult to conduct batch experiments without avoiding the sub-critical reactions that may occur. On the other hand, the continuous SCW flow process is comprised of four main sections or zones [6], including:

- Feed preparation
- Reactor Section
- Heat recovery and depressurization
- Product separation section

There have been several SCW lab-scale and pilot plants built so far in several institutions. In the following section, a brief description of the system built by the green engineering group at the University of Western Ontario, London, Ontario, Canada. This system consists of a small scale SCW batch and continuous flow units. The batch unit has been described in chapter 3, thus, the continuous flow unit will only be described solely in the following section:

Continuous flow system design & experimental procedures

Figure A2.1shows the schematic of the constructed experimental apparatus that is suitable for continuous operation at temperatures and pressures up to 650ºC and 350 bar, respectively. The system consists of four main zones: the pumping section, the reactor section, the cooling-depressurizing section, and the gas liquid separating-GC analysis section. The four zones are described as follows:

- The pumping zone:

A high-pressure pump (P1) capable of delivering 10,000 psi (Linc Milton Roy-86 Series Electric Pump, Ivyland PA U.S.A) with a nominal flow range between 0.31 and 1.29 L/h is used to feed in the aqueous solution. This pump is capable of delivering sewage sludge with mesh size < 70 μm. A Ball type check valve (High Pressure Equipment Company catalog no 60-41HF9, Erie, Pennsylvania U.S.A) was installed in the pump discharge line to insure flow in one direction only. The pump suction was connected to both the aqueous feed tank and de-ionized water tank (TK1 and TK2). The feed line contains a relief valve (RV1) (High Pressure Equipment Company. Erie, Pennsylvania U.S.A) proceeded by a 0-10000 psi pressure transducer (Noshok, Berea, OH, U.S.A) which was connected to the control and data acquisition system. The relief valve was installed to relieve pressure in case of excessive pressure. Additionally, a check valve (High Pressure Equipment Company. Erie, Pennsylvania U.S.A) was installed at the pump discharge to prevent back pressure during shutdown. The oxidant - aqueous H_2O_2 solution is pumped from the H_2O_2 tank (TK3) to the system by means of a syringe pump (ISCO Model 100 DX, Lincoln NE, USA).

The oxidant and the feed are pumped to the reactor through two separate lines, with each line preheated by means of two ultra high temperature heating tapes (OMEGA Model Number STH102-080, Laval, Quebec, Canada). The heating tapes were rated to 1400°F and the wires were double insulated with braided Samox and knitted into flat tapes for maximum flexibility. The feed and oxidant lines were connected to each other with a high pressure valve (20-11LF9, High Pressure Equipment Company, Erie, Pennsylvania U.S.A) which was used for flushing after each experimental run. After passing through the preheaters in the two separate lines and just before they enter the reactor, the oxidant and the feed were mixed together in a tee (30-23-

HF16 High Pressure Equipment Company, Erie, Pennsylvania U.S.A) at an angle of 90° to minimize the mixing effects as per the procedure described by Philip Marrone [29-30].

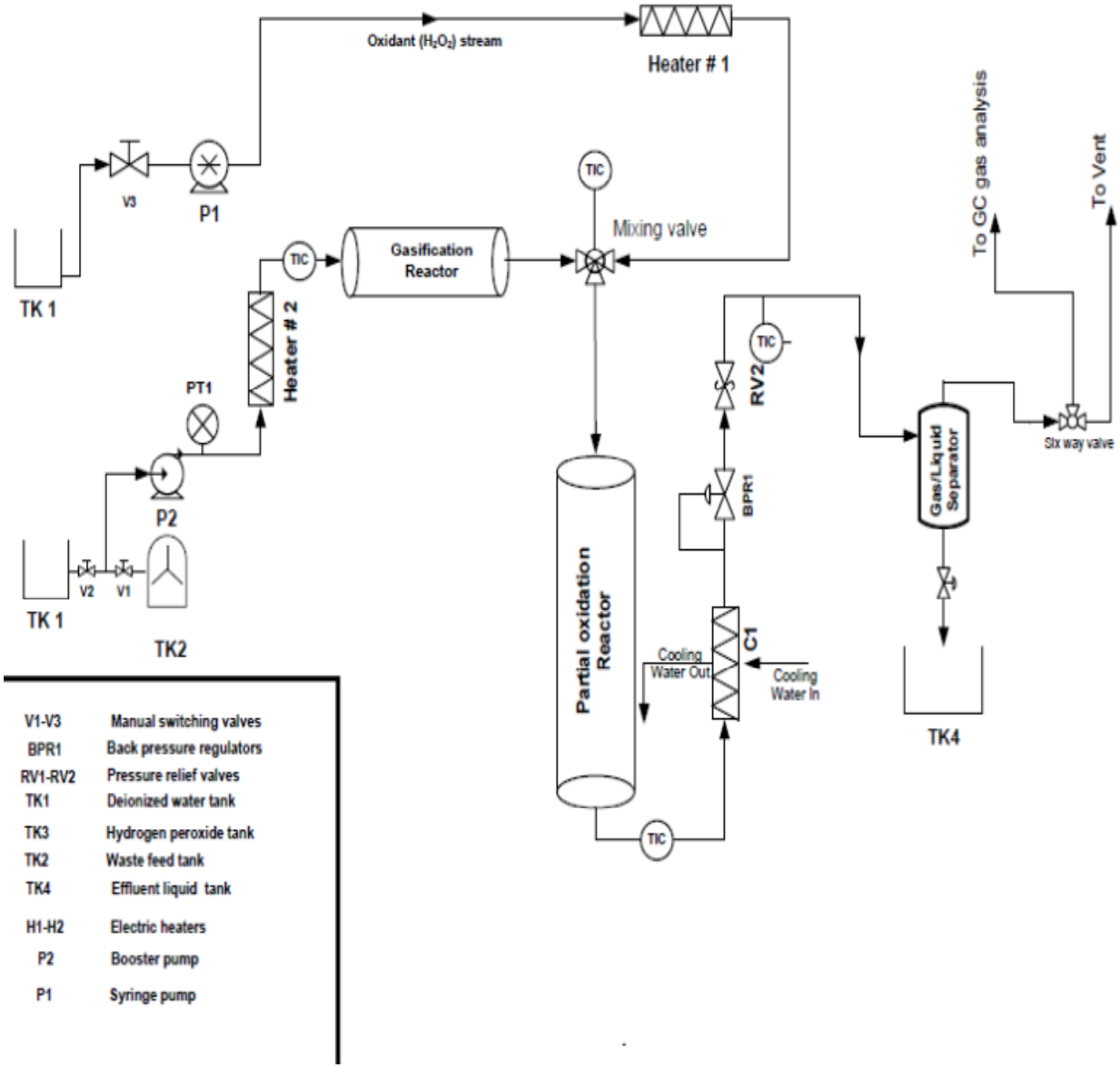

Fig. A2.1 Schematic diagram of the continuous SCW system apparatus constructed at the UWO.

- <u>The Reactor zone:</u>

The reactor section consists of two sections, namely, the gasification section followed by the partial oxidation section. The gasification section is where the preheated feed passed through the reactor and the catalyst. The catalyst was supported by stainless steel frits, fabricated at the

University of Western Ontario machine service, and placed at the inlet and outlet of the reactor. The design of gasification and partial oxidation reactors is based on the idea of a double pipe tube. In the gasification reactor, the outer pipe was made of 316 SS with dimensions of 0.562 inches I.D., 1inch O.D., 16 inch long, and a volume of 60 ml, to sustain the process operating pressure. An inner pipe made of Titanium (grade 2) was swaged perfectly inside the outer 316 SS pipe. The main purpose of using a Titanium inner tube is to prevent the fluid from contacting the outer tube and eventually preventing corrosion. Another purpose of using a Titanium inner tube was to eliminate the interference of the outer reactor wall as a catalyst in the gasification process as it is well known that 316 SS has high percent of nickel which can catalyze the reaction and mislead the gasification process results.

The partial oxidation reactor section was also designed based on the double pipe idea. However, the outer tube was made of 316 SS with dimensions of 0.562 inches I.D., 1inch O.D., 16 inch long, and a volume of 127 ml. An inner Titanium tube (grade 2) was swaged perfectly through the inner surface of the reactor. Therefore, the actual reactor internal volume was 120 ml. This inner tube was primarily employed to study the corrosion phenomena in the SCW process. Moreover, and for flexibility, the inner tube of the partial oxidation reactor section is easily replaceable. This design flexibility allows for easy replacement and testing of different alloys such as Inconel 625 and Hastelloy other than titanium for detailed corrosion studies and comparison between different alloys as mentioned earlier.

It also should be pointed out that most reactors used in the literature are either from Hastelloy C276 or Inconel because of their favourable anti-corrosion characteristics. Experience has shown that corrosion rates can be rapid when treating wastes containing halogens, such as chlorine. Corrosion-resistant alloys such as Hastelloy C-276 and Inconel 625 do not provide

adequate protection against chloride attack under the harsh oxidizing conditions found in SCW systems.

The products leave the second reactor (partial oxidation section) through a high pressure TEE (30-22-HF16 High Pressure Equipment Company, Erie, Pennsylvania U.S.A). The reactors are heated by two ultra high temperature heating tapes (OMEGA Model Number STH102-080*, Laval, Quebec, Canada). The heating tapes are rated at 750°C and the wires are double insulated with braided Samox and knitted into flat tapes for maximum flexibility. The heating tapes were procured to cover all the outer surface of the reactor tube to ensure consistent heating and temperature profiles. The temperature at the inlet and outlet of the reactor was monitored by means of thermocouples (Omega K type, Omega Engineering, Laval, Quebec, Canada) mounted on the inlet and outlet of the TEE. The thermocouples were mounted deep enough to be exposed to the fluid to ensure correct measurement of the feed inlet and outlet temperatures.

- Reactor Sizing:

The reactor was sized based on the following equation:

$$V_{reactor} = \{\tau \, X \, \rho_L \, (F_1+F_2)\} / \rho_{SC} \qquad (8)$$

Where τ is the reactor residence time; $F = (F_1+F_2)$ is the total volumetric flow rate of both oxidant and organic feed; ρ_L is the density of the pumped organic feed at the pump conditions; ρ_{SC} is the density of the pumped feed at the reactor conditions (T & P).

- The cooling-depressurization section

The effluent leaves the second reactor through an elbow (60-22 HF9, High Pressure Equipment Company, Erie, Pennsylvania U.S.A). The elbow is connected to a tee (60-23HF9, High Pressure Equipment Company. Erie, Pennsylvania U.S.A) in which the thermocouple is inserted deep until it reaches the outlet of the reactor. The effluents pass through a double pipe

heat exchanger that employs service water as a coolant. To ensure efficient cooling, the coolant flow is counter-current to the effluent. Another thermocouple is installed right after the heat exchanger and is connected to the data acquisition system. A back-pressure regulator (BPR-Tescom Series model number 26-1700, Emerson Process Management, TX, and U.S.A) is mounted at the end of the heat exchanger to control the system pressure. The pressure is monitored by the same Noshok pressure transducer just upstream of the back-pressure regulator. Another pressure reducing valve is mounted after the BPR for safety precautions in case the BPR fails to control the pressure. The pressure reducing valve is equipped with a pressure gauge (Swagelok, 0 - 7,500 psig), and a second relief valve (RV2) (High Pressure Equipment Company. Erie, Pennsylvania U.S.A) is connected to the pressure reducing valve in case of over pressurization.

- The gas liquid separating-GC analysis section.

After cooling and de-pressurizing, the reactor effluents are passed through a membrane gas liquid separator (Genie-Filters, Model 120, Gonzales, LA, U.S.A). It is ideal for low flow applications and can withstand high pressures of 210 bars in the housing. It also provides protection against liquids for on-line GC analysis. The separator has three ports, inlet, outlet, and bypass. Liquid products are collected from the bypass and the outlet port is connected to the gas chromatograph (Shimadzu 2014) equipped with TCD, FID, and FPD detectors for online gas analysis purposes.

- *Continuous flow system procedures*

Before starting any experiment, the data acquisition and all control system components are switched on. Each experiment starts with the feed and oxidant preparation in the feed and oxidant tanks (TK1 and TK3). The organics aqueous solution is purged with helium gas from the

helium cylinder prior to each experiment to reduce the amount of dissolved oxygen. The feed pump circulates purified water through the heating period and the BPR1 in figure 2 regulates the pressure. As the desired temperature is reached, the feed pump is switched to the feed tank by means of switching the three way valve that connects both the feed and purified water tanks (TK1 and TK2). The high pressure feed is preheated until it stabilizes to the desired experimental temperature. As the feed pressure and temperature stabilize, the unit is considered at steady state and samples are taken for the liquid effluent from the gas liquid separator as well as the gaseous stream from the top of the same device. A typical run would last between 2 to 6 hours based on the number of gas samples analyzed. At least, three GC injections are measured to ensure accuracy of the gas stream analysis. The oxidant (H_2O_2) solution is prepared in a similar manner to the feed stream and placed in the oxidant tank (TK3) and purged with helium gas to drive away any oxygen gas in the tank head space. The oxidant is then pumped to the reactor using an ISCO syringe pump. Thus, there is no need to install any pressure transducer in its line since The ISCO syringe pump is equipped with a control system that provides the flow rate and pressure parameters.

Appendix A3: SCW Performed Experiments

1- Performed Glucose Experiments

Catalyst type	Catalyst load(g)	Concentration (Molarity)	MR	Residence Time (min)	Temperature (°C)	No. of Runs	Status
N/A	N/A	0.25 M	0.7	30 min	400	1	R
N/A	N/A	0.25 M	0.7	30 min	400	1	R
N/A	N/A	0.25 M	0.5	30 min	400	1	R
N/A	N/A	0.25 M	0.8	30 min	400	1	R
N/A	N/A	0.25 M	0.9	30 min	400	1	R
N/A	N/A	0.25 M	0.8	30 min	450	1	R
N/A	N/A	0.25 M	0.8	30 min	500	2	R
Commercial (63 %wt Ni on silica-alumina)	0.5	0.25 M	0.8	30 min	500	1	R
Commercial (63 %wt Ni on silica-alumina)	0.5	0.25 M	0	30 min	500	1	R
Commercial (63 %wt Ni on silica-alumina)	1	0.25 M	0	30 min	500	2	R
Commercial (63 %wt Ni on silica-alumina)	0.5	0.25 M	0.56	30 min	500	1	R
7.5 wt % Ni theta Alumina	0.5	0.25 M	0.8	30 min	500	2	R
7.5 wt % Ni theta Alumina	1	0.25 M	0.8	30 min	500	1	R
11 wt % Ni theta Alumina	1	0.25 M	0.8	30 min	500	1	R
7.5wt % Ni Gamma Alumina	1	0.25 M	0.8	30 min	500	1	R

11 wt % Ni Gamma Alumina	0.5 & 1	0.25 M	0.8	30 min	500	2	R
18 wt % Ni theta Alumina	1 & 2	0.25 M	0.8	30 min	500	1	R
N/A	N/A	0.25 M	0.8	2 min	400	1	NR
N/A	N/A	0.25 M	0.8	4 min	400	1	NR
N/A	N/A	0.25 M	0.8	5 min	400	1	NR
N/A	N/A	0.25 M	0.8	6 min	400	2	NR
N/A	N/A	0.25 M	0.8	8 min	400	1	NR
N/A	N/A	0.25 M	0.8	10 min	400	1	NR
N/A	N/A	0.25 M	0.8	12 min	400	2	NR
N/A	N/A	0.25 M	0.8	15 min	400	1	NR
N/A	N/A	0.25 M	0.8	20 min	400	2	NR
N/A	N/A	0.25 M	0.8	22 min	400	1	NR
N/A	N/A	0.25 M	0.8	25 min	400	1	NR
N/A	N/A	0.25 M	0.8	30 min	400	4	NR
N/A	N/A	0.25 M	0.8	40 min	400	1	NR
N/A	N/A	0.25 M	0.8	45 min	400	1	NR
N/A	N/A	0.25 M	0.8	50 min	400	2	NR
N/A	N/A	0.25 M	0.8	60 min	400	1	NR
N/A	N/A	0.25 M	0.8	90 min	400	3	NR

R “reported”; NR “not reported”

2- **Performed Oleic acid Experiments**

Catalyst type	Catalyst load(g)	Concentration (Molarity)	MR	Residence Time (min)	Temperature (°C)	No. of Runs	Status
N/A	N/A	0.35 M	N/A	30 min	400	3	R
N/A	N/A	0.35 M	N/A	30 min	450	2	R
N/A	N/A	0.35 M	N/A	30 min	500	3	R
Ru/AC	1	0.35 M	N/A	30 min	500	5	R
Ru/Al_2O_3	1	0.35 M	N/A	30 min	500	5	R
Pd/AC	1	0.35 M	N/A	30 min	500	2	R
Pt/AC	1	0.35 M	N/A	30 min	500	2	R
commercial Iron catalysts (KATALCO)	1	0.35 M	N/A	30 min	500	2	R
AC	1	0.35 M	N/A	30 min	500	2	R
N/A	N/A	0.25 M	0.8	45 min	400	1	NR
Activated carbon(AC)	2.5	0.25 M	0.8	50 min	400	1	NR
Activated carbon(AC)	2.5	0.25 M	0.8	60 min	400	1	NR
Pd (Palladium)/AC	2.5	0.25 M	0.8	90 min	400	1	NR
Pd (Palladium)/AC	2.5	0.25 M	N/A	30 min	500	1	NR
Pt(Platinum)/AC	2.5	0.25 M	N/A	30 min	500	1	NR
Pt(Platinum)/AC	2.5	0.25 M	N/A	30 min	500	1	NR
Ni/silica-alumina	2.5	0.25 M	N/A	30 min	500	1	NR
Ni/silica-alumina	2.5	0.25 M	N/A	30 min	500	1	NR
KATALCO	2.5	0.25 M	N/A	30 min	500	1	NR
KATALCO	2.5	0.25 M	N/A	30 min	500	1	NR

R “reported”; NR “not reported”

3- **Performed Non-catalytic Starch & Catechol Kinetic Experiments**

Exp.No	Reaction time (min)	Temperature (°C)	Cat. Type	Status
1	5	400	No Catalyst	NR
2	5	425	No Catalyst	NR
3	5	450	No Catalyst	NR
4	5	500	No Catalyst	NR
5	15	400	No Catalyst	NR
6	15	425	No Catalyst	NR
7	15	450	No Catalyst	NR
8	15	500	No Catalyst	NR
9	20	400	No Catalyst	NR
10	20	425	No Catalyst	NR
11	20	450	No Catalyst	NR
12	20	500	No Catalyst	NR

Mixing ratio: (25 % S +75 % C), No oxidant, No. of Runs 1 for all

4- **Performed Non-catalytic Starch & Catechol Kinetic Experiments**

Time (min)	Temp(°C)	Catalyst	Starch	Catechol	Status
30	400	None	√	None	R
30	450	None	√	R	P
30	500	None	√	R	P
30	400	None	None	R	P
30	450	None	None	R	P
30	500	None	None	R	P
30	500	None	0.5	R	P
30	500	None	0.25	R	P
30	500	None	0.75	R	P
30	500	CaO	Opt (25 % S +75 % C)		R
30	500	AC	Opt (25 % S +75 % C)		R
30	500	AC + CaO	Opt (25 % S +75 % C)		R
30	500	TiO2 (nano-powder)	Opt (25 % S +75 % C)		R
30	500	None (Repeat exp 8)	R (25 % S +75 % C)		R
30	400	Opt (TiO2 (nano-powder) + CaO)	Opt (25 % S +75 % C)		R
30	425	Opt (TiO2 (nano-powder) + CaO)	Opt (25 % S +75 % C)		R
30	450	Opt (TiO2 (nano-powder) + CaO)	Opt (25 % S +75 % C)		R
30	500	Opt (TiO2 (nano-powder) + CaO)	Opt (25 % S +75 % C)		R

10	400	Opt (TiO2 (nano-powder) + CaO)	Opt (25 % S +75 % C)	R
10	425	Opt (TiO2 (nano-powder) + CaO)	Opt (25 % S +75 % C)	R
10	450	Opt (TiO2 (nano-powder) + CaO)	Opt (25 % S +75 % C)	R
10	500	Opt (TiO2 (nano-powder) + CaO)	Opt (25 % S +75 % C)	R
20	400	Opt (TiO2 (nano-powder) + CaO)	Opt (25 % S +75 % C)	R
20	425	Opt (TiO2 (nano-powder) + CaO)	Opt (25 % S +75 % C)	R
20	450	Opt (TiO2 (nano-powder) + CaO)	Opt (25 % S +75 % C)	R
20	500	Opt (TiO2 (nano-powder) + CaO)	Opt (25 % S +75 % C)	R
20	500	Opt (TiO2 (nano-powder) + CaO)	Opt (25 % S +75 % C)	R
25	400	Opt (TiO2 (nano-powder) + CaO)	Opt (25 % S +75 % C)	R
25	425	Opt (TiO2 (nano-powder) + CaO)	Opt (25 % S +75 % C)	R
25	450	Opt (TiO2 (nano-powder) + CaO)	Opt (25 % S +75 % C)	R
25	500	Opt (TiO2 (nano-powder) + CaO)	Opt (25 % S +75 % C)	R
30	400	No Catalyst	Opt (25 % S +75 % C)	R
30	425	No Catalyst	Opt (25 % S +75 % C)	R
30	450	No Catalyst	Opt (25 % S +75 % C)	R
30	**500**	None (Repeat exp 8)	**R (25 % S +75 % C)**	R
20	400	No Catalyst	Opt (25 % S +75 % C)	R
20	425	No Catalyst	Opt (25 % S +75 % C)	R
20	450	No Catalyst	Opt (25 % S +75 % C)	R
20	500	No Catalyst	Opt (25 % S +75 % C)	R
10	400	No Catalyst	Opt (25 % S +75 % C)	R
10	425	No Catalyst	Opt (25 % S +75 % C)	R
10	450	No Catalyst	Opt (25 % S +75 % C)	R

5- **Performed Cysteine Experiments**

Exp.No	Temp	Concentration (M)	Catalyst type	Reaction time (min)	Status	No.of runs
1	400	0.25	None	30	R	2
2	450	0.25	None	30	R	4
3	475	0.25	None	30	R	2
4	500	0.25	None	30	R	2
7	Opt	0.25	Ru/AC	30	R	2
8	Opt	0.25	Ru/Al_2O_3	30	R	2
9	Opt	0.25	AC	30	R	1
16	Opt	0.25	Pd/ AC	30	NR	2
17	Opt	0.25	Pt/ AC	30	NR	2

6- **Performed Hog Manure Experiments**

Exp.No	Temp (°C)	Concentration (mg COD/L)	Catalyst type	Reaction time (min)	Status	No.of runs
1	500	57000	None	10	NR	2
2	500	57000	None	30	R	3
3	500	57000	None	60	R	1
4	500	57000	None	90	R	3
7	500	57000	Ru/AC	30	R	2
8	500	57000	Ru/Al_2O_3	30	R	2
9	500	57000	AC	30	R	1
16	500	57000	Pd/ AC	30	NR	2
17	500	57000	Pt/ AC	30	NR	2
18	500	57000	NaOH	30	R	5

Curriculum Vitae

Emhemmed A Youssef

EDUCATION:

PhD in Chemical Engineering (July, 2011)
Department of Chemical and Biochemical Engineering, University of Western Ontario, Canada

Master of Science in Environmental Engineering (June, 2007)
Civil & Environmental Engineering, University of Windsor, Canada

Bachelor of Science in Chemical Engineering (July, 1997)
Department of Chemical Engineering, El-Fateh University, Tripoli, Libya

PROFESSIONAL EXPERINCE:

Sep 1999- April 2004: Process Engineer
Azzawiya Oil Refining Co, Azzawiya, Libya
May 2007- Dec 2007: Process Design Specialist
SNC-LAVALIN Engineers & Constructors, Sarnia, Ontario, Canada

RESEARCH EXPERIENCE:

Jan2006- April 2007: Research Assistant
Civil & Environmental Engineering, University of Windsor, Canada

Jan 2008- April 2011: Research Assistant
Department of Chemical and Biochemical Engineering, University of Western Ontario, Canada

SCHOLARSHIPS:

(1) Western Engineering Scholarship (2008-2011), University of Western Ontario, Canada.
(2) Graduate Scholarship (2004-2011), Libyan Post-Graduate Education Ministry. Libya

SELECTED PUBLICATIONS:

1. **Youssef, A., E**.; Nakhla, G.; Charpentier, P. Supercritical Water Gasification for Hydrogen Production. Accepted book Chapter in the Handbook of Hydrogen Energy, the book will be published by CRC Press⁄Taylor and Francis in early 2011.
2. **Youssef, A., E**.; M. B. I. Chowdhury, G. Nakhla, P. Charpentier, Effect of nickel loading on hydrogen production and chemical oxygen demand (COD) destruction from glucose oxidation and gasification in supercritical water, *Int. J. Hydrogen Energy,* 35, 2010.
3. **Youssef, A., E,** Elbeshbishy, E.; Hafez, H.; Nakhla, G.; Charpentier, P. Sequential Supercritical Water Gasification and Partial Oxidation of Hog Manure for Hydrogen Production. Int J Hydrogen Energy, 35 (2010) 11756-11767.
4. **Youssef, A., E**, Nakhla, G.; Charpentier, P. Oleic Acid Gasification over Supported Metal Catalysts in Supercritical Water; Hydrogen Production and Product Distribution. Int J Hydrogen Energy, 36 (2011) 4830-4842.
5. **Youssef, A., E**, Walid A. Al Gherwi, and Abdul-Fattah A. Asfour Densities and Kinematic Viscosities of Five Binary 1-Alkanol Liquid Systems at Temperatures of (293.15 and 298.15) K. Journal of Chemical & Engineering Data, je-2010 -000654. Submitted.
6. **Youssef, A., E,** Nakhla, G.; Charpentier, P. Co-Gasification of Starch and Catechol over TiO_2 nano-catalyst for hydrogen production in supercritical water; Effect of CaO as a CO_2 absorber. Submitted.
7. **Youssef, A., E,** Nakhla, G.; Charpentier, P. Behavior of Sulfur during Gasification of Cysteine as protein model compound in Supercritical Water for Hydrogen Production. Submitted.